Establishing a rodent model of long-term consumption of sugar-sweetened beverages

Natasha Darné Driescher

Thesis presented in fulfilment of the requirements for the degree of Masters in Science in the Faculty of Science at Stellenbosch University

Supervisor: Professor M. Faadiel Essop

December 2014

Guard your heart above all else,

for it determines the course of your life.

Proverbs 4:23, NLT

Declaration

By submitting this thesis electronically, I declare that the entirety of the work contained therein is my own, original work, that I am the sole author thereof (save to the extent explicitly otherwise stated), that reproduction and publication thereof by Stellenbosch University will not infringe any third party rights and that I have not previously in its entirety or in part submitted it for obtaining any qualification.

Signature:_____Date:_____

Abstract

Introduction- Cardiovascular complications contribute dramatically to morbidity and mortality incidence amongst individuals who have developed type 2 diabetes (T2D), with myocardial insulin resistance (IR) playing an important role. Poor lifestyle choices and dietary habits such as increased sugar-sweetened beverage (SSB) consumption have emerged as key contributors to the global 'epidemic' of obesity, diabetes and heart disease. However, the underlying mechanisms whereby SSBs drive the onset of cardio-metabolic complications remain unclear. For the current study, we hypothesized that long-term SSB consumption will trigger downstream glucose metabolic pathways with physiologically damaging outcomes. Specifically we proposed that increased glucose availability (due to SSB consumption) activates non-oxidative glucose pathways (NOGPs), i.e. polyol pathway, hexosamine biosynthetic pathway (HBP), advanced glycation end-products (AGE), and PKC activation that may in turn contribute to cardio-metabolic complications.

Methodology- Male Wistar rats (~200 g) were gavaged daily with 3-5.1 mL of well-known, local SSBs and ASBs for a total period of six months. Dietary behavior and phenotypic changes were monitored on a weekly basis, while systemic (fasted) triglyceride, cholesterol and glucose levels at various time points during the study period. Furthermore, we performed oral glucose tolerance tests (OGTTs) biweekly, and also determined overall weight gain and organ tissue mass. Myocardial NOGPs were evaluated using commercially available kits and by Western blotting techniques.

Results- Our data reveal that after six months the different soda groups displayed minimal macroscopic changes, therefore possibly representing a relatively early stage in terms of SSB-mediated cardio-metabolic complications. However, we also found several changes at the biochemical level but with distinct signatures for the Jive® group compared to the Coca Cola® and Coke Light® groups. Here Jive® consumption for six months resulted in early signs of cardiac and skeletal muscle hypertrophy, together with increased liver mass and perturbed adipocyte ultrastructure. We also established that the majority of the myocardial NOGPs were activated that may have contributed to some of the changes already found and that may lead to the onset of future complications. The Coca Cola® and

Coke Light® groups exhibited alterations in liver mass and altered adipocyte ultrastructure together with lower glucose clearance after six months suggesting onset of IR. These data also clearly show that the HBP may be a universal pathway that was activated in all of the soda groups, with potential long-term detrimental physiological effects.

Conclusion- This study managed to successfully establish a novel *in vivo* rat model of chronic SSB and artificially sweetened beverage (ASB) consumption. We demonstrated that SSB consumption resulted in minimal macroscopic alterations but that it did trigger variable postprandial excursions together with the induction of several myocardial NOGPs. Thus the current study shows that long-term SSB intake activates potentially detrimental metabolic pathways that may place organisms at risk of developing cardio-metabolic complications despite an apparently "healthy" phenotype.

Opsomming

Inleiding- Kardiovaskulêre komplikasies is verantwoordelik vir die bydrae tot morbiditeit en mortaliteit onder individue wat tipe 2 Diabetes ontwikkel het, waar miokardiale insulien weerstanigheid (IW) ‘n belangrike rol speel. Swak lewenstylkeuses en dieetgewoontes soos byvoorbeeld verhoogde suikerversoete drankies (SVDs) inname ‘n ‘n sleutel bydraende faktor vir die wêreld epidemie, vetsugtugheid, Diabetes en hartsiektes. Die onderliggende meganismes waarby SVDs die aanvang van kardio-metaboliese komplikasies aandryf bly steeds onduidelik. Vir die huidige studie is ons hipotese dat langtermyn SVD inname, afstroom glukose metaboliese weë met fisiologies-skadelike effekte sal ontlok met ongewensde uitkomste. Ons stel spesifiek voor dat die verhoogde glukose beskikbaarheid (a.g.v. SVD inname) die nie-oksidatiewe glukose weë (NOGW) aktiveer, i.e. poliolweg, heksosamienbiosintetiese weg (HBP), gevorderde glukeringseindprodukte (GGE), en PKC aktivering wat op sy beurt tot kardiometaboliese komplikasies bydra.

Metodologie – Manlike Wistar rotte (~200 g) is daagliks met 3-5.1 mL van ‘n bekende lokale SVD vir ‘n periode van ses maande deur middel van orale toegediening gevoed. Ons het dieetgedrag en fenotipiese veranderinge gemonitor op ‘n weeklikse basis en ook sistemiese (vastende) trigliseried, cholesterol en glukose vlakke op verskeie tydspunte gedurende die ses maande toetsperiode gemonitor. Verder het ons ‘n orale glukose toleransie toets (OGTT) twee-weekliks uitgevoer en ook die algehele gewigstoename en orgaanweefselmassa gemonitor. Miokardiale NOGWs is met behulp van kommersiëel beskikbare toetse en deur middel van Westerse blottegnieke bepaal.

Resultate – Ons data het na ses maande aangedui dat daar minimale makroskopiese veranderinge tussen die verskillende soda groepe waargeneem is. Dit kan ‘n relatiewe vroeë stadium, in terme van SSB-gemediëerde kardiometaboliese komplikasies is. Verder het ons verskeie biochemiese veranderinge waargeneem met uitsluitlike kenmerke vir die Jive® groep vergeleke met die Coca Cola® en Coke Light® groepe. Hier het Jive® gebruik vir ses maande in vroeë tekens van kardiale en skeletspierhipertrofie gelei – tesame met verhoogde lewermassa en versteurde adiposietultrastruktuur. Ons het ook vasgestel dat die meerderheid van die miokardiale NOGWs geaktiveer was en dat dit mag

bydra tot die veranderinge wat reeds gevind is met die aanvang van toekomstige komplikasies. Die Coca Cola® en Coke Light® groepe het wysigings in lewermassa en adiposietultrastruktuur getoon met laer glukose opruiming na ses maande wat moontlik die aanvang van insulienweerstandigheid kan voorstel. Hierdie data toon duidelik aan dat die HBP ‘n unversiele weg is wat geaktiveer word in al die soda groepe, met potensiële langtermyn newe effekte.

Gevolgtrekking – Hierdie studie het daarin geslaag om ‘n sukesvolle nuwe *in vivo* rot model van ‘n chroniese SSB/ASB inname te vestig. Ons het ook bevind dat die SSB inname ‘n minimale makroskopiese wysigings teweeg bring en dat dit verskeie post prandiale veranderinge tesame met die induksie van verskeie miokardiale NOGWs tot gevolg bring. Dus, het die huidige studie getoon dat langtermyn SSB inname potensiëel skadelike metaboliese weë aktiveer en dat dit individue met verhoogde risiko vir kardiovaskulêre komplikasiese verhoog ten spyte van ‘n gesonde fenotipe.

Acknowledgements

I thank God for giving me the talent and ability to have come this far. All the glory goes to Him.

I would like to express my gratitude to the following persons for their contributions to me personally and this project:

My supervisor and mentor, Professor M. Faadiel Essop. You are truly such an inspiration, not only to me and the department, but also the whole scientific community. I would like to thank you for your leadership and support. Thank you for all the patience, guidance and believing in me as I developed my scientific skills. Thank you for all the work you have put in into making me not only scientifically minded, but also developing my creative side. I can only hope to one day be as good a sculptor as you.

I would also like to thank all the people in the physiology department (my second home). Without your support the experience would not have been the same. I would like to extend a special thank you to Theo and Grazelda for all their help and administrative input behind the scenes.

Thank you to the CMRG group for the friendships, assistance and intellectual discussion during our early morning meetings. Thank you for all the laughter and great times together.

I would also like to extend my gratitude to Lydia for all her help, not only in the laboratories, but also as a mentor and advisor.

A special thanks to Danzil and Rudo for all their help with the animals, experiments and most importantly for helping to edit this thesis. Thank you for adding laughter to my life and making my days interesting.

I would like thank Marna for all the heated discussions and debates during our much needed coffee breaks and dinner dates. Thank you for always listening to me and being there when I needed encouragement during the past six years.

Most importantly thank you to my family for all their prayers and support throughout the years and encouraging my dreams and aspirations. I would not be where I am today without your love.

Table of Content

List of Figures

List of Tables

List of Abbreviations

ADP	Adenosine diphosphate
AGE	Advanced glycation end-product
ANOVA	One-way analysis of variance
ANP	Atrial natriuretic peptide
AR	Aldose reductase
ASB	Artificially sweetened beverages
ATP	Adenosine triphosphate
BMI	Body mass index
BNP	B-type natriuretic peptide
CI	Confidence intervals
COA and CO-Q	Coenzyme A and Coenzyme Q
CPT-1	Carnitine palmitoyltransferase 1
CuZnSOD	*C*opper-zinc superoxide dismutase
CV	Cardiovascular
CVD	Cardiovascular diseases
DAG	*Diacylglycerol*
ddH_2O	Distilled water
DNA	*Deoxyribonucleic acid*
e^-	*Electrons*
EcSOD	*E*xtracellular dismutase
eNOS	Endothelial nitric oxide synthase
ETC	Electron transport chain
F-3-P	Fructose-3-phosphate
F-6-P	Fructose-6-phosphate
FA	Fatty acid
$FADH_2$	Flavin adenine dinucleotide reduced
FAT	Fatty acid translocase
FFA	Free fatty acids
G-3-P	Glucose-3-phosphate
GAPDH	Glyceraldehyde-3-phosphate dehydrogenase
GFAT	Glutamine: fructose-6 phosphate amidotransferase

GLUT4	Glucose transporter four
GLUT5	Glucose transporter five
GSH	Glutathione
GSSG	Glutathione disulfide
H_2O_2	Hydrogen peroxide
HBP	Hexosamine biosynthetic pathway
HFCS	high fructose corn syrups
HOMA	homeostatic model assessment
HR	Hazard rates
IDF	International Diabetes Federation
IGT	Impaired glucose tolerance
IR	Insulin resistance
IRS	Insulin receptor substrate
MG	Methylglyoxal
MnSOD	Manganese superoxide dismutase
NADH	Nicotinamide adenine dinucleotide reduced
NFκB	*Nuclear factor kappa b*
NHLS	National Health Laboratory Service
NO	Nitric oxide
NOGP	Non-oxidative glucose pathways
NOX	NADPH oxidase
$O_2^{\bullet}$	Superoxide
OGA	N-acetylglucosaminidase
O-GlcNAc	*O*-linked N-acetyl glucosamine
OGT	*O*-linked GlcNAc transferase
OGTT	Oral glucose tolerance tests
OH	Hydroxide
PARP	Poly adenosine diphosphate ribose polymerase
PDH	Pyruvate dehydrogenase
PI(3)K	*P*hosphatidylinositol-3-OH kinase
PKC	Protein kinase C
PMSF	Phenylmethylsulfonyl fluoride
RAGE	AGE receptor
ROS	Reactive oxygen species

SA	South Africa
SBTI	Soyabean Trypsin inhibitor
SDH	Sorbitol dehydrogenase
SEM	Standard error of the mean
SOD	Superoxide dismutase
SSB	sugar sweetened beverage
SSBs	sugar sweetened beverages
T2D	Type 2 diabetes
TCA	Tricarboxylic acid cycle
UDP	Uridine diphosphate
UDP-GlcNAc	Uridine diphosphate-N-acetyl glucosamine
USA	The United States of America
WHO	World Health Organization

Units of Measurement

%	percent/percentage
~	approximately
°C	degrees Celsius
µg	microgram
µg/ml	microgram per millilitres
µL	microliter
µm	micrometre
μm^2	micrometre squared
AU	arbitrary units
g	grams
g/kg	grams per kilogram
g/L	grams per litre
kg	kilograms
kg/m^2	kilograms per meter squared
L	litre
M	molar
mA	milliamps
mg	milligrams
min	minutes
ml	millilitres
mM	millimolar
mmol/L	millimoles per litre
MW	molecular weight
n	number

ng	nanograms
ng/µg	nanograms per microgram
nm	nanometres
V	volts
w/v	weight per volume

Chapter 1

Perspective

1.1 Defining Diabetes

The term Diabetes Mellitus describes a metabolic disorder with numerous defects characterized by chronic hyperglycemia and the disturbances of carbohydrate, fat and protein metabolism, thus resulting in impaired insulin secretion and/or action. Diabetes may be classified into two categories, i.e. Type 1 Diabetes - the inability to produce little or no insulin which is usually genetically inherited; and Type 2 Diabetes (T2D) - the ability to produce insulin but with a lack of insulin effects (due to insulin resistance and/or β-cell dysfunction) that is often accompanied by obesity and poor lifestyle choices (Alberti and Zimmet, 1998). Persons can be placed into three groups with regards to Diabetes classifications: 1) non-diabetic, 2) pre-diabetic (impaired glucose tolerance [IGT] or impaired fasting glucose) and 3) diabetic. Each category has its own range of glycemic levels used in order to classify individuals with different stages of Diabetes (The Diabetes Forum, [s.a.]) as shown in Table 1.1.

Each stage of Diabetes also comes with a broad range of pathogenic complications. Such complications typically include long-term damage, dysfunction and failure of various organs as well as progressive development of distinct tissue-related complications. For example, individuals with Diabetes are at an increased risk of developing cardiovascular, peripheral vascular and cerebrovascular diseases. Several pathogenic processes are involved in the onset of Diabetes; these include processes that damage pancreatic β-cells with the eventual onset of insulin deficiency, while others can result in resistance of target cells to insulin action. The abnormalities of carbohydrate, fat and protein metabolism are due to deficient action(s) of insulin on target tissues resulting from insensitivity or lack of insulin (Alberti and Zimmet, 1998). Of concern, such damaging effects of Diabetes are now rapidly becoming a global pandemic.

Table 1.1: Values for diagnosing Diabetes Mellitus and other classes of hyperglycemia (adapted from: The Diabetes Forum, [s.a.], adapted from The International Diabetes Federation [IDF]).

Target Levels by Type	Fasting (pre-prandial)	2 hours after meals (postprandial)
Non-diabetic	4.0 to 5.9 mmol/L	under 7.8 mmol/L
Pre-diabetic	6.0 to 6.9 mmol/L	under 7.9 to 11.1 mmol/L
Type 1 Diabetes	> 7 mmol/L	under 9 mmol/L
Type 2 Diabetes	> 7 mmol/L	under 8.5 mmol/L

1.2 Global Diabetes prevalence

T2D is recognized as a public health pandemic with the rise in incidence becoming more alarming than predicted (Boyle *et al*., 2001). According to the World Health Organization (WHO) the prevalence for persons living with Diabetes has shifted from ~135 million in 1998 to ~171 million in the year 2000; with estimates indicating that this number will continue to rise to ~366 million by 2030 (Bradshaw *et al*., 2007) - Figure1.1 indicates the prevalence of Diabetes worldwide and the predicted values for 2030. The reasons for this are multi-factorial but key drivers for the increased prevalence include growing populations, urbanization and most importantly an increase in physical inactivity together with the increased consumption of unhealthy diets (Wild *et al*., 2004). This rising prevalence is in turn a central contributor to morbidity and premature mortality, both in developed and developing countries (Levitt *et al*., 1999).

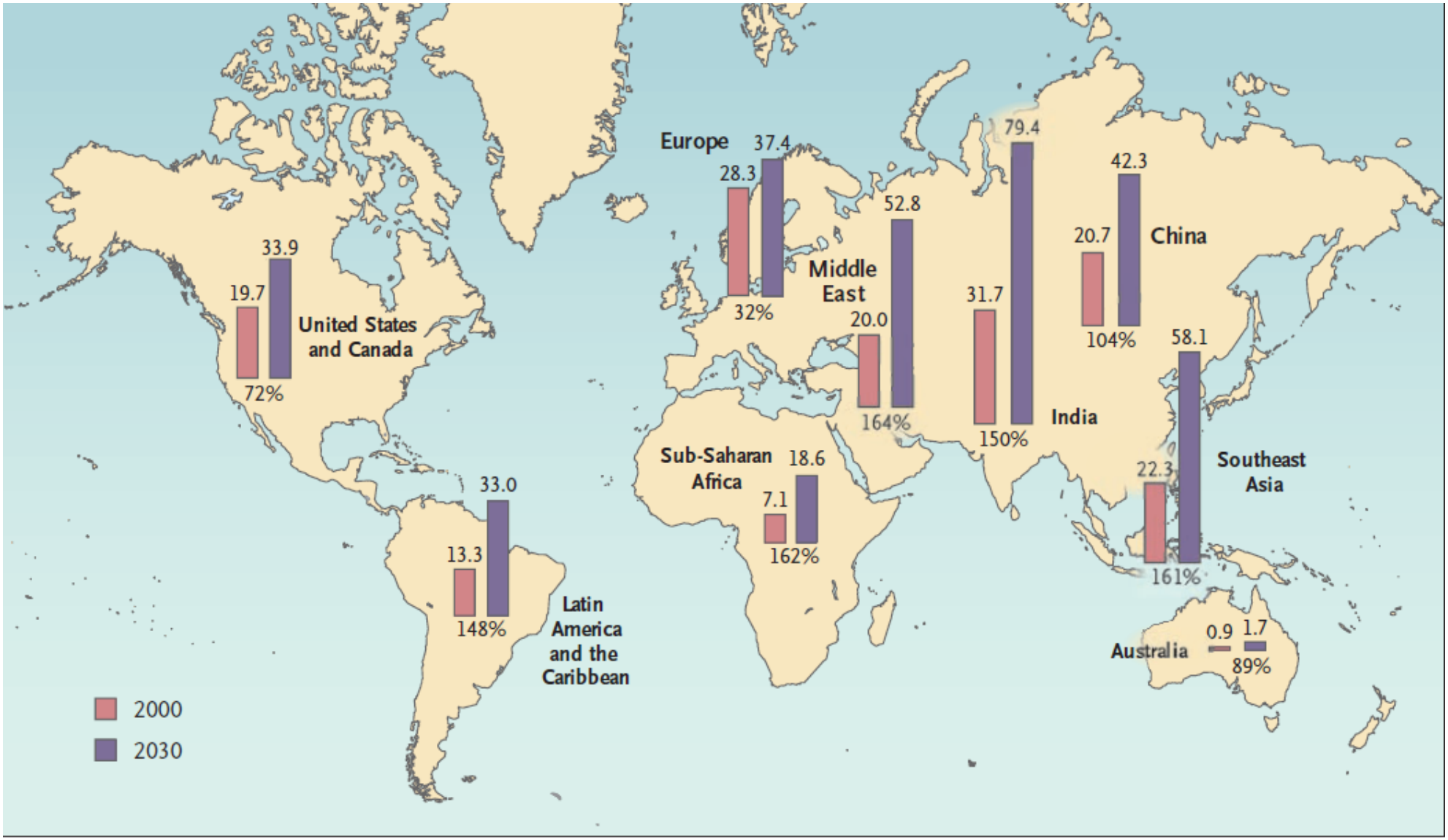

Figure 1.1: A schematic representation of the diabetic prevalence in 2000 and the predicted values for 2030 worldwide. Numbers are presented in millions and calculated percentages are included (Hossain *et al*., 2007).

1.3 Diabetes in developing nations

As developing countries grow and their economies expand, non-communicable diseases such as Diabetes will become more prevalent largely because of the adoption of a so-called 'Western' lifestyle and its accompanying risk factors (Wild *et al*., 2004). As discussed, most of the increase in Diabetes prevalence will occur in developing countries that are also strongly linked with growing urbanization (Bradshaw *et al*., 2007; Guariguata *et al*., 2014). Such countries fall within the following continents; Asia, some countries in Europe, South America and sub-Saharan Africa (discussed by Prentice, 2006). Although Diabetes Mellitus was initially considered to be rare in sub-Saharan Africa this has dramatically changed with it now emerging as a significant medical concern within such a developing continent (Motala *et al*., 2003).

The burden of T2D in South Africa (SA) is excessively high compared to the rest of the African continent, with the prevalence expected to rise to ~ 1.6 million by 2030 (Shaw *et al*., 2010). Furthermore, Diabetes is the seventh most common cause of mortality in SA and several studies suggest that high blood glucose levels can increase cardiovascular mortalities and thus further fuel the overall burden of disease. This increase in diabetic incidence in the SA population is closely linked with urbanization together with sedentary lifestyle choices and unhealthy dietary behavior (Bradshaw *et al*., 2007). Here T2D is also closely associated with obesity (poor lifestyle and genetic influences) and cardiovascular complications. Alarmingly, the number of obese individuals has increased in relatively "health conscious'' nations , therefore making it one of the most important contributors to T2D onset (Seidell, 2000).

1.4 The associated risk factors of Diabetes

"Obesity has emerged as one of the greatest health challenges of the 21st century" (Caprio, 2012). Worldwide obesity is fast becoming a problem of epidemic proportions and with it increasing risks of premature death. For example, the WHO estimated that ~700 million persons will be obese by the year 2015 (Malik *et al*., 2010) and this will increase the risk of developing T2D and cardiovascular disorders. Intriguingly, such risks may in some cases present in individuals with normal body mass index (BMI) ranges (Van Gaal *et al*., 2006). Studies have described an inverse relationship between obesity and heart failure which is

referred to as the 'obesity-mortality paradox' (Ahima and Lazar, 2013). For example, studies done by Flegal *et al*. (2013b) showed that obesity alone was not associated with higher mortality compared to normal weight (BMI 18 to less than 25 kg/m^2) individuals.

Obesity can manifest as a result of a variety of factors, e.g. physical inactivity, inadequate nutrient intake, sedentary lifestyles, as well as genetic factors. Obese individuals are at an increased risk for developing T2D and related cardiovascular diseases (CVD). Insulin resistance (IR) has emerged as an important mechanism that may play a role in the development of such conditions.

IR can be defined as a condition where the body is unable to respond to physiological concentrations of insulin resulting in impaired glucose utilization. Obesity itself also exacerbates the degree of IR and these factors are associated with cardiovascular risk factors such as hypertension, dyslipidemia and development of the metabolic syndrome (leads to the development of T2D and CVD). For cardiovascular tissues, IR can have a multi-faceted effect and lead to the inhibition of a variety of metabolic pathways which can further decrease glucose uptake and ultimately impede normal cardiac function (Van Gaal *et al*., 2006).

Obesity and IR can contribute to progressive damage to the vasculature and result in endothelial dysfunction (Caballero, 2003). Endothelial dysfunction can be described as partial or complete loss of stability between vasodilators and vasoconstrictors (Caballero, 2003); therefore, endothelial dysfunction may contribute to the development of contractile dysfunction and micro-vascular complications in Diabetes. One of the proposed mechanisms linking obesity and IR is the pathogenic effect of oxidative stress and subsequent endothelial dysfunction (Van Gaal *et al*., 2006). However, such mechanisms are complex and pathways often cross-talk between each other. The collaborate effects of such risk factors (IR, obesity and T2D) play a role in the onset of CVD (Figure 1.2). It is important to note that many factors play a role in developing CVD i.e. genetics, therefore, Figure 1.2 is a simplified schematic representation of disease onset.

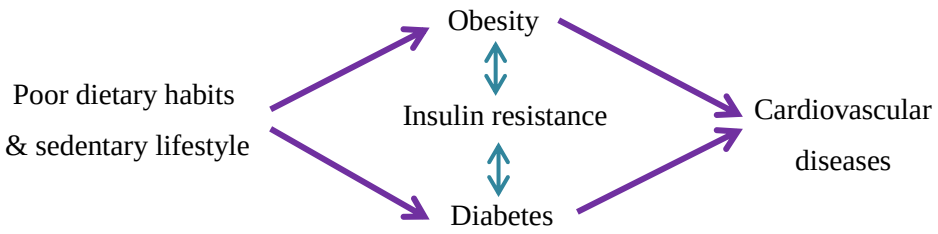

Figure 1.2: A schematic representation of cross-talk between complex mechanisms leading to CVD onset.

In 2005, the WHO estimated that there will be ~20 million CVD deaths in 2015, accounting for ~30% of all mortalities worldwide. Researchers have projected that by 2030 non-communicable diseases will constitute for more than three-quarters of deaths worldwide. Here CVD alone will be responsible for more deaths in developing countries than infectious diseases, including HIV/AIDS and tuberculosis (WHO, 2005). Thus, CVD is the leading contributor to global mortality - Figure 1.3 alerts to the number of global mortalities due to CVD (WHO, 2008). CVD onset can be attributed to a multitude of factors that generally overlap with what was discussed so far in this chapter. One of these factors includes urbanization or 'Westernization' which will now be discussed in more detail.

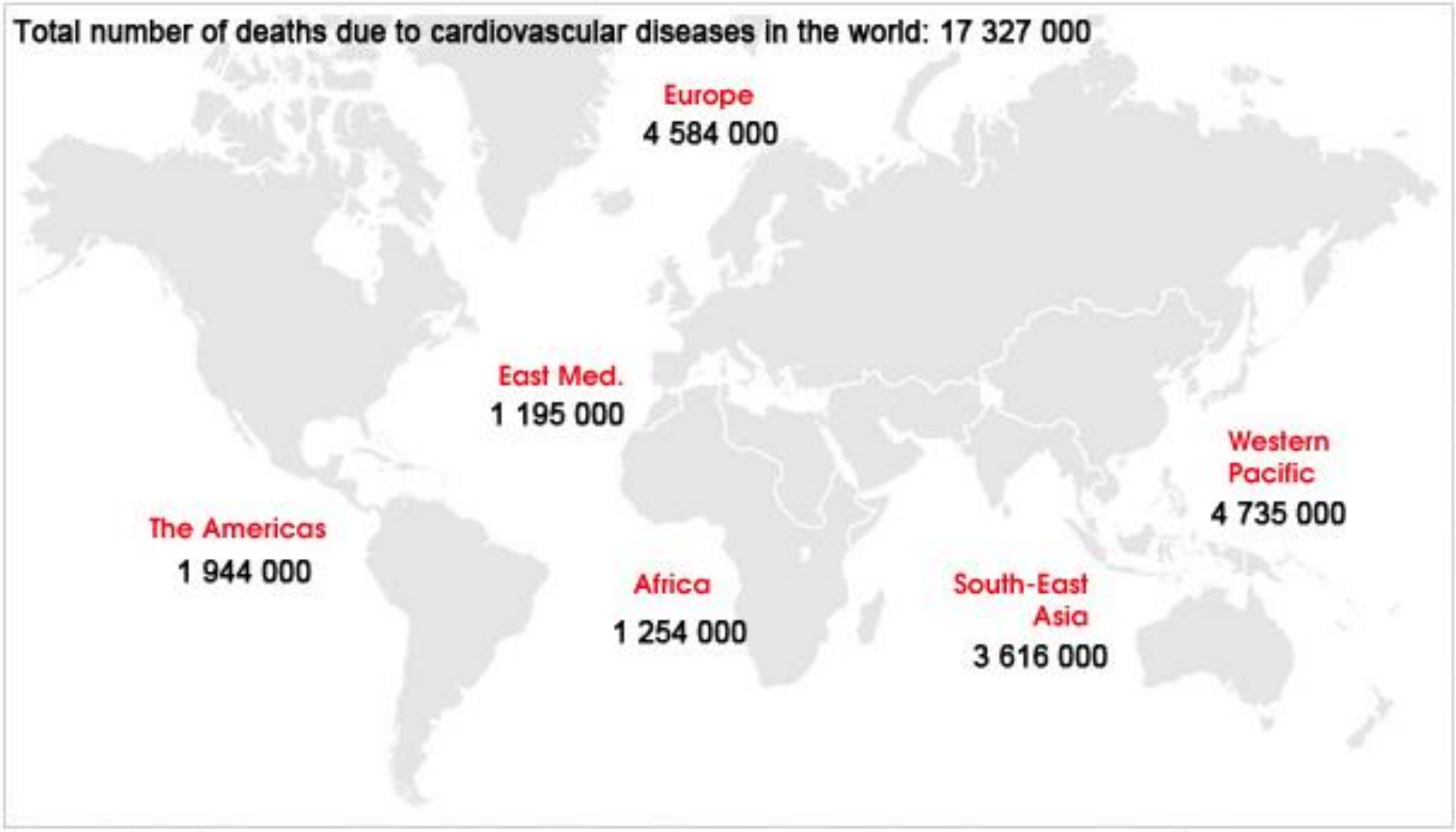

Figure 1.3: The total number of deaths due to CVD worldwide (WHO, 2008).

1.5 The 'Western' influence on Diabetes

T2D and obesity arise from related lifestyle-dependent risk factors, including poor dietary habits and lack of physical activity. Furthermore, with increased urbanization these risk factors are becoming more common in developing nations (Danaei *et al*., 2013). Dietary behavior and specific food content (such as sugar-sweetened beverages [SSB]) are associated with CVD and T2D with detrimental outcomes, for example, hypertension, obesity, hyperglycemia and insulin resistance (He *et al*., 2013; Mozaffarian *et al*., 2011; Sacks *et al*., 2009).

Investigating dietary patterns and food consumption offers an added dimension where one can assess the relationship between dietary behavior and disease risk/development (Fung *et al*., 2001). For example, in recent times more individuals are ingesting increased amounts of fats and refined carbohydrates that typically accompany decreased physical activity to constitute the more commonly referred to 'Western' diet or lifestyle. This shift in dietary behavior is not only observed in developed countries, but is rapidly becoming more frequent in developing nations (Popkin, 2001). The so-called 'Western' diet is also closely linked to higher caloric intake by increased SSB consumption (the focus of this research project) (Fung *et al*., 2001; Welsh *et al*., 2011).

1.6 Sugar-sweetened beverages in the Western diet

1.6.1 Classification of sugar-sweetened beverages

Soda beverages can be classified into two categories, i.e. caloric sweeteners which include sucrose- and fructose-sweetened beverages (SSBs), and non-caloric sweetened beverages which include those that are sweetened with artificial sweeteners (ASB) such as aspartame (Bray *et al*., 2004). Several studies have been conducted in order to elucidate the effects of these beverages on the body, which will be discussed in more detail below.

1.6.2 The effects of consuming sugar-sweetened beverages

There has been a sharp increase in the global consumption of caloric beverages in the last few decades (Brownell *et al*., 2009). Numerous adverse effects and disease risk factors arise due to SSB consumption (De Ruyter *et al*., 2012) as the body does not compensate for the excess calories consumed. Here detrimental outcomes may include weight gain, fatty liver disease, T2D and cardio-metabolic changes (De Ruyter *et al*., 2012; Popkin, 2012). In addition, SSB intake may not trigger the satiety response and this may be an important link between elevated liquid calories and increased health risk. Studies have linked the ingestion of SSBs to numerous risk factors which may lead to the development of CVD. These factors include increased visceral deposition, elevated triglyceride and cholesterol metabolites, and an increase in body weight (or BMI) (De Ruyter *et al*., 2012; Ebbeling *et al*., 2012; Malik *et al*., 2010).

One of the world's most popular SSBs is Coca Cola®. Here the main ingredient present is high fructose corn syrup (HFCS) which is made up of ~50% sucrose and ~50% fructose. In addition, the majority of processed foods also contain HFCS as a main ingredient. As HFCS is much sweeter than table sugar, this constitutes a major reason for its popularity within the food industry (Raatz *et al*., 2014). Fructose and glucose not only differs in taste but is also absorbed differently in the gastrointestinal tract.

Both glucose and fructose are absorbed in the small intestine, however, glucose is taken up through GLUT 4 transporters and fructose trough GLUT 5 transporters. Fructose does not induce the same insulin response as glucose due to there being very little GLUT 5 transporters in the pancreas (Johnson *et al*., 2013).

Evidence suggests that fructose may be a key factor at play with high SSB intake. It is found in approximately equal amounts in corn syrup compared to sucrose and other sugar forms that are present in SSBs. In fact, fructose alone elicited detrimental effects on blood pressure, visceral fat deposition, weight gain and IR (Caprio, 2012; Popkin, 2012). The mechanisms that contribute to the associated risk factors for IR, obesity and T2D may include an incomplete reduction in energy intake after consumption of SSBs and glycemic effects with rapid spikes in blood glucose levels (hyperglycemia) and insulin concentrations (Fagherazzi *et al*., 2013; Qi *et al*., 2012).

Although few studies have investigated the relationship between SSB consumption and the onset of associated diseases, the evidence suggests a link between SSBs and weight gain, CVD and T2D (Qi *et al*., 2012) (refer to Figure 1.4). The consumption of various carbohydrate forms (sugars and HFCS) contribute to high dietary glycemic load, inflammation and IR- irrespective of obesity (Ludwig, 2002). Moreover, the consumption of both SSBs and ASBs lead to a dramatic increase in blood glucose and insulin concentrations (Anton *et al*., 2010; Fagherazzi *et al*., 2013; Malik *et al*., 2010), that can directly impede hepatic insulin signaling and thereby promote IR (Swarbrick *et al*., 2008). However, despite advances in this field there is - to our knowledge - no clear molecular mechanisms that have been proposed to describe the association between the consumption of SSB, increased hyperglycemia and the onset of T2D and CVD.

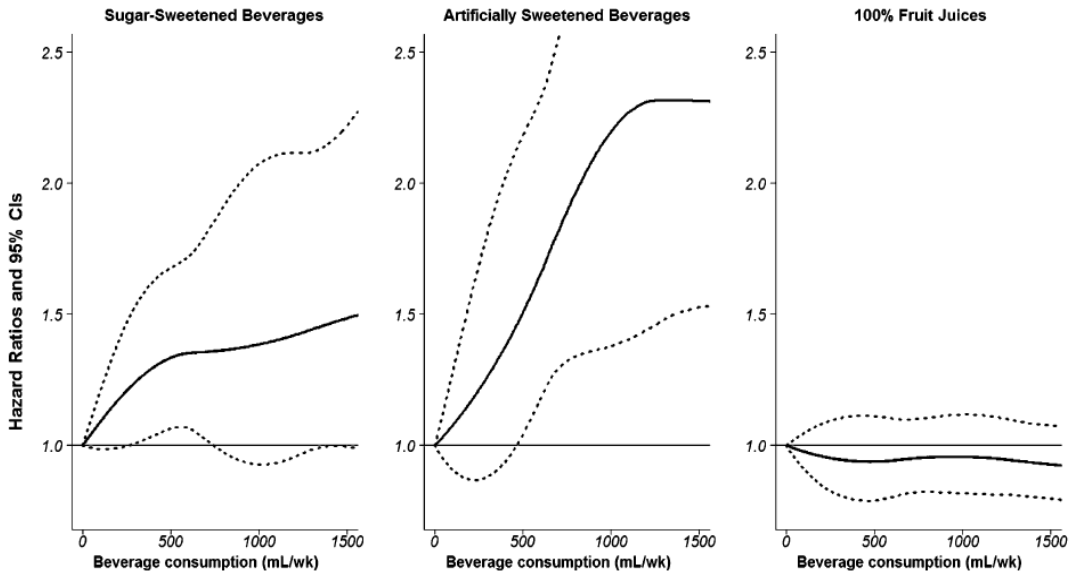

Figure 1.4: The risk evaluation of developing Type 2 Diabetes with the consumption of sugary-sweetened beverages, artificially sweetened beverages and fruit juices.
Solid lines correspond to hazard ratios (HR) and the dotted lines correlate to the 95% confidence intervals (CI) (adapted from Fagherazzi *et al*., 2013).

1.7 Problem statement

To summarize, metabolic dysfunction triggered by SSB consumption plays an important role in causing various lifestyle diseases and thus contributing to the overall health care burden (morbidity and mortality). However, the underlying molecular mechanisms are poorly understood and require urgent investigation.

With developing countries such as SA becoming increasingly 'Westernized', there is already evidence of greater manifestation of obesity and associated complications such as T2D and CVD. As discussed, this rise can be attributed to sedentary lifestyles, poor dietary habits and increased caloric intake from SSBs. This study was therefore initiated to begin to explore this intriguing question in order to gain novel mechanistic insights. Our laboratory proposes that acute hyperglycemic episodes may be present with the early onset of Diabetes or as a result of high glycemic dietary intake (Joseph *et al*., 2014). For this study, we propose that hyperglycemic episodes due to SSB intake will elicit downstream effects that will lead to the perturbation of specific metabolic pathways (of non-oxidative glucose metabolism) in the heart. We employed a novel approach to assess such mechanisms by establishing – for the first time as far as we are aware - an *in vivo* rat model of long-term SSB consumption.

This chapter summarized the global pandemic of T2D and CVD with specific focus on the consumption of SSBs in developing countries. Chapter 2 will deal with cardio-metabolism under normal physiological conditions, and thereafter Chapter 3 with focus on metabolic derangement in the myocardium.

References

1. Ahima, R. S., & Lazar, M. A. (2013). Physiology. The health risk of obesity-better metrics imperative. *Science (New York, N.Y.)*, *341*(6148), 856–8.

2. Alberti, K. G. M. M., & Zimmet, P. Z. (1998). Definition, Diagnosis and Classification of Diabetes Mellitus and its Complications Part 1 : Diagnosis and Classification of Diabetes Mellitus Provisional Report of a WHO Consultation. *Diabetic Medicine*, *15*, 539–553.

3. Anton, S. D., Martin, C. K., Han, H., Coulon, S., Cefalu, W. T., Geiselman, P., & Williamson, D. A. (2010). Effects of stevia, aspartame, and sucrose on food intake, satiety, and postprandial glucose and insulin levels. *Appetite*, *55*(1), 37–43.

4. Boyle, J. P., Honeycutt, A. A., Narayan, K. M., Hoerger, T. J., Geiss, L. S., Chen, H., & Thompson, T. J. (2001). Projection of Diabetes burden through 2050: impact of changing demography and disease prevalence in the U.S. *Diabetes Care*, *24*(11), 1936–40.

5. Bradshaw, D., Norman, R., Pieterse, D., & Levitt, N. (2007). Estimating the burden of disease attributable to Diabetes in South Africa in 2000. *South African MEdical Journal*, *97*(7), 700–706.

6. Bray, G. A., Nielsen, S. J., & Popkin, B. M. (2004). Consumption of high-fructose corn syrup in beverages may play a role in the epidemic of obesity. *Am J Clin Nutr*, *79*(4), 537–543.

7. Brownell, K. D., Farley, T., Willett, W. C., Popkin, B. M., Chaloupka, F. J., Thompson, J. W., & Ludwig, D. S. (2009). The public health and economic benefits of taxing sugar-sweetened beverages. *The New England Journal of Medicine*, *361*(16), 1599–605.

8. Caballero, A. E. (2003). Endothelial dysfunction in obesity and insulin resistance: a road to Diabetes and heart disease. *Obesity Research*, *11*(11), 1278–89.

9. Caprio, S. (2012). Calories from soft drinks-do they matter? *The New England Journal of Medicine*, *367*(15), 1462–3.

10. Danaei, G., Singh, G. M., Paciorek, C. J., Lin, J. K., Cowan, M. J., Finucane, M. M., & Ezzati, M. (2013). The global cardiovascular risk transition: associations of four metabolic risk factors with national income, urbanization, and Western diet in 1980 and 2008. *Circulation*, *127*(14), 1493–502,

11. De Ruyter, J. C., Olthof, M. R., Seidell, J. C., & Katan, M. B. (2012). A trial of sugar-free or sugar-sweetened beverages and body weight in children. *The New England Journal of Medicine*, *367*(15), 1397–406.

12. Ebbeling, C. B., Feldman, H. A, Chomitz, V. R., Antonelli, T. A, Gortmaker, S. L., Osganian, S. K., & Ludwig, D. S. (2012). A randomized trial of sugar-sweetened beverages and adolescent body weight. *The New England Journal of Medicine*, *367*(15), 1407–16.

13. Fagherazzi, G., Vilier, A., Sartorelli, D. S., Lajous, M., & Balkau, B. (2013). Consumption of artificially and sugar-sweetened beverages and ´ miologique aupre ` s des incident type 2 Diabetes in the Etude Epide ´ ne ´ rale de l ' Education Nationale – European femmes de la Mutuelle Ge Prospective Investigation into Cancer and Nutri, (1), 517–523.

14. Flegal, K. M., Kit, B. K., & Graubard, B. I. (2013b). Overweight, obesity, and all-cause mortality-reply. *JAMA*, *309*(16), 1681–2.

15. Fung, T. T., Rimm, E. B., Spiegelman, D., Rifai, N., Tofler, G. H., Willett, W. C., & Hu, F. B. (2001). Association between dietary patterns and plasma biomarkers of obesity and cardiovascular disease risk. *The American Journal of Clinical Nutrition*, *73*(1), 61–7.

16. Guariguata, L., Whiting, D. R., Hambleton, I., Beagley, J., Linnenkamp, U., & Shaw, J. E. (2014). Global estimates of Diabetes prevalence for 2013 and projections for 2035. *Diabetes Research and Clinical Practice*, *103*(2), 137–49.

17. He, F. J., Li, J., & Macgregor, G. A. (2013). Effect of longer term modest salt reduction on blood pressure : Cochrane systematic review and meta-analysis of randomised trials, *1325*(April), 1–15.

18. Hossain, P., Kawar, B., & Nahas, M. (2007). Obesity and Diabetes in the Developing World — A Growing Challenge. *New England Journal of Medicine*, *356*(3), 213–215.

19. Joseph, D., Kimar, C., Symington, B., Milne, R., & Essop, M. F. (2014). The detrimental effects of acute hyperglycemia on myocardial glucose uptake. *Life Sciences*, *105*(1-2), 31–42.

20. Levitt, N. S., Steyn, K., Lambert, E. V., Reagon, G., Lombard, C. J., Fourie, J. M., & Hoffman, M. (1999). Modifiable risk factors for Type 2 Diabetes Mellitus in a peri-urban community in South Africa. *Diabetic Medicine*, *16*(11), 946–950.

21. Ludwig, D. S. (2002). The Glycemic Index Physiological Mechanisms Relating to Obesity, Diabetes, and Cardiovascular Disease. *Journal American Medical Association*, *287*(18), 2414–2423.

22. Malik, V. S., Popkin, B. M., Bray, G. A, Després, J.-P., & Hu, F. B. (2010). Sugar-sweetened beverages, obesity, type 2 Diabetes Mellitus, and cardiovascular disease risk. *Circulation*, *121*(11), 1356–64.

23. Motala, A. A., Omar, M. A. K., & Pirie, F. J. (2003). Epidemiology of Type 1 and Type 2 Diabetes in Africa. *European Journal of Cardiovascular Prevention & Rehabilitation*, *10*(2), 77–83.

24. Mozaffarian, D., Hao, T., Rimm, E. B., Willett, W. C., & Hu, F. B. (2011). Changes in diet and lifestyle and long-term weight gain in women and men. *The New England Journal of Medicine*, *364*(25), 2392–404

25. Prentice, A. M. (2006). The emerging epidemic of obesity in developing countries. *International Journal of Epidemiology*, *35*(1), 93–9.

26. Popkin, B. M. (2001). Symposium : Obesity in Developing Countries : Biological and Ecological Factors The Nutrition Transition and Obesity in the Developing World 1. *The Journal of Nutrition*, *131*, 871–873.

27. Popkin, B. M. (2012). Sugary beverages represent a threat to global health. *Trends in Endocrinology and Metabolism: TEM*, *23*(12), 591–3.

28. Qi, Q., Chu, A. Y., Kang, J. H., Jensen, M. K., Curhan, G. C., Pasquale, L. R., & Qi, L. (2012). Sugar-sweetened beverages and genetic risk of obesity. *The New England Journal of Medicine*, *367*(15), 1387–96.

29. Raatz, S., Beals, K., Johnson, L., & Picklo, M. (2014). Chronic intake of honey, sugar and high fructose corn syrup exert equivalent effects on glucose and insulin (1039.4). *FASEB J*, *28*(1_Supplement), 1039.4.

30. Sacks, F. M., Bray, G. A., Carey, V. J., Smith, S. R., Ryan, D. H., Anton, S. D., & Williamson, D. A. (2009). Comparison of weight-loss diets with different compositions of fat, protein, and carbohydrates. *The New England Journal of Medicine*, *360*(9), 859–73.

31. Seidell, J. C. (2000). Obesity, insulin resistance and Diabetes--a worldwide epidemic. *The British Journal of Nutrition*, *83 Suppl 1*(2000), S5–8.

32. Shaw, J. E., Sicree, R. A, & Zimmet, P. Z. (2010). Global estimates of the prevalence of Diabetes for 2010 and 2030. *Diabetes Research and Clinical Practice*, *87*(1), 4–14.

33. Swarbrick, M. M., Stanhope, K. L., Elliott, S. S., Graham, J. L., Krauss, R. M., Christiansen, M. P., & Havel, P. J. (2008). Consumption of fructose-sweetened beverages for 10 weeks increases postprandial triacylglycerol and apolipoprotein-B concentrations in overweight and obese women. *The British Journal of Nutrition*, *100*(5), 947–952.

34. The Diabetes Forum. Diabetes Digital Media Ltd- the global Diabetes community. Blood sugar level ranges. 2014. [s.a.] [Online]. Available: http://www.diabetes.co.uk/diabetes_care/blood-sugar-level-ranges.html [2014, September 20]

35. Van Gaal, L. F., Mertens, I. L., & De Block, C. E. (2006). Mechanisms linking obesity with cardiovascular disease. *Nature*, *444*(7121), 875–80.

36. Welsh, J. A, Sharma, A., Cunningham, S. A, & Vos, M. B. (2011). Consumption of added sugars and indicators of cardiovascular disease risk among US adolescents. *Circulation*, *123*(3), 249–57.

37. Wild, S., Roglic, G., King, H., Green, A & Sicree, R. (2004). Global Prevalence of Diabetes Estimates for the year 2000 and projections for 2030. *Diabetes Care*, *27*(5), 1047–1053.

38. WHO. Preventing chronic diseases: A vital investment. 2005. [S.a.] [Online]. Available: http://www.who.int/chp/chronic_disease_report/full_report.pdf [2014, September 20].

39. WHO causes of death 2008 summary tables. [s.a.] [Online]. Available: http://apps.who.int/gho/data/node.main.A865 [2014, September 21].

Chapter 2

Cardiac-metabolism and its dysregulation

2.1 Introduction

Mortality from cardiovascular complications is a common outcome for persons living with Diabetes. As Diabetes is a multifaceted disease, many factors play a role in its progression to cardiovascular complications such as heart failure and diabetic cardiomyopathy (Chavali *et al*., 2013). As outlined in Chapter 1, a number of detrimental consequences arise from poor lifestyle choices, therefore, confirming a robust link between metabolic perturbations and cardiac abnormalities. It is thus essential to understand the driving mechanisms which mediate the dysregulation of glycolysis in a hyperglycemic setting.

The surge in inactivity, poor lifestyle choices and greater liquid calorie consumption has added to the incidence of hyperglycemia (e.g. by increased postprandial spikes) (Fagherazzi *et al*., 2013). However, the role of SSBs and its effects on hyperglycemia remain poorly understood (Ludwig, 2002). Our laboratory's focus has been on hyperglycemia-mediated metabolic alterations and its role in the onset of cardio-metabolic complications (Joseph *et al*., 2014; Mapanga *et al*., 2012). For the current study we aimed to extend this hypothesis and our proposal is that hyperglycemia will be relevant within the context of chronic SSB consumption. In broad terms, the central hypothesis suggests that hyperglycemia is associated with the formation of reactive oxygen species (ROS) which play a central role in cardiac-metabolic derangements (Brownlee, 2005; Rubin *et al*., 2012). Such oxidative stress is linked with disrupted metabolic flux through the glycolytic pathway, that may increase flux through non-oxidative glucose pathways (NOGPs), thus leading to harmful vascular complications that are typically associated with Diabetes (Brownlee, 2005; Giaccari *et al*., 2009). However, these ideas have largely centered on chronically elevated hyperglycemia, whereas our laboratory's recent work focused on changes observed with short-term/acute hyperglycemia (Joseph *et al*., 2014)- interestingly, this hypothesis (that hyperglycemia leads to metabolic perturbations in the myocardium) remains true for both these conditions.

The focus of this study is therefore to investigate the overall effects of SSB consumption by establishing a novel in vivo rat model, with emphasis on the activation of NOGPs. Such research should therefore – in the longer term - provide more insight into mechanisms driving SSB-mediated onset of obesity, Diabetes and cardiovascular complications.

2.2 Cardiac-metabolism

2.2.1 Fuel substrates

As the heart has to nourish the entire body via the circulatory system, it has high energy demands to maintain contractile function and general homeostasis. The major energy production site of the heart is the mitochondrial electron transport chain (ETC) which generates adenosine triphosphate (ATP), the chemical energy source of myocardial cells. ATP can be generated by oxidative phosphorylation in the mitochondrial tricarboxylic acid (TCA) cycle. Here, energy inputs to drive mitochondrial oxidative phosphorylation are provided by transferred electrons from carbon-based fuel sources which generate reducing-equivalents, nicotinamide adenine dinucleotide reduced (NADH) and flavin adenine dinucleotide reduced ($FADH_2$). Both glucose and fatty acids (FAs) provide energy inputs in the form of reducing equivalents, although FA β-oxidation is the main fuel source of the normal mammalian heart (Stanley *et al*., 2005).

Under normal physiological conditions, the adult heart uses FA as its major fuel substrate i.e. approximately 60-90% of acetyl-CoA is formed as a result of FA β-oxidation and ~10-40% from pyruvate oxidation (*via* glycolysis). High FA oxidation rates inhibit glucose oxidation in the heart (reviewed by Fillmore and Lopaschuk, 2011; Gertz *et al*., 1988). The mechanism through which FA regulate/inhibits glucose utilization is referred to as the Randle cycle. This reaction occurs because the initial event, triggered by fatty acid oxidation, is an increase in the mitochondrial ratios of [acetyl-CoA]/[CoA] and [NADH]/[NAD^+], both of which inhibit pyruvate dehydrogenase (PDH) activity (a key enzyme which converts pyruvate into acetyl-CoA within the mitochondrion). Under these conditions, part of the glucose that is not oxidized is re-routed to glycogen formation (reviewed by Hue and Taegtmeyer, 2009) (refer to Figure 2.1).

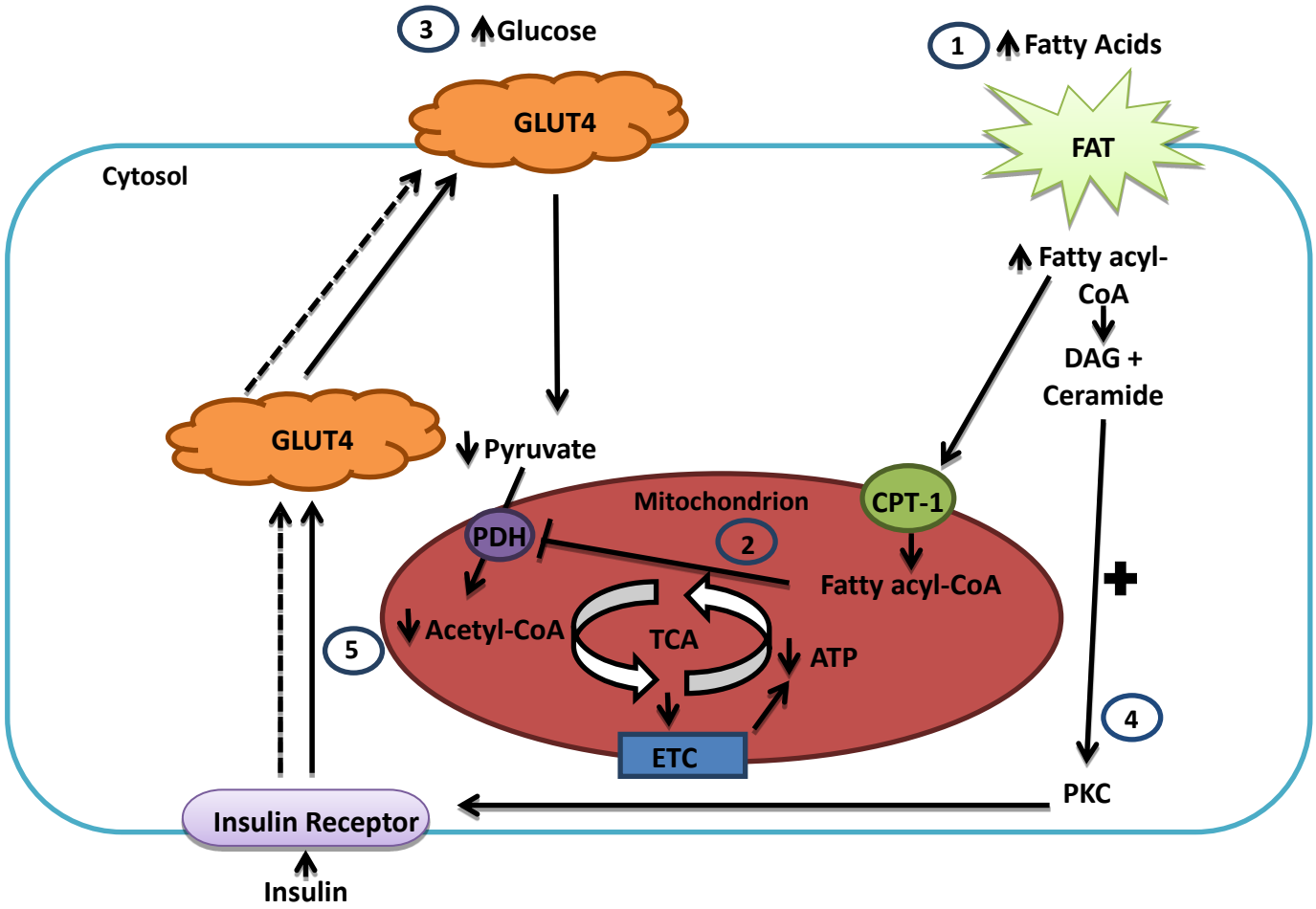

Figure 2.1: A schematic representation of the production of ATP in the myocardium. 1- Fatty acids are the main substrates utilized. 2- The production of fatty acyl-CoA inhibits the action of PDH in mitochondria. 3- With higher glucose availability (e.g. postprandially) it is utilized as the main fuel substrate. 4 and 5- With high FA availability, DAG can activate PKC, which reacts with insulin signaling subsequently interfering with GLUT4 membrane recruitment and increasing intracellular glucose concentrations.

Abbreviations: Glucose transporter four (GLUT4), fatty acid translocase (FAT), adenosine triphosphate (ATP), tricarboxylic acid cycle (TCA), electron transport chain (ETC) and carnitine palmitoyltransferase 1 (CPT-1).

FA can indirectly decrease the uptake of glucose by acting on the insulin signaling pathway. This occurs when FA enter into the cell and form diacylglycerol (DAG) and ceramides. DAG allows for the activation of PKC (which will be discussed later), which subsequently interferes with the insulin signaling pathway. The mechanisms behind this remain unclear, however, correlations have been made between decreased insulin activity and the activation of insulin receptor substrate (IRS) -associated phosphatidylinositol-3-OH kinase (PI(3)K) when PKC activity was elevated (Montell *et al*., 2001; Saltiel and Kahn, 2001). Although FA are the main fuel source of the normal mammalian heart, this may change according to circumstances, e.g. under hyperglycemic conditions when substrate utilization is altered. Thus glucose can become a major fuel substrate of the heart following a meal when its circulating levels robustly increase. In this instance, the myocardium is exposed to higher glucose availability (in circulation) and hence there is greater glucose uptake and increased utilization that is used to fuel ATP production (Bertrand *et al*., 2008).

The TCA cycle is fuelled by acetyl-CoA that may be derived from pyruvate decarboxylation and/or from FA β-oxidation. The latter results in the formation of reducing equivalents used for oxidative phosphorylation in the ETC. The TCA cycle can thus be considered to be the main mediator in cardiac energy supplies. As discussed, the heart can also alter fuel sources depending on substrate availability, oxidation rates and energy demands (Atkinson *et al*., 2002; King *et al*., 2005). Such alterations in the balance between FA and carbohydrates as energy sources can contribute to differing cardiac efficiency in producing ATP (Fillmore and Lopaschuk., 2011); e.g. greater glycolysis may serve as a cardio-protective mechanism during ischemia (versus increased FA utilization) since higher FA utilization can cause mitochondrial uncoupling and hence a loss of ATP production (Essop, 2007). An indirect result is decreased myocardial utilization of glucose and decreased protective glycolysis – due to the Randle cycle. Therefore, switching from FA to increased glycolysis during ischemic events may aid the heart as it can generate ATP in a more oxygen-efficient manner versus FA (Essop and Opie, 2004).

2.2.2 Glucose utilization

The major sources of glycolytic substrates are exogenous glucose and endogenous glycogen stores. Glycolysis can be stimulated by adrenergic stimulation, exercise and depleted ATP levels in the myocardium. Although glycogen has a high turnover rate, its availability is relatively small in the heart when compared to skeletal muscle (Hue *et al*., 1995; Stanley *et al*., 1992). Dietary carbohydrates therefore contribute largely to glucose availability in the myocardium – especially postprandially. Upon entry into the cell, glucose is rapidly converted to glucose-6-phosphate, which can then enter the glycolytic pathway. This phosphorylation is catalyzed by hexokinase-2 that effectively traps glucose-6-phosphate in the cell as it cannot penetrate the sarcolemma (Bouché *et al*., 2004). A series of phosphorylation and cleavage steps thereafter convert glucose-6-phosphate to pyruvate. An important glycolytic enzyme in the context of high glucose availability is glyceraldehyde-3-phosphate dehydrogenase (GAPDH) that will be discussed in further detail in Chapter 3. Net flux through glycolysis contributes to ~10% of the myocardial ATP production (Opie and Knuuti, 2009).

When pyruvate enters the mitochondrial matrix it is decarboxylated to form acetyl-CoA - PDH then converts pyruvate (irreversibly) to acetyl-CoA. Thus, the PDH complex is a vital mediator in glucose metabolism which couples glycolysis to oxidative phosphorylation (Randle, 1986; Vincent *et al*., 2004). PDH is regulated via many mechanisms, however, its regulation through increased FA oxidation inhibits glucose metabolism, as shown above in Figure 2.1 (Panchal *et al*., 2000). FAs lead to the inactivation of PDH which in turn increases citrate concentrations. This inhibits phosphofructokinase which is a key regulator in glycolysis. Therefore, intracellular glucose concentrations increases, resulting in decreased glucose uptake which may subsequently lead to IR (Shulman, 2000). When glycolytic flux increases the TCA cycle does so in parallel fashion, i.e. during hyperglycemic events flux is increased through the TCA cycle, as next discussed in further detail.

2.2.3 Tricarboxylic acid cycle and electron transport chain

Mitochondria are the “powerhouses” of the cell as it is the major site of ATP production. Cardiomyocytes are enriched with mitochondria to maintain its ATP requirements (Dobson and Himmelreich, 2002). After acetyl-CoA (from FA β–oxidation and glycolysis) is

converted to reducing equivalents, the latter is employed to produce ATP (Kavazis *et al*., 2009). The major products formed in the TCA cycle include NADH and FADH2 which are used as electron donors to form ATP in the ETC (Gibala *et al*., 2000). NADH and FADH2 can therefore be described as the link between the breakdown of fuel substrates and the conversion of this fuel into energy. Reducing equivalents generated by the TCA next move into the ETC where it is utilized for energy production.

The ETC is a complex composition of proteins located within the inner membrane of mitochondria - which includes complexes I, II, III, IV and ATP synthase (complex V). Such complexes transfer electrons from NADH and FADH2 to oxygen during the formation of ATP (Cecchini, 2003). Between complex II and III there is a mobile electron carrier, coenzyme Q or ubiquinone (Co-Q), which donates electrons to oxygen thus producing superoxide (O2•). This step plays a vital role in the formation of ROS and will be discussed in more detail in Chapter 3.

2.3 Summary

This chapter summarized myocardial metabolism under normal physiological conditions and briefly focused both on FA and carbohydrate metabolism - highlighting the most important aspects of glycolysis, the TCA cycle and the ETC. The next chapter will focus on metabolic derangements that can occur with hyperglycemia and subsequent pathogenic effects.

References

1. Atkinson, L. L., Fischer, M. A, & Lopaschuk, G. D. (2002). Leptin activates cardiac fatty acid oxidation independent of changes in the AMP-activated protein kinase-acetyl-CoA carboxylase-malonyl-CoA axis. *The Journal of Biological Chemistry*, *277*(33), 29424–30.

2. Bertrand, L., Horman, S., Beauloye, C., & Vanoverschelde, J.-L. (2008). Insulin signalling in the heart. *Cardiovascular Research*, *79*(2), 238–48.

3. Bouché, C., Serdy, S., Kahn, C. R., & Goldfine, A. B. (2004). The cellular fate of glucose and its relevance in type 2 Diabetes. *Endocrine Reviews*, *25*(5), 807–30.

4. Brownlee, M. (2005). The pathobiology of diabetic complications: a unifying mechanism. *Diabetes*, *54*(6), 1615–25.

5. Cecchini, G. (2003). Function and structure of complex II of the respiratory chain. *Annual Review of Biochemistry*, *72*, 77–109.

6. Chavali, V., Tyagi, S. C., & Mishra, P. K. (2013). Predictors and prevention of diabetic cardiomyopathy. *Diabetes, Metabolic Syndrome and Obesity : Targets and Therapy*, *6*, 151–60.

7. Dobson, G. P., & Himmelreich, U. (2002). Heart design: free ADP scales with absolute mitochondrial and myofibrillar volumes from mouse to human. *Biochimica et Biophysica Acta*, *1553*(3), 261–7.

8. Essop, M. F. (2007). Cardiac metabolic adaptations in response to chronic hypoxia. *The Journal of Physiology*, *584*(Pt 3), 715–26.

9. Essop, M. F., & Opie, L. H. (2004). Metabolic therapy for heart failure. *European Heart Journal*, *25*(20), 1765–8.

10. Fagherazzi, G., Vilier, A., Sartorelli, D. S., Lajous, M., & Balkau, B. (2013). Consumption of artificially and sugar-sweetened beverages and ´ miologique aupre ` s des incident type 2 Diabetes in the Etude Epide ´ ne ´ rale de l ' Education Nationale – European femmes de la Mutuelle Ge Prospective Investigation into Cancer and Nutri, (1), 517–523.

11. Fillmore, N and Lopaschuk, G, D. (2011). Impact of fatty acid oxidation on cardiac efficiency. *Heart and Metabolism*, *53*, 33–37.

12. Gertz, E. W., Wisneski, J. A, Stanley, W. C., & Neese, R. A. (1988). Myocardial substrate utilization during exercise in humans. Dual carbon-labeled carbohydrate isotope experiments. *The Journal of Clinical Investigation*, *82*(6), 2017–25.

13. Giaccari, A, Sorice, G., & Muscogiuri, G. (2009). Glucose toxicity: the leading actor in the pathogenesis and clinical history of type 2 Diabetes - mechanisms and potentials for treatment. *Nutrition, Metabolism, and Cardiovascular Diseases*, *19*(5), 365–77.

14. Gibala, M. J., Young, M. E., & Taegtmeyer, H. (2000). Anaplerosis of the citric acid cycle: role in energy metabolism of heart and skeletal muscle. *Acta Physiologica Scandinavica*, *168*(4), 657–65.

15. Hue, L., Depre, C., Lefebvre, V., Rider, M. H., & Veitch, K. (1995). Regulation of glucose metabolism in cardiac muscle. *Biochemical Society Transactions*, *23*(2), 311–4.

16. Hue, L., & Taegtmeyer, H. (2009). The Randle cycle revisited: a new head for an old hat. *American Journal of Physiology. Endocrinology and Metabolism*, *297*(3), E578–91.

17. Joseph, D., Kimar, C., Symington, B., Milne, R., & Essop, M. F. (2014). The detrimental effects of acute hyperglycemia on myocardial glucose uptake. *Life Sciences*, *105*(1-2), 31–42.

18. Kavazis, A. N., Alvarez, S., Talbert, E., Lee, Y., & Powers, S. K. (2009). Exercise training induces a cardioprotective phenotype and alterations in cardiac subsarcolemmal and intermyofibrillar mitochondrial proteins. *American Journal of Physiology. Heart and Circulatory Physiology*, *297*(1), H144–52.

19. King, K. L., Okere, I. C., Sharma, N., Dyck, J. R. B., Reszko, A. E., McElfresh, T. A., & Stanley, W. C. (2005). Regulation of cardiac malonyl-CoA content and fatty acid oxidation during increased cardiac power. *American Journal of Physiology. Heart and Circulatory Physiology*, *289*(3), H1033–7.

20. Ludwig, D. S. (2002). The Glycemic Index Physiological Mechanisms Relating to Obesity, Diabetes, and Cardiovascular Disease. *Journal American Medical Association*, *287*(18), 2414–2423.

21. Mapanga, R. F., Rajamani, U., Dlamini, N., Zungu-Edmondson, M., Kelly-Laubscher, R., Shafiullah, M., & Essop, M. F. (2012). Oleanolic acid: a novel cardioprotective agent that blunts hyperglycemia-induced contractile dysfunction. *PloS One*, *7*(10), e47322.

22. Montell, E., Turini, M., Marotta, M., Roberts, M., Noé, V., Ciudad, C. J., & Gómez-Foix, A, M. (2001). DAG accumulation from saturated fatty acids desensitizes insulin stimulation of glucose uptake in muscle cells. *American Journal of Physiology. Endocrinology and Metabolism*, *280*(2), E229–37.

23. Opie, L. H., & Knuuti, J. (2009). The adrenergic-fatty acid load in heart failure. *Journal of the American College of Cardiology*, *54*(18), 1637–46.

24. Panchal, A. R., Comte, B., Huang, H., Kerwin, T., Darvish, A, des Rosiers, C., & Stanley, W. C. (2000). Partitioning of pyruvate between oxidation and anaplerosis in swine hearts. *American Journal of Physiology. Heart and Circulatory Physiology*, *279*(5), H2390–8.

25. Randle, P. J. (1986). Fuel selection in animals. *Biochemical Society Transactions*, *14*(5), 799–806.

26. Rubin, J., Matsushita, K., Ballantyne, C. M., Hoogeveen, R., Coresh, J., & Selvin, E. (2012). Chronic hyperglycemia and subclinical myocardial injury. *Journal of the American College of Cardiology*, *59*(5), 484–9.

27. Saltiel, A. R., & Kahn, C. R. (2001). Insulin signalling and the regulation of glucose and lipid metabolism. *Nature*, *414*(6865), 799–806.

28. Shulman, G. I. (2000). Cellular mechanisms of insulin resistance. *The Journal of Clinical Investigation*, *106*(2), 171–6.

29. Stanley, W. C., Hall, J. L., Stone, C. K., & Hacker, T. A. (1992). Acute myocardial ischemia causes a transmural gradient in glucose extraction but not glucose uptake. *The American Journal of Physiology*, *262*(1 Pt 2), H91–6.

30. Stanley, W. C., Recchia, F. A., & Lopaschuk, G. D. (2005). Myocardial substrate metabolism in the normal and failing heart. *Physiological Reviews*, *85*(3), 1093–129.

31. Vincent, G., Bouchard, B., Khairallah, M., & Des Rosiers, C. (2004). Differential modulation of citrate synthesis and release by fatty acids in perfused working rat hearts. *American Journal of Physiology. Heart and Circulatory Physiology*, *286*(1), H257–66.

Chapter 3

Metabolic derangements in the myocardium

The previous chapter focused on myocardial metabolism under normal physiological conditions. We now turn our attention to metabolic derangements that may result in downstream pathological consequences, with the emphasis on SSB consumption (as it is the focus of this study). Here the spotlight will be on the effects of hyperglycemia on oxidative stress and flux through the NOGPs. These pathways are an important focus of our laboratory and we propose that their activations play a key role in the development of insulin resistance and diabetic cardiovascular complications.

3.1 Introduction

The homeostatic control of glucose is dependent on its uptake by various tissues. For example, after the ingestion of a carbohydrate-rich meal, blood glucose levels increase and a corresponding response is initiated, i.e. insulin produced by pancreatic β-cells acts to lower circulating blood glucose levels again. Moreover, insulin availability allow target tissues to respond to the hyperglycemic state by increasing glucose uptake, metabolic utilization and glycogen storage. Insulin increases glucose transport in fat and muscle cells by stimulating the translocation of GLUT4 from intracellular sites to the plasma membrane (Saltiel and Kahn, 2001). This therefore shows the crucial role insulin plays in glucose utilization, and if the insulin response becomes dysfunctional this can severely impact on mechanisms regulating glucose utilization. The relative lack of insulin action on target cells is referred to as IR, a multi-faceted and progressive condition that is normally associated with diabetic individuals (Shulman, 2000).

IR is associated with a variety of metabolic disorders, with poor lifestyle and dietary behavior, such as SSB consumption, contributing greatly to its progression. Although skeletal muscle and adipose tissues are the main target organs of insulin action, IR and subsequent derangement of glucose utilization may also impact on cardiac metabolism and function (Hu *et al*., 2008; reviewed by Poornima *et al*., 2006).

The influence of hyperglycemia (e.g. pre-Diabetes/Diabetes, poor dietary choices like increased SSB consumption, etc.) on the dysregulation of glucose homeostasis, IR and the development of cardiovascular complications has not been given much attention in the literature. It is therefore of great importance to address this topic. Since hyperglycemic episodes may lead to IR, T2D and CVD over time, the controlled regulation of SSB consumption could potentially play a significant role to prevent such detrimental outcomes (Brownell *et al*., 2009; Joseph *et al*., 2014; Mapanga *et al*., 2012).

The aim of this study is to investigate the role of SSBs within this context and to assess if it induces hyperglycemia and thereby dysregulates myocardial glucose metabolism, i.e. by NOGP activation, and the subsequent onset of IR and CVD. This chapter therefore reviews mechanisms whereby hyperglycemia alters glucose metabolism, resulting in oxidative stress and the consequent activation of the NOGPs leading to IR, endothelial dysfunction and other cardiovascular complications.

3.2 Hyperglycemia

Two forms of hyperglycemia exist, i.e. chronic and acute. Chronic hyperglycemia is defined as constantly elevated blood glucose levels over a prolonged period of time and has been linked with obesity and CVD (Rubin *et al*., 2012). Acute hyperglycemia is defined as a sudden and dramatic spike in blood sugar, and can sometimes be a serious condition that can result in immediate and/or lasting damage (Raposeiras-Roubín *et al*., 2011)- which will be discussed later. We will focus on acute hyperglycemia, as there is limited evidence for the potential damaging effects of acute hyperglycemia e.g. caused by increased SSB consumption. Furthermore, understanding the early molecular events which perturbs glucose metabolic pathways may help us to gain insight into effective intervention strategies to blunt such effects.

A number of studies implicate hyperglycemia as an active, causative factor for cardio-metabolic and vascular dysfunction. For example, our laboratory found that short-term hyperglycemic exposures play an essential role in the progression of IR and cardiac dysfunction (Joseph *et al*., 2014; Mapanga *et al*., 2012). For the current study we therefore hypothesize that increased consumption of SSBs induces abnormal postprandial

hyperglycemic excursions subsequently leading to perturbed myocardial glucose metabolism, with detrimental consequences.

3.2.1 Acute hyperglycemia

Postprandial hyperglycemia is a normal phenomenon to clear blood glucose levels following a meal, however higher glucose levels may persist when glucose homeostasis is dysfunctional and insulin fails to restore blood glucose levels postprandially. The latter condition usually manifests during the progression towards T2D when insulin action becomes impaired (Del Prato and Tiengo, 2001). The rate of glucose uptake is generally regulated by fasting hyperglycemia, and is increased in individuals with higher fasting glucose levels - this is due to the mass action effects of hyperglycemia (Mapanga *et al*., 2012). Acute hyperglycemia may present in undiagnosed diabetic cases, IGT or in response to a severe stress episode (Lazzeri, 2009). IGT precedes the onset of T2D and is defined as a condition where fasting plasma glucose levels decrease below 7 mmol/L, and is associated with a two-hour postprandial excursion of between 7.8 and 11 mmol/L (The Diabetes Forum, [s.a.] as adapted from the IDF*)* (as discussed in Chapter 1).

Hyperglycemia in itself can also cause pancreatic β–cell dysfunction, or cause cell death in other tissues like the heart - a phenomenon sometimes referred to as ‘‘glucotoxicity’’. In the case of the pancreas, this can be caused by the higher demands for insulin stimulation, therefore causing hyperinsulinemia which can directly compromise β–cell function. With high SSB consumption there is more insulin secretion than normal and this state of hyperinsulinemia may in turn lead to IR (Anton *et al*., 2010; Fagherazzi *et al*., 2013; Ludwig, 2002).

3.2.2 Sugar-sweetened beverages and hyperglycemia

The metabolic effects of long term SSB consumption are linked to increased visceral obesity and decreased insulin sensitivity (Stanhope *et al*., 2009). Clinical studies found that fructose-sweetened beverage consumption increased fasting glucose concentrations within two weeks and also strongly elevated postprandial glucose levels. The inverse was true for insulin secretion i.e. after a period of two and ten weeks of fructose consumption, significantly lower insulin levels were found versus baseline levels (Swarbrick *et al*., 2008). Studies have shown

that fructose does not stimulate the insulin response as is the case with glucose exposure. This is due to the liver being its major site of metabolism as well as the relatively low levels of fructose transporters (GLUT5) expressed in pancreatic β–cells. Both glucose and fructose are absorbed in the small intestine, however, glucose is taken up through GLUT 4 transporters and fructose through GLUT 5 transporters. Fructose does not induce the same insulin response as glucose due to there being very little GLUT 5 transporters in the pancreas (Johnson et al., 2013). Further evidence suggests that the long-term consumption of SSBs will increase the risk of developing CVD due to the above mentioned factors (De Koning et al., 2012; *Tasevska et al., 2014).*

Thus, these studies show that SSB consumption may trigger hyperglycemia (Anton *et al*., 2010) which subsequently leads to the dysregulation of cardio-metabolism (Joseph and Essop, 2014). In addition, other related effects may also include oxidative stress that in turn may cause various CV complications (Fagherazzi *et al*., 2013; Ludwig, 2002).

3.3 Dysregulation of glucose metabolism and diabetic complications

As discussed, hyperglycemia can contribute to a series of vascular complications by initiating detrimental molecular events. The mechanisms whereby hyperglycemia may cause metabolic derangements remain unclear but increased free radicals and oxidative stress are proposed to be key factors in this process (Mapanga *et al*., 2012; Robins and Swanson, 2014). Here increased caloric intake may help explain such detrimental effects, i.e. additional energy expenditure increases flux through the TCA cycle and enhances NADH and subsequent ROS generation (Van Gaal *et al*., 2006). Such an upregulation of oxidative stress plays an essential role in a range of complications – e.g. β-cell dysfunction and IR onset - making it a central factor for the dysregulation of glucose metabolism (Joseph *et al*., 2014; King and Loeken, 2004). Therefore, with increased hyperglycemic episodes, subsequent flux in cardiac glycolytic pathways is increased forming ROS which causes oxidative stress triggering downstream detrimental effects.

3.3.1 Oxidative stress

Oxidative stress is defined as the inability to remove excess oxidants faster than the production thereof. The formation of ROS may be triggered by several stimuli, including an

elevation in metabolic fuel substrates (reviewed by King and Loeken, 2004). For example, studies demonstrated that hyperglycemia may cause an increase in $O_2^{\bullet}$ levels, while hyperlipidemia could elevate $O_2^{\bullet}$ and peroxynitrite levels (Baynes and Thorpe, 1999; Ceriello *et al*., 2002). Such free radicals formed can damage proteins, lipids and nucleic acids, resulting in detrimental outcomes. Moreover, increased levels of oxidative stress have strong correlations to the development of IR and related conditions, as well as T2D complications (Brownlee, 2005). Therefore oxidative stress is proposed to be the common pathogenic factor indicating the development of IR, as well as its progression to Diabetes. In addition, oxidative stress is also considered a risk factor for developing CVD (Sugamura & Keaney, 2011). In light of this, the specific mechanisms linked to the production of ROS will now be further described.

3.3.2 The sources of reactive oxygen species

The primary site of ROS production is the mitochondrial ETC. This is where the substrates from carbohydrate and FA metabolism are utilized as described in Chapter 2. The ETC drives the electron donors (NADH and $FADH_2$) through its protein complexes to form a proton gradient which in turn results in the generation of ATP (discussed by Cecchini, 2003). Various signals drive mitochondrial ATP production i.e. increased ATP requirement during stress responses or greater physical activity, and hence mitochondrial function is tightly regulated – the latter includes the production of mitochondrial ROS subsequent to increased ETC activity.

Under stressed conditions mitochondria can generate amplified amounts of ROS (reviewed by Du *et al*., 2000). For example, hyperglycemia-mediated ETC-generated ROS production is strongly linked to mitochondrial damage associated with diabetic complications (Guzik *et al*., 2002). Of note, hyperglycemia (from SSB consumption) also adds to elevated ROS production by increasing glycolytic flux which consequently triggers greater oxidative stress production (Park at el., 2005). The upregulation of oxidative stress thus plays a significant role in a diverse range of complications and may be relevant within the context of chronic SSB consumption.

The mitochondrion generates ROS by the passage of increased electron flow through the ETC. Under hyperglycemic conditions the ETC becomes impaired and electrons leak out via Co-Q and react with oxygen to form free radicals, e.g. $O_2^{\bullet}$, which is highly reactive because

of its unpaired electrons (Ceriello, 2005; Joseph *et al*., 2014). The electrons mainly leak out between complexes II and III, and this is evident by the production of $O_2^{\bullet}$ ions in diabetic rats in response to glycation of complex III (Brownlee, 2005; Rosca *et al*., 2005). Figure 3.1 illustrates the chain of events during hyperglycemia-mediated ROS production in the mitochondria due to electron leakage. However, whether mitochondrial defects are causative factors or consequences of IR is still under debate (Rabøl *et al*., 2006).

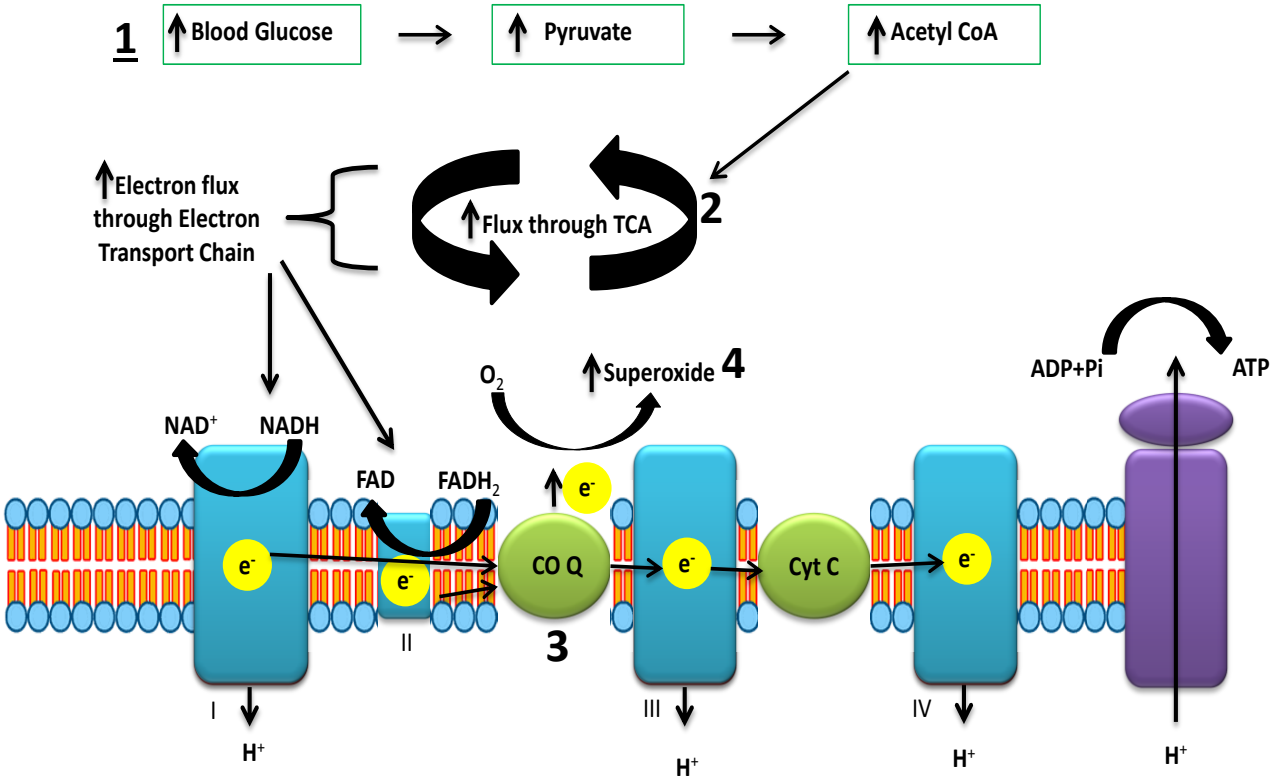

Figure 3.1: Possible mechanism of how increased blood glucose levels lead to the production of superoxide. 1-This may occur with the diabetic phenotype or also with greater caloric intake by 'Western' dietary habits that may increase blood glucose levels due to postprandial hyperglycemia. 2- Increased flux through the TCA cycle forms abundant NADH and $FADH_2$ electron donors. 3- This generates excess flux though the ETC, causing a build-up of electrons between the II and III complexes. 4- Electrons then react with oxygen to form increased superoxide levels.

Abbreviations: Tricarboxylic acid cycle (TCA), nicotinamide adenine dinucleotide reduced (NADH), flavin adenine dinucleotide reduced ($FADH_2$), adenosine triphosphate (ATP), adenosine diphosphate (ADP), co-enzyme Q (CO-Q), electrons (e^-).

As discussed, although $O_2^{\bullet}$ is implicated in downstream effects such as IR, another species, e.g. hydrogen peroxide (H_2O_2) may also play a role in the dysregulation of insulin signaling mechanisms (Anderson *et al*., 2009). This is evident as mitochondrial dysfunction was discovered when examining the morphology of muscle tissue in diabetic patients.

Although mitochondria are a major source of ROS production, recent data suggest that higher levels of ROS generation from sources in the cytosol may also play a pathophysiologic role (Joseph *et al*., 2014; Zhou *et al*., 2010). These include glucose autoxidation, NADPH oxidase (NOX) as well as lipogenase, xanthine oxidase, peroxidases and peroxisomes (Ceriello *et al*., 2002; Nishikawa *et al*., 2000). For example, NOX activity as well as $O_2^{\bullet}$ production was increased in vascular tissue from diabetic patients (Guzik *et al*., 2002). ROS produced by NOX can additionally participate in myocardial apoptosis during hyperglycemic conditions, further exacerbating cardio-metabolic problems (Balteau *et al*., 2011). Thus both mitochondrial and extra-mitochondrial ROS sources are vital in the manifestation of cardio-metabolic pathologies. It is proposed that the initiating event is the formation of mitochondrial $O_2^{\bullet}$ which triggers initial ROS generation, which in turn further fuels greater ROS generation from other extra-mitochondrial sources.

The other side of the coin is of course that cells do possess antioxidant mechanisms to help maintain ROS homeostasis (Dhar *et al*., 2008). Here mitochondria contain intracellular antioxidant mechanisms which alleviate the formation of ROS in order to maintain homeostasis, e.g. glutathione reductase and peroxidase recycles glutathione between its reduced phase (GSH) and its oxidized phase (GSSG). It acts as an antioxidant, converting $O_2^{\bullet}$ to H_2O_2. Superoxide dismutase (SOD) also modifies $O_2^{\bullet}$ to H_2O_2 which is then converted to water via catalase (which is also an antioxidant). Three forms of superoxide dismutase exist; mitochondrial manganese superoxide dismutase (MnSOD, SOD2), cytosolic copper-zinc superoxide dismutase (CuZnSOD, SOD 1) and extracellular dismutase (EcSOD, SOD3) (discussed by Tiebosch, 2014). SOD1 is found in the cytoplasm, whereas SOD2 and SOD3 are found in the mitochondrion and extracellular matrix respectively (McCord and Edeas, 2005). However, such intracellular antioxidant defence mechanisms are overwhelmed during extreme conditions such as hyperglycemia (Brownlee, 2005; Joseph *et al*., 2014; King and Loeken, 2004) with damaging cardio-metabolic outcomes. The focus will now be on

downstream metabolic perturbations and the research interest of our laboratory, i.e. increased activation of NOGPs.

3.4 Reactive oxygen species and the activation of non-oxidative glucose pathways

Glucose utilization begins with glycolysis (cytoplasm) that forms NADH and pyruvate. Pyruvate is subsequently transported into the mitochondrion and further oxidized in the TCA cycle. However, with enhanced glucose availability and utilization, ROS generation increases. As discussed, hyperglycemia-driven flow through the ETC is the source of excessive ROS production in the mitochondrion (Nishikawa *et al*., 2000). In addition, increased FA oxidation leads to the formation of NADH and $FADH_2$, therefore, also contributing to ROS formation by similar mechanisms as described before (Brownlee, 2005). It is proposed that excessive ROS production cause downstream activation of NOGPs which will now be discussed in more detail.

3.4.1 Activation of non-oxidative glucose pathways

Under normal physiological conditions, a relatively small percentage of glucose-derived intermediates are shunted into the NOGPs. However, these pathways are markedly upregulated upon additional glucose substrate availability – acute and chronic hyperglycemia (Fagherazzi *et al*., 2013). Hyperglycemia-mediated oxidative stress (especially $O_2^{\bullet}$) is proposed to play an essential role in NOGP activation (Brownlee, 2005; Ceriello, 2005). The model currently favored is that the production of $O_2^{\bullet}$ under hyperglycemic conditions acts as a unifying mechanism in the induction of NOGPs.

The idea put forward is that hyperglycemia-mediated ROS causes DNA damage. $O_2^{\bullet}$ reacts with nitric oxide (NO) to reduce bioavailability, which in turn produces peroxynitrite which can also cause DNA damage (Guzik *et al*., 2002). The damaged DNA subsequently activates the repair enzyme poly adenosine diphosphate ribose polymerase (PARP). However, PARP can attenuate GAPDH, a key glycolytic enzyme. As a result upstream glycolytic intermediates accumulate and can be shunted into upstream NOGPs, i.e. the formation of advanced glycation end-product (AGE) pathway, the activation of protein kinase C (PKC) and its isoforms, the polyol pathway and the hexosamine biosynthetic pathway (HBP)

(Ceriello and Motz, 2004; Giacco and Brownlee, 2010; Nishikawa *et al*., 2000) (refer to Figure 3.2). Our laboratory proposes that both mitochondria and NOX-derived ROS can result in NOGP activation under hyperglycemic conditions (Joseph *et al*., 2014, Joseph and Essop, 2014). The next section will provide a more detailed discussion of the pathophysiological roles of NOGPs.

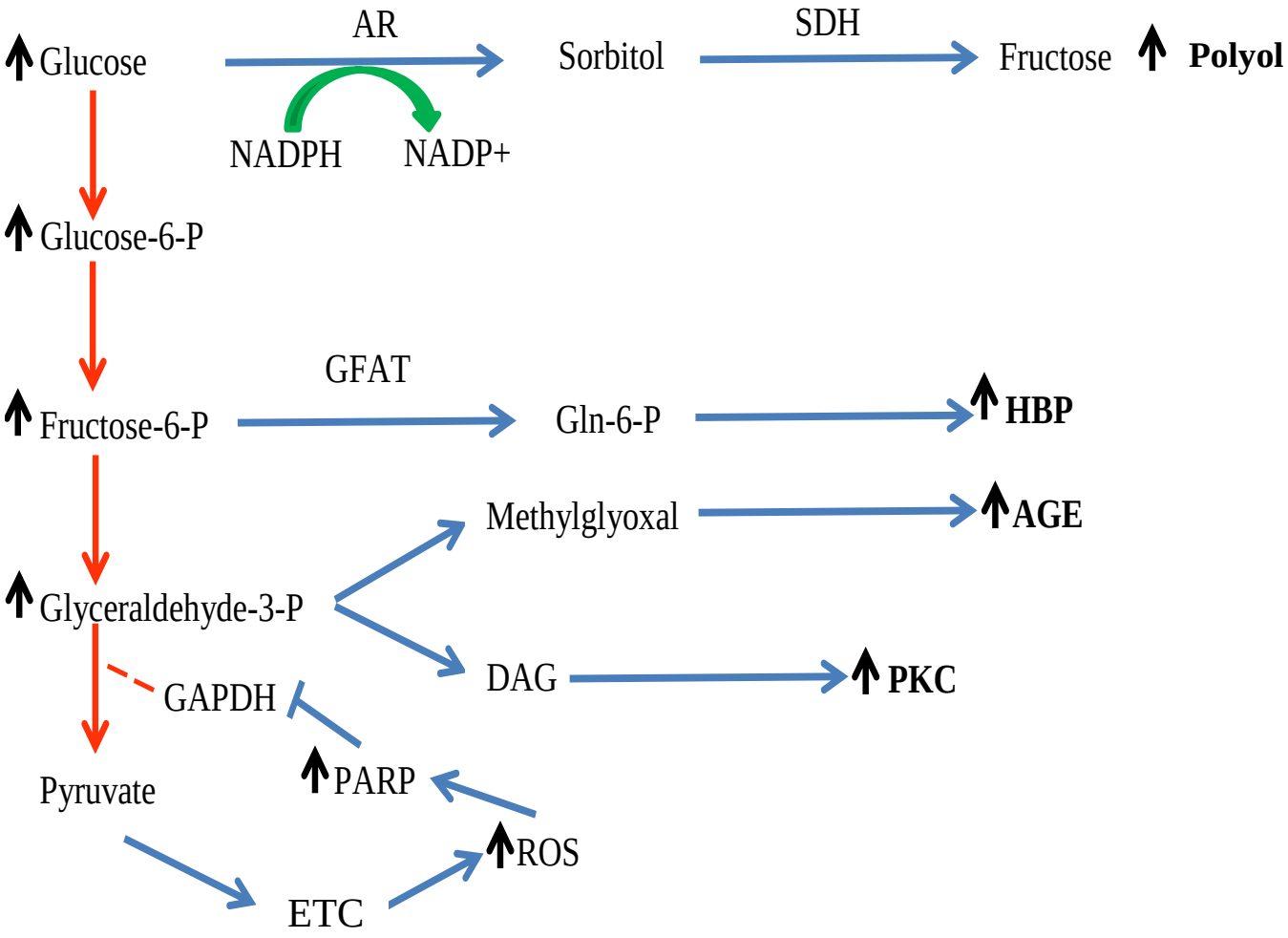

Figure 3.2: A schematic representation of increased flux through the glycolytic pathway as well as the TCA cycle forming ROS. This in turn induces DNA damage, subsequently activating PARP which tries to rectify the damage done to the DNA but simultaneously limits the actions of GAPDH. Glucose intermediates are subsequently shunted into upstream NOGPs, i.e. Polyol, HBP, PKC and AGE.
Abbreviations: aldose reductase (AR), sorbitol dehydrogenase (SDH), glutamine:fructose-6-phosphate amidotransferase (GFAT), diacylglycerol (DAG), glyceraldehyde-3-phosphate dehydrogenase (GAPDH), poly adenosine diphosphate ribose polymerase (PARP), reactive oxygen species (ROS), electron transport chain (ETC).

3.4.2 Non-oxidative glucose pathways

As explained, elevated blood glucose levels may therefore contribute significantly to observed adverse effects on the myocardium. A brief description of the four NOGPs will now be provided.

3.4.2.1 Advanced glycation end products

AGE compounds are complex and have been linked with Diabetes-related complications (Singh *et al*., 2001; *Vlassara & Uribarri, 2014*). *Here r*educed carbohydrates such as carbonyl compounds and glucose form methylglyoxal (MG) derivatives from a non-enzymatic reaction. This occurs in the Maillard reaction and the products are referred to as AGEs. The production of intracellular AGE precursors is an important mechanism to induce intracellular stress (Hartog *et al*., 2007), and can accumulate in response to oxidative stress under diabetic conditions.

AGE precursors can cause damage to cells in various ways. Firstly, it can act by modification of intracellular proteins, including those required for gene transcription. AGE precursors can also diffuse from the cell and modify extracellular molecules thereby altering cell signaling that can subsequently cause cellular dysfunction. Finally, AGE precursors can diffuse out of cells and alter circulating proteins e.g. circulating albumins. Such modified proteins may trigger a cascade of events by binding to AGE receptors (RAGE), activating the production of inflammatory cytokines and/or growth factors, which in turn can cause vascular complications (Brownlee, 2005, Doi *et al*., 1992). The activation of AGEs through RAGEs alters enzymatic structure and function by promoting free radical formation (Baynes and Thorpe, 1999; McCarthy *et al*., 2001). Furthermore, studies found that AGE-modified matrix protein inhibits cell migration and adhesion of human T-cells (cells responsible for cell-mediated immunity) (Haucke *et al*., 2013).

High amounts of MG can accumulate during hyperglycemic excursions which may directly increase AGE precursors by the accumulation of glucose-3-phosphate (G-3-P) in the glycolytic pathway (Singh *et al*., 2001; Vlassara and Uribarri, 2014). AGEs are implicated in the progression of heart failure in both diabetic and non-diabetic individuals. The formation of AGE induces the production of free radicals and also depletes NO concentrations, which

can fuel oxidative stress. As NO exerts its effects on vasodilation and anti-proliferation, AGE accumulation may therefore result in vascular thickening and endothelial cell dysfunction (Singh *et al*., 2001). Furthermore, the oxidative stress state caused by AGEs activates nuclear factor kappa B (NFκB) a pro-inflammatory transcription factor, which in turn can enhance cytokine production and contribute to vascular pathology (Brownlee, 2005) (Figure 3.3).

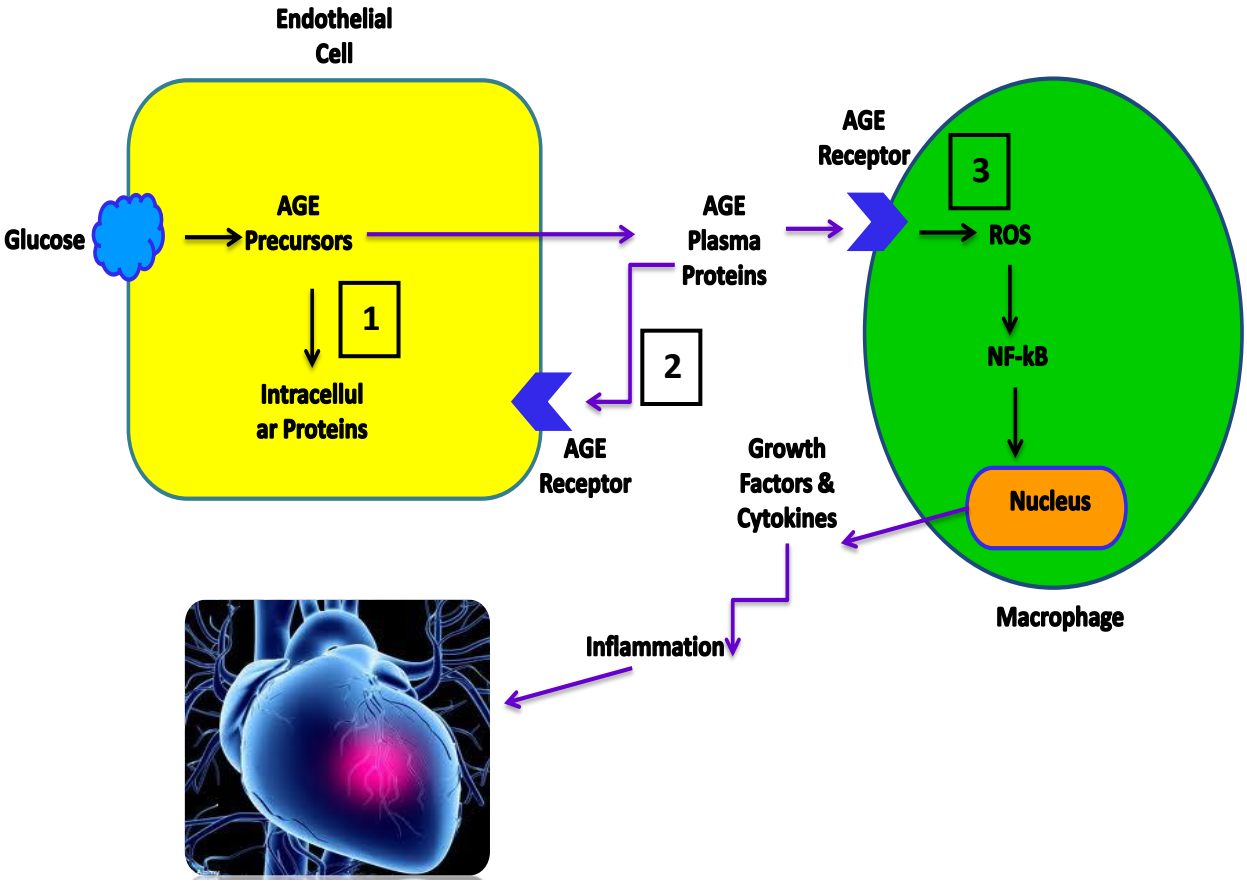

Figure 3.3: A schematic representation of three different mechanisms whereby AGE precursors exert harmful effects, causing vascular pathologies. 1- Modifies intracellular proteins. 2- Moves out of the cell and modifies extracellular proteins, therefore impacting on cell signaling. 3- Activates AGE receptors (RAGE) and cause a variety of downstream effects.

3.4.2.2 Protein kinase C activation

The hyperglycemia-mediated accumulation of glycolytic metabolites, e.g. glyceraldehyde-3-phosphate in glycolysis may drive the synthesis of DAG. DAG in turn will recruit PKC to the plasma membrane, allowing for its activation. The levels of DAG content in the heart is directly proportional to its blood glucose levels, therefore hyperglycemic episodes result in elevated DAG concentrations (Liu *et al*., 2012). The PKC family consists of a variety of different isoforms with the purpose to control functionality of other proteins – accomplished by phosphorylating mainly threonine or serine residues. The main PKC isoforms identified includes PKC α, β, and δ (Koya *et al*., 1997; Mapanga *et al*., 2012). FA may also trigger the formation of active PKC thus bringing into play another metabolite that is typically elevated with Diabetes (Koya *et al*., 1997). The activation of PKC may have detrimental downstream effects including decreasing the amount of endothelial nitric oxide synthase (eNOS) (causing abnormal blood flow), increasing inflammatory markers (e.g. NFκB) and stimulating NOX production (thereby increasing already elevated ROS levels) (Ceriello, 2005; Xia *et al*., 2006). Furthermore, the dual actions of PKC, i.e. diminishing eNOS and elevating NOX may play an important role in the development of IR (Joseph *et al*., 2014) (Figure 3.4.).

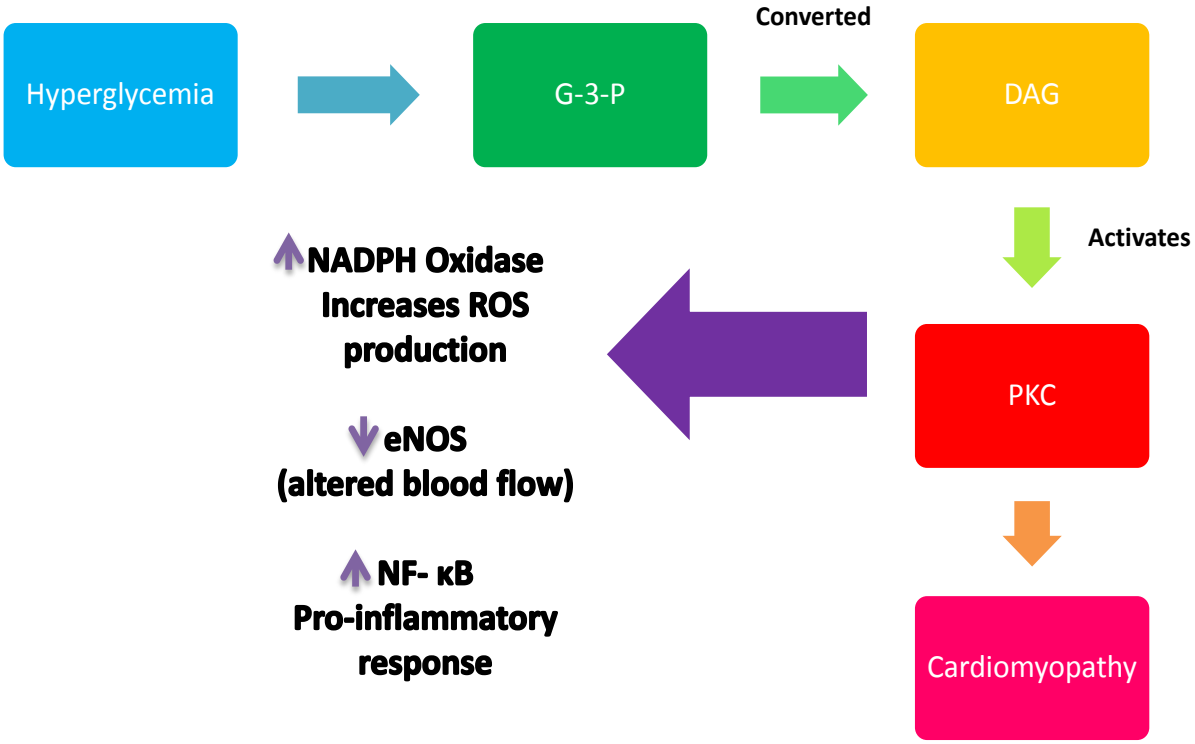

Figure 3.4: A schematic representation of the activation of protein kinase C (PKC) and the detrimental effects thereof. Glucose-3-phosphate is converted into diacylglycerol (DAG) which in turn activates PKC isoforms with detrimental outcomes e.g. increased ROS production and inflammatory responses.

3.4.2.3 Polyol pathway

As glucose concentrations become elevated, aldose reductase (AR) (normally reduces toxic aldehydes to inactive alcohols) reduces glucose to sorbitol, which is then oxidized to fructose. The AR reaction (i.e. reduction of glucose to sorbitol) consumes NADPH. As NADPH is a vital co-factor for the reduction of GSSG to GSH this decreases NADPH availability and thus increases intracellular susceptibility to oxidative stress (Brownlee, 2005; Liu *et al*., 2012).

There are three potential mechanisms by which the polyol pathway could contribute to oxidative stress: 1) AR depletes NADPH cofactors as described above, 2) upon the conversion of sorbitol to fructose, sorbitol dehydrogenase (SDH) converts NAD^+ to NADH which in turn is a precursor for the formation of NOX, and 3) the converted sorbitol to fructose leads to the formation of fructose-3-phosphate (F-3-P), which is converted to AGE precursors downstream (Chung *et al*., 2003) (Figure 3.5).

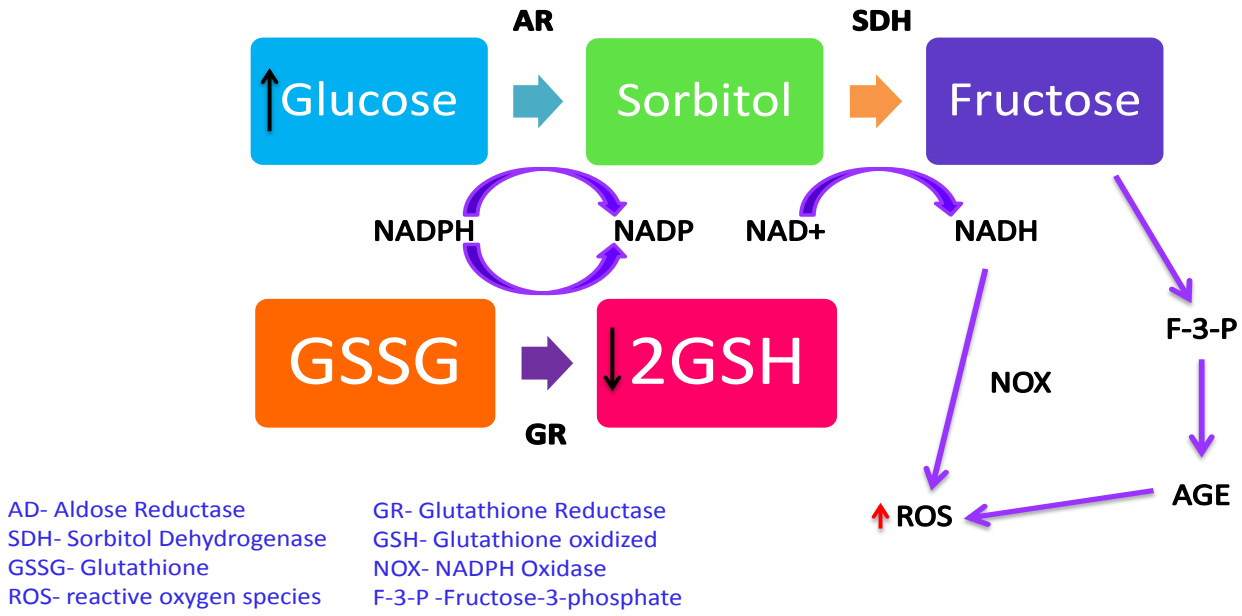

Figure 3.5: A schematic representation of increased flux through the polyol pathway during hyperglycemia. Glucose is converted to sorbitol by AR; this subsequently depletes NADPH required in the reduction of GSSG to the anti-oxidant GSH. ROS levels subsequently increase thereby contributing to intracellular damage. Fructose also increases cellular ROS production as its downstream effects activate AGE, thus contributing to intracellular damage.

3.4.2.4 Hexosamine Biosynthetic Pathway

The HBP is regarded as a metabolic sensor, i.e. it can 'tag' metabolic fuel substrates (when in excess) to be stored in various storage depots within the host organism (Rossetti, 2000). Under normal physiological conditions ~3% of glycolytic intermediates are shunted into this pathway. However, this can sharply increase with hyperglycemia (Robinson et al., 1995). Here glucose is progressively shunted into the HBP, which converts fructose-6-phosphate to glucosamine-6-phosphate and finally to uridine diphosphate (UDP) N-acetyl glucosamine after a series of reactions. The fructose to glucosamine-6-phosphate reaction is catalyzed by the rate-limiting enzyme, glutamine: fructose-6-phosphate amidotransferase (GFAT). The N-acetyl glucosamine is tagged onto serine and threonine residues of various intracellular proteins, in an O-linked fashion i.e. O-GlcNAc. The proteins are modified using the following enzymes: O-linked GlcNAc transferase (OGT) catalyzes the addition of the sugar residue onto nucleocytoplasmic proteins; and N-acetylglucosaminidase (OGA) which hydrolyzes the removal of the sugar moiety (discussed by Myslicki et al., 2014).

Excessive HBP modification can result in pathogenic changes in gene expression and protein function and greater O-GlcNAcylation may contribute to the pathogenesis of IR, diabetic and cardiovascular complications (Brownlee, 2005; Du et al., 2000; Jacobsen et al., 1996). The HBP also plays a role in modifying the pentose phosphate pathway (PPP), reducing NADPH levels and attenuating the anti-oxidative properties of GSH (Joseph et al., 2014; Mapanga et al., 2012; Li et al., 1996). Figure 3.6 demonstrates the flux through the HBP and shows how proteins are O-GlcNAcylated.

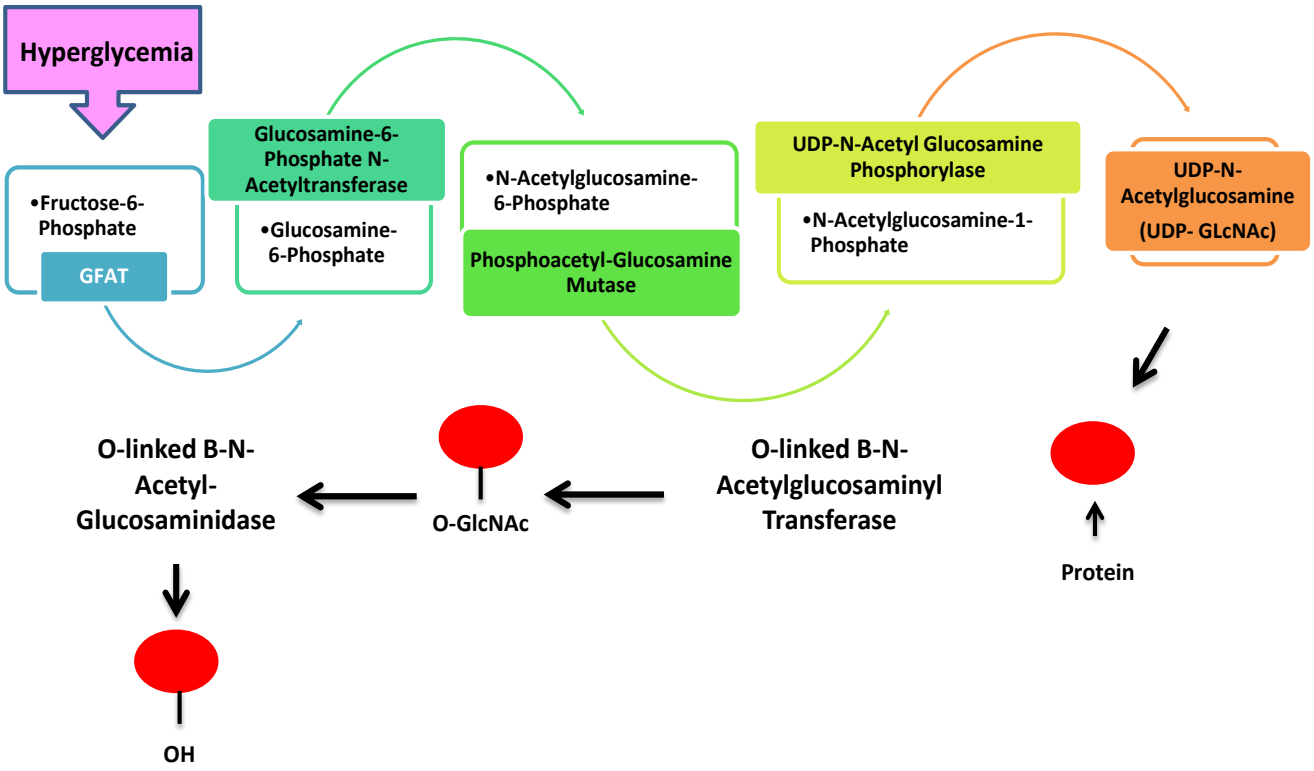

Figure 3.6: Hyperglycemia increases flux through the HBP. The above is a schematic representation of how proteins become *O*-GlcNAcylated which could lead to damaging outcomes. Under hyperglycemic conditions fructose-6-phosphate is converted - by a variety of downstream reactions - into uridine diphosphate-N-acetyl glucosamine (UDP-GlcNAc). This substrate gets tagged onto proteins which may result in pathophysiologic outcomes.

Abbreviations: *O*-linked N-acetyl glucosamine (*O*-GlcNAc), glutamine: fructose-6-phosphate amidotransferase (GFAT), uridine diphosphate (UDP), hydroxyl (OH).

3.5 Summary

Hyperglycemia exerts glucose metabolic derangements with detrimental downstream effects on cellular function. The literature discussed in Chapter 3 demonstrates that hyperglycemic events perturb glucose utilization and also causes oxidative damage. The downstream molecular derangements induce a series of "unfortunate events'' that result in activation of NOGPs, each contributing to various forms of damage in the myocardium and beyond.

As discussed earlier, various studies have linked SSBs to hyperglycemia and also to detrimental outcomes for the host organism. However, the underlying mechanisms whereby this *actually* occurs remain elusive and no study has investigated whether NOGPs can be activated with SSB consumption. Moreover, from a more general perspective there is a paucity of data regarding mechanisms whereby SSBs may mediate potential detrimental effects. In light of this, we therefore initiated this particular project in order to investigate the effects of SSB and ASB consumption, respectively, with the aim to establish a unique, chronic SSB model that will allow for a comprehensive investigation of underlying mechanisms (this work will extend beyond the current MSc study). As a first step in this process, this MSc study entailed pioneering research work to establish and characterize the experimental SSB model and also examined NOGP activation in the rat heart. The methodology is described in Chapter 4, while Chapters 5 and 6 describes our unique findings in this regard.

3.6 Hypothesis

Our central hypothesis is that long-term SSB consumption will perturb glucose metabolism, enhance intracellular oxidative stress, leading to NOGP activation in the heart. We further propose that such activation may in turn lead to IR and decreased cardiac function – note the broader parts of our hypothesis will be investigated at a later stage and does not form part of this MSc study.

3.7 Aims

Our aims for this study are:

- Establish a novel *in vivo* rat model of chronic SSB and ASB consumption (up to six months)
- Monitor dietary behaviour and phenotypic changes
- Evaluate fasting blood triglyceride, cholesterol and glucose levels
- Perform oral glucose tolerance tests (OGTTs), biweekly
- Measure activation of myocardial NOGPs

References

1. Anderson, E. J., Lustig, M. E., Boyle, K. E., Woodlief, T. L., Kane, D. A., Lin, C., & Neufer, P. D. (2009). Mitochondrial H_2O_2 emission and cellular redox state link excess fat intake to insulin resistance in both rodents and humans. The Journal of Clinical Investigation, 119(3), 573–81.

2. Anton, S. D., Martin, C. K., Han, H., Coulon, S., Cefalu, W. T., Geiselman, P., & Williamson, D. A. (2010). Effects of stevia, aspartame, and sucrose on food intake, satiety, and postprandial glucose and insulin levels. *Appetite*, *55*(1), 37–43.

3. Balteau, M., Tajeddine, N., de Meester, C., Ginion, A., Des Rosiers, C., Brady, N. R., Beauloye, C. (2011). NADPH oxidase activation by hyperglycaemia in cardiomyocytes is independent of glucose metabolism but requires SGLT1. *Cardiovascular Research*, *92*(2), 237–46.

4. Baynes, J. W., & Thorpe, S. R. (1999). Role of oxidative stress in diabetic complications: a new perspective on an old paradigm. *Diabetes*, *48*(1), 1–9.

5. Brownell, K. D., Farley, T., Willett, W. C., Popkin, B. M., Chaloupka, F. J., Thompson, J. W., & Ludwig, D. S. (2009). The public health and economic benefits of taxing sugar-sweetened beverages. *The New England Journal of Medicine*, *361*(16), 1599–605.

6. Brownlee, M. (2005). The pathobiology of diabetic complications: a unifying mechanism. *Diabetes*, *54*(6), 1615–25.

7. Cecchini, G. (2003). Function and structure of complex II of the respiratory chain. *Annual Review of Biochemistry*, *72*, 77–109.

8. Ceriello, A. (2005). Postprandial hyperglycemia and Diabetes complications: is it time to treat? *Diabetes*, *54*(1), 1–7.

9. Ceriello, A., & Motz, E. (2004). Is oxidative stress the pathogenic mechanism underlying insulin resistance, Diabetes, and cardiovascular disease? The common soil hypothesis revisited. *Arteriosclerosis, Thrombosis, and Vascular Biology*, *24*(5), 816–23.

10. Ceriello, A., Quagliaro, L., D'Amico, M., Di Filippo, C., Marfella, R., Nappo, F., Giugliano, D. (2002). Acute Hyperglycemia Induces Nitrotyrosine Formation and Apoptosis in Perfused Heart From Rat. *Diabetes*, *51*(4), 1076–1082.

11. Chung, S. S. (2003). Contribution of Polyol Pathway to Diabetes-Induced Oxidative Stress. *Journal of the American Society of Nephrology*, *14*(90003), 233S–236.

12. De Koning, L., Malik, V. S., Kellogg, M. D., Rimm, E. B., Willett, W. C., & Hu, F. B. (2012). Sweetened beverage consumption, incident coronary heart disease, and biomarkers of risk in men. *Circulation*, *125*(14), 1735–41, S1.

13. Del Prato, S., & Tiengo, A. (2001). The importance of first-phase insulin secretion: implications for the therapy of type 2 Diabetes Mellitus. Diabetes/metabolism Research and Reviews, 17(3), 164–74.

14. Dhar, A., Desai, K., Kazachmov, M., Yu, P., & Wu, L. (2008). Methylglyoxal production in vascular smooth muscle cells from different metabolic precursors. *Metabolism: Clinical and Experimental*, 57(9), 1211–20.

15. Doi, T., Vlassara, H., Kirstein, M., Yamada, Y., Striker, G. E., & Striker, L. J. (1992). Receptor-specific increase in extracellular matrix production in mouse mesangial cells by advanced glycosylation end products is mediated via platelet-derived growth factor. Proceedings of the National Academy of Sciences of the United States of America, 89(7), 2873–7.

16. Du, X. L., Edelstein, D., Rossetti, L., Fantus, I. G., Goldberg, H., Ziyadeh, F., & Brownlee, M. (2000). Hyperglycemia-induced mitochondrial superoxide overproduction activates the hexosamine pathway and induces plasminogen activator

inhibitor-1 expression by increasing Sp1 glycosylation. *Proceedings of the National Academy of Sciences of the United States of America*, *97*(22), 12222–6.

17. Fagherazzi, G., Vilier, A., Sartorelli, D. S., Lajous, M., & Balkau, B. (2013). Consumption of artificially and sugar-sweetened beverages and ´ miologique aupre ` s des incident type 2 Diabetes in the Etude Epide ´ ne ´ rale de l ' Education Nationale – European femmes de la Mutuelle Ge Prospective Investigation into Cancer and Nutri, (1), 517–523.

18. Giacco, F., & Brownlee, M. (2010). Oxidative stress and diabetic complications. *Circulation Research*, *107*(9), 1058–70.

19. Guzik, T. J. , Mussa, S. , Gastaldi, D. , Sadowski, J. , Ratnatunga, C. , Pillai, R., and Channon, K. M. (2002). Mechanisms of Increased Vascular Superoxide Production in Human Diabetes Mellitus: Role of NAD(P)H Oxidase and Endothelial Nitric Oxide Synthase. *Circulation*, *105*(14), 1656–1662.

20. Hartog, J. W. ., Voors, A. A., Bakker, S. J. L., Smit, A. J., & van Veldhuisen, D. J. (2007). Advanced glycation end-products (AGEs) and heart failure: pathophysiology and clinical implications. *European Journal of Heart Failure*, *9*(12), 1146–55.

21. Haucke, E., Navarrete-Santos, A., Simm, A., Silber, R.-E., & Hofmann, B. (2013). Glycation of extracellular matrix proteins impairs migration of immune cells. *Wound Repair and Regeneration : Official Publication of the Wound Healing Society [and] the European Tissue Repair Society*, *22*(2), 239–45.

22. Hu, J., Klein, J. D., Du, J., & Wang, X. H. (2008). Cardiac muscle protein catabolism in Diabetes Mellitus: activation of the ubiquitin-proteasome system by insulin deficiency. *Endocrinology*, *149*(11), 5384–90.

23. Jacobsen, S. E., Binkowski, K. A, & Olszewski, N. E. (1996). SPINDLY, a tetratricopeptide repeat protein involved in gibberellin signal transduction in Arabidopsis. *Proceedings of the National Academy of Sciences of the United States of America*, *93*(17), 9292–6.

24. Johnson, R. J., Nakagawa, T., Sanchez-Lozada, L. G., Shafiu, M., Sundaram, S., Le, M., & Lanaspa, M. A. (2013). Sugar, uric acid, and the etiology of diabetes and obesity. Diabetes, 62(10), 3307–15.

25. Joseph, D., & Essop, M. F. (2014). The effects of thiamine treatment on pre-diabetic versus overt diabetic rat hearts: Role of non-oxidative glucose pathways. *International Journal of Cardiology*, 7–9.

26. Joseph, D., Kimar, C., Symington, B., Milne, R., & Essop, M. F. (2014). The detrimental effects of acute hyperglycemia on myocardial glucose uptake. *Life Sciences*, *105*(1-2), 31–42.

27. King, G. L., & Loeken, M. R. (2004). Hyperglycemia-induced oxidative stress in diabetic complications. *Histochemistry and Cell Biology*, *122*(4), 333–8.

28. Koya, D., Jirousek, M. R., Lin, Y. W., Ishii, H., Kuboki, K., & King, G. L. (1997). Characterization of protein kinase C beta isoform activation on the gene expression of transforming growth factor-beta, extracellular matrix components, and prostanoids in the glomeruli of diabetic rats. *The Journal of Clinical Investigation*, *100*(1), 115–26.

29. Lazzeri, C., Tarquini, R., Giunta, F., & Gensini, G. F. (2009). Glucose dysmetabolism and prognosis in critical illness. *Internal and Emergency Medicine*, *4*(2), 147–56.

30. Li, Y. M., Mitsuhashi, T., Wojciechowicz, D., Shimizu, N., Li, J., Stitt, A, Vlassara, H. (1996). Molecular identity and cellular distribution of advanced glycation endproduct receptors: relationship of p60 to OST-48 and p90 to 80K-H membrane proteins. *Proceedings of the National Academy of Sciences of the United States of America*, *93*(20), 11047–52.

31. Liu, J.-W., Liu, D., Cui, K.-Z., Xu, Y., Li, Y.-B., Sun, Y.-M., & Su, Y. (2012). Recent advances in understanding the biochemical and molecular mechanism of diabetic cardiomyopathy. *Biochemical and Biophysical Research Communications*, *427*(3), 441–3.

32. Ludwig, D. S. (2002). The Glycemic Index Physiological Mechanisms Relating to Obesity, Diabetes, and Cardiovascular Disease. *Journal American Medical Association*, *287*(18), 2414–2423.

33. Mapanga, R. F., Rajamani, U., Dlamini, N., Zungu-Edmondson, M., Kelly-Laubscher, R., Shafiullah, M., Essop, M. F. (2012). Oleanolic acid: a novel cardioprotective agent that blunts hyperglycemia-induced contractile dysfunction. *PloS One*, *7*(10), e47322.

34. McCarthy, A. D., Etcheverry, S. B., & Cortizo, A. M. (2001). Effect of advanced glycation endproducts on the secretion of insulin-like growth factor-I and its binding proteins: role in osteoblast development. *Acta Diabetologica*, *38*(3), 113–122.

35. McCord, J. M., & Edeas, M. A. (2005). SOD, oxidative stress and human pathologies: a brief history and a future vision. *Biomedicine & Pharmacotherapy*, *59*(4), 139–42.

36. Myslicki, J. P., Belke, D. D., & Shearer, J. (2014). Role of O-GlcNAcylation in nutritional sensing, insulin resistance and in mediating the benefits of exercise. *Applied Physiology, Nutrition, and Metabolism*, *9*(July), 1–9.

37. Nishikawa, T., Edelstein, D., Du, X. L., Yamagishi, S., Matsumura, T., Kaneda, Y., Brownlee, M. (2000). Normalizing mitochondrial superoxide production blocks three pathways of hyperglycaemic damage. *Nature*, *404*(6779), 787–90.

38. Park, S., Ryu, J., & Lee, W. (2005). O-GlcNAc modification on IRS-1 and Akt2 by PUGNAc inhibits their phosphorylation and induces insulin resistance in rat primary adipocytes. *Experimental Molecular Medicine*, 37(3), 220-229.

39. Poornima, I. G., Parikh, P., & Shannon, R. P. (2006). Diabetic cardiomyopathy: the search for a unifying hypothesis. *Circulation Research*, *98*(5), 596–605.

40. Rabøl, R., Boushel, R., & Dela, F. (2006). Mitochondrial oxidative function and type 2 Diabetes. *Applied Physiology, Nutrition, and Metabolism*, *31*(6), 675–83.

41. Raposeiras-Roubín, S., Barreiro Pardal, C., Ocaranza, R., Cid, B., & González-Juanatey, J. R. (2011). Acute hyperglycemia: is really a new risk marker for contrast-induced nephropathy in patients with acute myocardial infarction without Diabetes and normal renal function? *American Heart Journal*, *162*(1), e7; author reply e9.

42. Robbins, N. M., & Swanson, R. A. (2014). Opposing effects of glucose on stroke and reperfusion injury: acidosis, oxidative stress, and energy metabolism. *Stroke*, 45(6), 1881–6.

43. Robinson, K. A., Weinstein, M. L., Lindenmayer, G. E., & Buse, M. G. (1995). Effects of Diabetes and hyperglycemia on the hexosamine synthesis pathway in rat muscle and liver. *Diabetes*, *44*(12), 1438–46.

44. Rosca, M. G., Mustata, T. G., Kinter, M. T., Ozdemir, A. M., Kern, T. S., Szweda, L. I., Weiss, M. F. (2005). Glycation of mitochondrial proteins from diabetic rat kidney is associated with excess superoxide formation. *American Journal of Physiology. Renal Physiology*, *289*(2), F420–30.

45. Rossetti, L. (2000). Perspective: Hexosamines and nutrient sensing. *Endocrinology*, *141*(6), 1922–5.

46. Rubin, J., Matsushita, K., Ballantyne, C. M., Hoogeveen, R., Coresh, J., & Selvin, E. (2012). Chronic hyperglycemia and subclinical myocardial injury. *Journal of the American College of Cardiology*, *59*(5), 484–9.

47. Saltiel, A. R., & Kahn, C. R. (2001). Insulin signalling and the regulation of glucose and lipid metabolism. *Nature*, *414*(6865), 799–806.

48. Shulman, G. I. (2000). Cellular mechanisms of insulin resistance. *The Journal of Clinical Investigation*, *106*(2), 171–6.

49. Singh, R., Barden, A, Mori, T., & Beilin, L. (2001). Advanced glycation end-products: a review. *Diabetologia*, *44*(2), 129–46.

50. Stanhope, K. L., Schwarz, J. M., Keim, N. L., Griffen, S. C., Bremer, A. A., Graham, J. L., & Havel, P. J. (2009). Consuming fructose-sweetened, not glucose-sweetened, beverages increases visceral adiposity and lipids and decreases insulin sensitivity in overweight/obese humans. *The Journal of Clinical Investigation*, *119*(5), 1322–34.

51. Sugamura, K., & Keaney, J. F. (2011). Reactive oxygen species in cardiovascular disease. *Free Radical Biology & Medicine*, *51*(5), 978–92.

52. Swarbrick, M. M., Stanhope, K. L., Elliott, S. S., Graham, J. L., Krauss, R. M., Christiansen, M. P., Havel, P. J. (2008). Consumption of fructose-sweetened beverages for 10 weeks increases postprandial triacylglycerol and apolipoprotein-B concentrations in overweight and obese women. *The British Journal of Nutrition*, *100*(5), 947–952.

53. Tasevska, N., Park, Y., Jiao, L., Hollenbeck, A., Subar, A. F., & Potischman, N. (2014). Sugars and risk of mortality in the NIH-AARP Diet and Health Study. *The American Journal of Clinical Nutrition*, *99*(5), 1077–88.

54. Tiebosch, M. H. (2014). Antioxidant adaptations in liver fibrogenesis. Unpublished doctoral dissertation. The Netherlands: *De Nederlandse Vereniging voor de Hepatologie*, (pp. 53–77).

55. The Diabetes Forum. Diabetes Digital Media Ltd- the global Diabetes community. Blood sugar level ranges. 2014. [S.a.] [Online]. Available: http://www.diabetes.co.uk/diabetes_care/blood-sugar-level-ranges.html [2014, September 20]

56. Van Gaal, L. F., Mertens, I. L., & De Block, C. E. (2006). Mechanisms linking obesity with cardiovascular disease. *Nature*, *444*(7121), 875–80.

57. Vlassara, H., & Uribarri, J. (2014). Advanced glycation end products (AGE) and Diabetes: cause, effect, or both? *Current Diabetes Reports*, *14*(1), 453.

58. Xia, L., Wang, H., Goldberg, H. J., Munk, S., Fantus, I. G., & Whiteside, C. I. (2006). Mesangial cell NADPH oxidase upregulation in high glucose is protein kinase C dependent and required for collagen IV expression. *American Journal of Physiology. Renal Physiology*, *290*(2), F345–56.

59. Zhou, L., Aon, M. A, Almas, T., Cortassa, S., Winslow, R. L., & O'Rourke, B. (2010). A reaction-diffusion model of ROS-induced ROS release in a mitochondrial network. *PLoS Computational Biology*, *6*(1), e1000657.

Chapter 4

Materials and Methods

4.1 Experimental design and research chapter layout

The aim of this study was to investigate the effects of SSB consumption on weight gain, food intake, insulin-mediated glucose metabolism (oral glucose tolerance tests [OGTTs]), and blood metabolites such as triglycerides and cholesterol. Furthermore, organ/tissue weights (heart, liver, gastrocnemius and visceral adipose) were evaluated and documented as a percentage of the rat's body weight. Histological analysis was conducted along with analysis of the degree of NOGP activation in heart tissues. We aimed to gain an improved understanding of how SSB intake may contribute to the onset of cardiovascular disease and Type 2 diabetes. This approach would provide greater insight into biochemical mechanisms and pathways of an intact organism which an *in vitro* model would not allow.

4.2 Animals and ethics statement

Animals were treated adhering to the Guide for the Care and Use of Laboratory Animals of the National Academy of Science (NIH publication No. 85-23, revised 1996). This study was executed with the approval of the Animal Ethics Committees of Stellenbosch University (South Africa), (Ethics # SU-ACUM13-00012) (Appendix A).

For the experimental procedure, male Wistar rats (n=72) weighing ~200 grams and containing no clinical signs of infection were divided into six groups. The groups were classified as follows: control, water, Coca Cola®, Coke Light®, Jive® and butter (n=12) and further divided into three or six month groups (n=6) (Figure 4.1). The rats were housed three per cage with *ad libitum* access to water and standard chow.

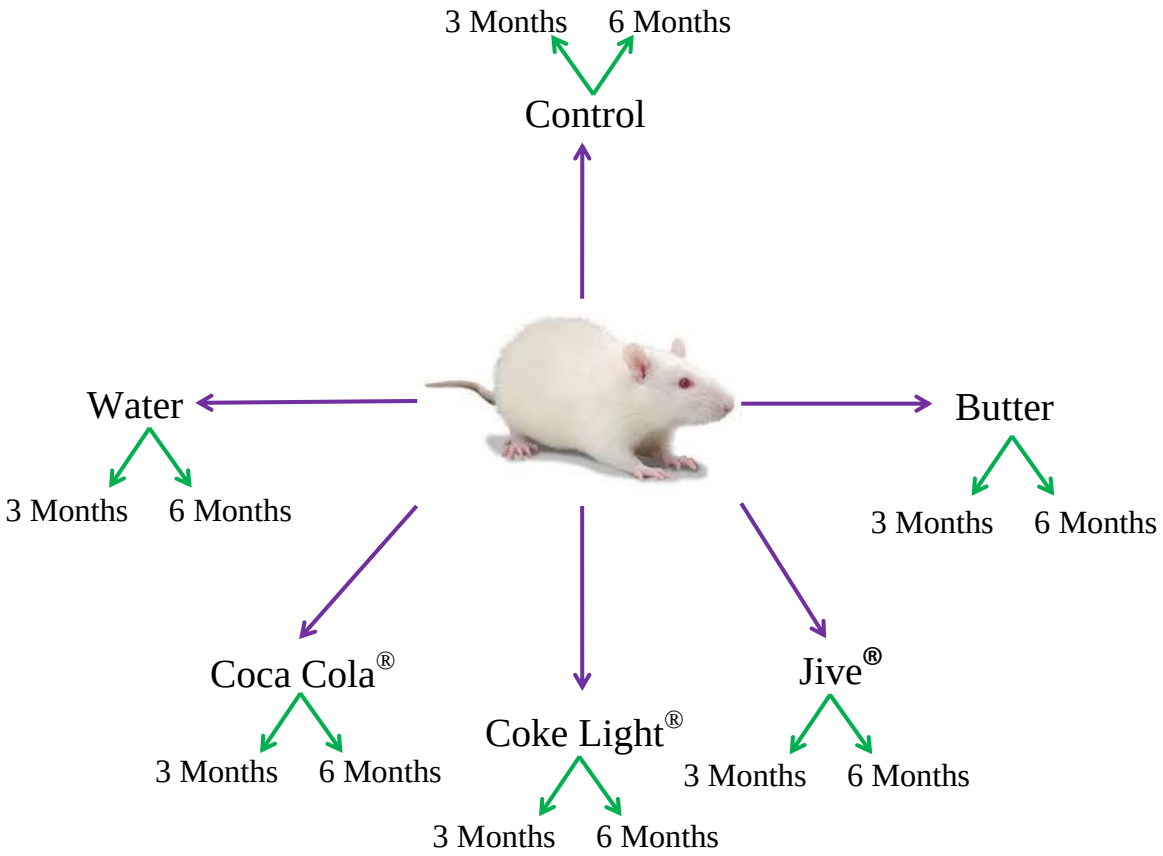

Figure 4.1: A schematic representation of the various group allocations for this experiment.

4.3 Experimental procedure

4.3.1 Experimental dosages

The rats were gavaged on a daily basis with an experimental dosage depending on their group allocation and body weight classification. The dosage volumes were calculated using their surface area to volume ratio (Reagan-Shaw *et al.*, 2007) and animals were gavaged with the equivalent of 125 ml (54 calories) of Coca Cola® for a 60 kg adult human being. The water and Coke Light® groups received the same volume of experimental dosage as the Coca Cola® group. Furthermore, the Jive® and butter group volumes were equivalent to the number of calories as for the Coca Cola® group (54 calories). Rats were also allocated to a non-gavaged control group. Table 4.1 specifies the amount of experimental dosages that the animals received in milliliters according to their weight classification.

Table 4.1: Experimental dosage volumes for the different groups according to their body weight classifications.

	Treatment Volume According to Weight Classification				
Treatment	**250-300 g**	**300-350 g**	**350-400 g**	**400-450 g**	**>450 g**
Water	3.2 ml	3.8 ml	4.5 ml	5.1 ml	5.8 ml
Coca Cola®	3.2 ml	3.8 ml	4.5 ml	5.1 ml	5.8 ml
Coke Light®	3.2 ml	3.8 ml	4.5 ml	5.1 ml	5.8 ml
Jive®	2.4 ml	2.9 ml	3.4 ml	3.8 ml	4.4 ml
Butter	0.3 ml	0.37 ml	0.43 ml	0.5 ml	0.56 ml

4.3.2 Weight and food consumption

Rats were weighed on a weekly basis in order to record percentage body weight gain and assess the development of obesity. Food intake was monitored weekly by measuring food consumption within and amongst the different groups. This was achieved by initially weighing normal rat chow and placing the pellets into rat cages; where after pellets were removed and re-weighed after seven days. The difference between the two measurements equated to food consumed per cage. This allowed for quantification of food intake per week and thereafter the calculation of the average daily consumption per rat. This procedure continued for the duration of the study (24 weeks).

4.3.3 Blood sampling

The animals were fasted overnight (at least 12 hours) in preparation for blood sampling. The rats were first sedated using 3% isoflurane (Piramal, Bethlehem PA, USA) and thereafter 1 ml of blood was drawn from the right jugular vein. Food was subsequently provided *ad libitum* and rats were monitored to assess their overall well-being. The blood samples were then centrifuged (Spectrafuge™ 24D, Labnet, Edison NJ, USA) at 13, 952 x g for 5 minutes to separate serum that was collected and stored at -80^{0}C until further analysis. Blood was drawn at the following time points: week #1 (baseline), week #8, week #12 (three months), week #16 and week #24 (six months). The blood samples were sent to the National Health Laboratory Service (NHLS) at Tygerberg Hospital to evaluate triglyceride and total cholesterol levels (mmol/L).

4.3.4 Oral glucose tolerance tests (OGTT)

Oral glucose tolerance tests were performed every two weeks (bi-weekly) for the duration of the 24 weeks. The rats were fasted overnight to ensure accurate determination of fasting blood glucose levels. A small skin prick was made at the tip of the rat's tail to allow blood droplets to form and a glucometer then used to test blood glucose levels (mmol/L). Baseline fasting glucose levels were initially tested where after glucose powder was dissolved in distilled water (0.86 g/kg) (Mapanga *et al*., 2012) and rats gavaged and monitored for 120 minutes. Readings were taken at the following time points (in minutes): baseline (0), 5, 10, 15, 30, 45, 60 and 120. Once the procedure was completed the animals re-gained access to their food and water, and were monitored to ensure their general well-being.

4.3.5 Tissue and organ harvest

Upon the completion of the experimental procedures for both the three and six month groups, respectively, rats were euthanized and their organs harvested for further analysis. Here rats were sedated using 5% isoflurane (Piramal, Bethlehem PA) and pedal reflexes tested before blood was collected and stored as previously stated. Thereafter, heart, liver, gastrocnemius muscle and visceral adipose tissue were collected, weighed, and snap-frozen in liquid nitrogen for long-term storage at -80ºC. We also collected visceral adipose tissue for the six month groups - stored in formalin for histological analysis. Due to limited animal numbers we were only able to focus on adipose tissue for histological analyses – other organs will be harvested at a future date.

4.4 Analyses

4.4.1 Tissue sample preparation

Proteins were extracted from the tissue samples for various analytical procedures. Tissues were homogenized in ice-cold RIPA buffer (see Appendix B), and then stored at -80ºC. Protein content was evaluated by the Bradford method (Appendix C) and the lysates obtained were used for both Western blotting and NOGP analysis (using ELISA kits).

4.4.2 Evaluation of non-oxidative glucose metabolic pathways activation

Commercial kits were used to evaluate markers of NOGP activation: AGE precursors were analyzed using the OxiSelect™ Methylglyoxal ELISA kit (Cell Biolabs, San Diego CA,USA), PKC kinase activity (Abcam, Global Biotech Company, San Francisco CA, USA), polyol pathway using a D-sorbitol colorimetric detection kit (Biovision Research Products, Mountain View CA, USA). Western blotting was employed to determine HBP activation – assessment of total *O*-GlcNAc levels (Joseph *et al*., 2014; Mapanga *et al*., 2012).

4.4.2.1 Methylglyoxal levels (AGE pathway)

Reduced carbohydrates such as carbonyl compounds and glucose form methylglyoxal (MG) derivatives in a non-enzymatic reaction, i.e. the Maillard reaction -products formed are referred to as AGEs. The OxiSelect™ Methylglyoxal ELISA kit (Cell Biolabs, San Diego CA) was therefore employed as it measures MG derivatives as markers for the activation of the AGE pathway. The kit measures MG concentrations in protein samples by comparing absorbance values to that of known MG-BSA standard curves.

The previously prepared protein lysates were pipetted into the 96-well plate provided and it was incubated overnight at 4°C to allow MG markers to attach to the wells. It was subsequently probed with an anti-MG specific monoclonal antibody for one hour at room temperature on an orbital shaker. The plate was washed seven times followed by an HRP-conjugate secondary antibody and the plate was incubated at room temperature for an hour on the shaker. A substrate solution was added and left for 5-20 minutes to allow for color development. A stop solution was then added to the wells to stop the previous enzymatic reaction. Thereafter, the plate was immediately read at a wavelength of 450 nm using a microplate reader (El 800 KC Junior Universal Microplate reader, Bio-Tek Instruments, Winooski VT). MG marker levels were then quantified from the standard curve and were expressed as ng per µg protein.

4.4.2.2 Protein kinase C activity assay

The PKC assay was carried out using an ELISA-based method where a synthetic substrate is used for PKC activation. This is measured using an antibody that recognizes the phosphorylated form of PKC. Detailed instructions were included in the kit to perform the assay (PKC kinase activity [Abcam, Global Biotech Company, San Francisco CA]).

In order to prepare the plate (provided), each well was soaked in a Kinase Assay Dilution Buffer (50 µL) at room temperature for 10 minutes where after the solution in the wells were aspirated. Protein samples, as well as positive and negative controls were added to the wells as detailed in the instruction manual. The reaction was initiated by adding 10 µL of ATP to each well and the plate was then incubated at 30°C for 90 minutes with gentle mixing every 20 minutes. The reaction was thereafter terminated by emptying the wells and patting dry the plate. A phosphospecific substrate antibody (40 µL) was then added to each well followed by a 60 minute incubation period, with shaking every 20 minutes. After several washing steps (with wash buffer provided), diluted anti-rabbit IgG: HRP conjugate was added to the wells (1:1000 dilution) and incubated for 30 minutes at room temperature. TMB substrate (60 µL) was then added to each well and the plate incubated for 30-60 minutes (this time was determined by the color development). Stop Solution was added to the wells to stop the reaction and the color intensity was recorded at a wavelength of 450 nm using a microplate reader (El 800 KC Junior Universal Microplate reader, Bio-Tek Instruments, Winooski VT, USA). PKC activity was determined using the standard curve and expressed per volume lysate per minute and values normalized to relative standard controls.

4.4.2.3 D-sorbitol levels (Polyol pathway)

When glucose is reduced by aldose reductase, sorbitol is formed and eventually converted into fructose. D-sorbitol is an intermediate in the polyol pathway and was here employed as a marker of this pathway's activation. D-sorbitol was measured using a D-sorbitol colorimetric detection kit (Biovision Research Products, Mountain View CA). The standards, as well as the samples were loaded into the 96-well plate as detailed in the kit's instruction manual. The reaction mix was prepared and pipetted into each well (50 µL) and left to incubate at 37°C for 30 minutes. Sorbitol levels were determined by evaluating the oxidation of sorbitol to fructose. The reaction's absorbance was determined at 560 nm with a microplate reader (El

800 KC Junior Universal Microplate reader, Bio-Tek Instruments, Winooski VT). The sorbitol concentration (C) was calculated using the sample amount (nmol) from the standard curve (S_a), sample volume used (S_v) and the dilution factor (D); $C = S_a / S_v \times D$.

4.4.2.4 Hexosamine Biosynthetic Pathway (HBP)

We employed Western blotting to determine myocardial HBP activation (Appendix D). Collected heart tissues were used to prepare lysates (as previously described) and samples stored at -80°C. *O*-GlcNAc expression was determined using SDS-PAGE electrophoresis and Western Blotting (refer Appendix D) with an *O*-GlcNAc antibody (CTD110.6, Santa Cruz Biotechnology, Santa Cruz CA, USA) together with an appropriate secondary antibody (anti-mouse IgG, HRP-linked, Cell Signaling Technology®, Danvers MA, USA). Final *O*-GlcNAc amounts were determined using Image Lab™ Software version 4.0, quantification analysis (BIO-RAD, Berkley CA, USA). A more detailed description of the imaging process can be found in Appendix D.

4.4.3 Histology samples

The collected visceral adipose tissue was fixed in formalin and stained with hematoxylin and eosin stain (H&E) to produce histology slides (refer to Appendix E). Tissues slides were examined using a Nikon Microscope (Nikon Eclipes E400, Tokyo Japan) at a 10X magnification and photographed with NIS Elements (Imaging software version 4.10, Tokyo Japan). The surface area of the adipose tissue was calculated using ImageJ software (ImageJ 1.47v, Java 1.6.0_20).

4.5 Statistical analysis

The data is presented as mean ± standard error of the mean (SEM). Differences between groups were analyzed using Mann-Whitney unpaired t-tests. Where more than two groups were present, the one-way analysis of variance (ANOVA) was used. All statistical analyses were conducted using Graphpad Prism 5.01 (Graphpad Software Inc, San Diego CA, USA). Values were considered significant when $P<0.05$.

References

1. Joseph, D., Kimar, C., Symington, B., Milne, R., & Essop, M. F. (2014). The detrimental effects of acute hyperglycemia on myocardial glucose uptake. *Life Sciences*, *105*(1-2), 31–42.

2. Mapanga, R. F., Rajamani, U., Dlamini, N., Zungu-Edmondson, M., Kelly-Laubscher, R., Shafiullah, M., & Essop, M. F. (2012). Oleanolic acid: a novel cardioprotective agent that blunts hyperglycemia-induced contractile dysfunction. *PloS One*, *7*(10), e47322.

3. Reagan-Shaw, S., Nihal, M., & Ahmad, N. (2008). Dose translation from animal to human studies revisited. *FASEB Journal : Official Publication of the Federation of American Societies for Experimental Biology*, *22*(3), 659–61.

Chapter 5

Chronic SSB model – baseline characterization (weights, metabolite levels)

Although limited studies have previously linked SSBs to hyperglycemia, no-one (as far as we know) has undertaken a comprehensive investigation to evaluate how SSB consumption may mediate detrimental physiological effects on the heart. In light of this, this study aimed to investigate the effects of chronic consumption of different SSBs and ASBs by establishing a unique *in vivo* rat model. As this thesis was the beginning of this challenge, we began by performing some baseline characterization of SSB treatment in terms of weight changes and key systemic metabolites – covered in Chapter 5. We also investigated whether myocardial NOGPs – our laboratory's research focus – would be activated in our newly established rat model of chronic SSB consumption – Chapter 6.

5.1 Percentage weight gain (from baseline)

We initially evaluated the percentage increase in body weight (from baseline [day 1]) over a period of 24 weeks for each of the different experimental groups here investigated (Figure 5.1). Our data reveal that there were no significant differences detected for any of the groups – for the entire duration of the experiment.

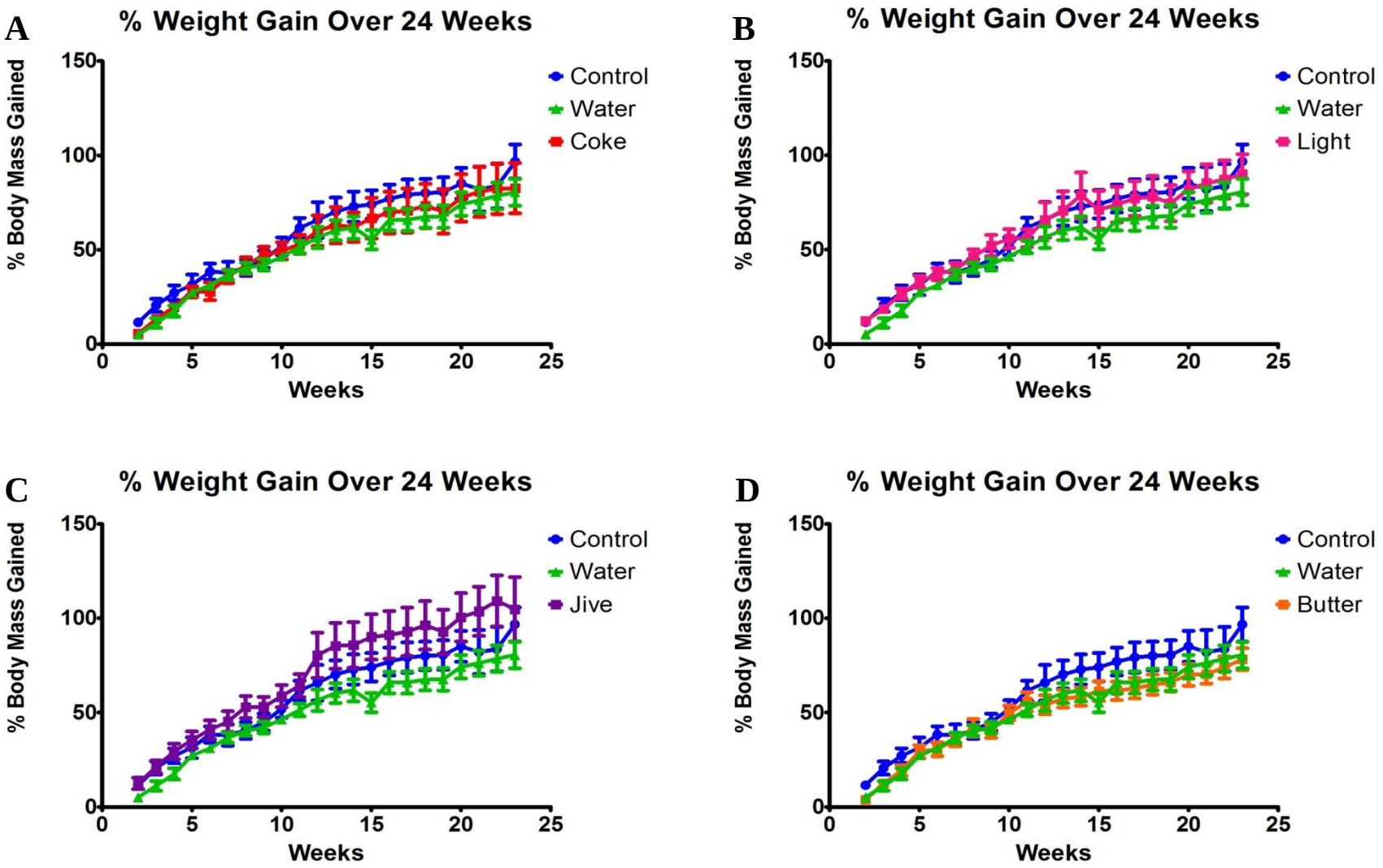

Figure 5.1: The percentage weight gain over a period of 24 weeks. A: Coca Cola®, B: Coke Light®, C: Jive®, D: butter. Weeks 1 - 12, n=12; weeks 13 to 24, n=6 – for all groups except butter. For the butter group: weeks 1 - 12, n=11; weeks 13 - 24, n=5.

5.2 Food consumption

The food consumption of the rats was also monitored for the entire duration of the experiment (Figure 5.2). However, we found no significant differences in food consumed by the four different groups here investigated.

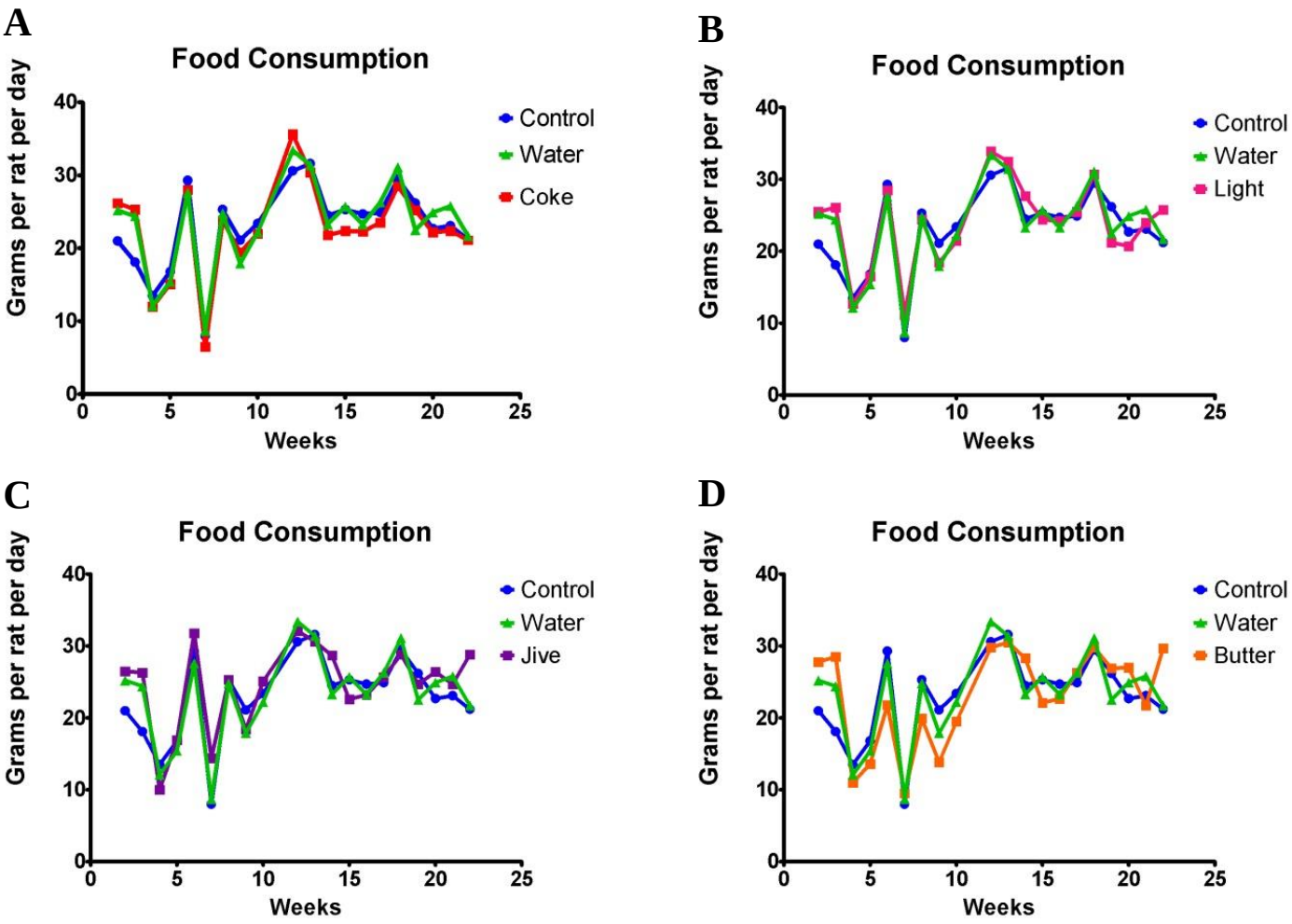

Figure 5.2: Food consumption over 24 weeks. A: Coca Cola®, B: Coke Light®, C: Jive®, D: butter. Weeks 1 - 12, n=12; weeks 13 - 24, n=6 – for all experimental groups except the butter group. Butter group: week 1 - 12, n=11; weeks 13 - 24, n=5.

5.3 Key systemic metabolites

To gain further insights into the effects of SSB consumption, we also determined total plasma cholesterol, triglyceride and glucose levels (fasted) at various time intervals (Figures 5.3 - 5.7). Each treatment group's results are shown separately.

5.3.1 Coca Cola®

The Coca Cola® group exhibited no differences in cholesterol levels at baseline, two, four and six months. However, at three months, there were higher cholesterol levels compared to the water group ($P<0.05$). For triglyceride levels there were no differences at baseline, three, four and six months. However triglyceride levels for the Coca Cola® group were higher than the water group at the two month time point ($P<0.05$) (refer to Figure 5.3). For the glucose measurements, during week one there was significance with Coca Cola® presenting higher fasting blood glucose levels than those of the control group ($P<0.05$). At three months fasting blood glucose levels were lower compared to the control group ($P<0.001$). No significant differences were noted at six months with regards to fasting blood glucose levels (Figure 5.7).

5.3.2 Coke Light®

No significance was seen at baseline and four months between the three groups. There were elevated cholesterol levels in the Coke Light® group at two and three months, respectively, when compared to the water group ($P<0.05$). After six months the Coke Light® group showed decreased cholesterol levels compared to the water group ($P<0.05$). The triglyceride data revealed no changes at baseline, two, three and four months, respectively. However, we found a reduction at the six month time point when compared to the control and water groups ($P<0.05$) (refer to Figure 5.4). Results from week 1 indicated no significant fasting blood glucose levels. At three months Coke Light® had reduced fasting glucose levels compared to the control group ($P<0.001$). The six month results revealed no significant differences between the groups fasting blood glucose levels (Figure 5.7).

5.3.3 Jive®

The Jive® group displayed no differences for cholesterol levels after two and six months, respectively, however, the baseline results reflecting higher levels than the control group ($P<0.05$). After three and four months, respectively, the Jive® group showed elevated cholesterol levels compared to the water group ($P<0.001$ & $P< 0.05$, respectively). There

were no significant differences observed for triglyceride levels during any of the measured time points (refer to Figure 5.5). During week 1, Jive® showed elevated glucose levels at baseline (fasting glucose) versus both the control and water groups ($P<0.001$ and $P<0.01$, respectively). At the three month time point, Jive® presented with lower fasting glucose levels when compared to respective control and water groups ($P<0.001$ and $P<0.05$, respectively). At six months there were no significant differences between the three groups (Figure 5.7).

5.3.4 Butter

The baseline cholesterol tests for the butter group revealed no significant differences as well as after four and six months, respectively. However, after two months the butter group exhibited elevated cholesterol metabolites compared to the water group ($P< 0.05$). After three months the butter group displayed significance between the control and water groups ($P< 0.05$). The triglyceride levels remained unchanged at baseline, three, four and six months, respectively, but at two months it showed higher triglyceride levels than both the control and water groups ($P<0.01$) (refer to Figure 5.6). Week one's results revealed no significance between the groups fasting blood glucose levels. At three months the butter group exhibited elevated fasting blood glucose levels compared to the water group ($P<0.01$). Again at six months, the butter group had higher fasting glucose levels compared to the water group ($P<0.05$) (Figure 5.7).

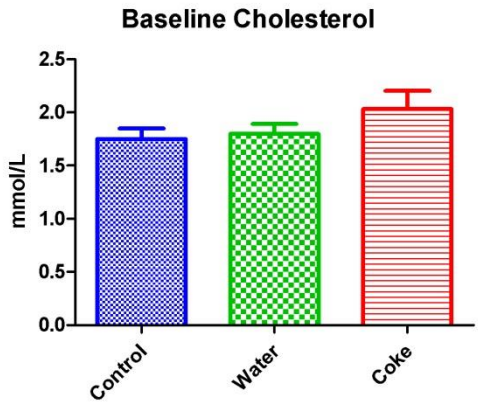

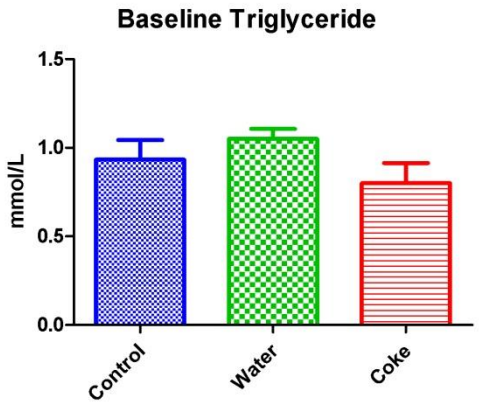

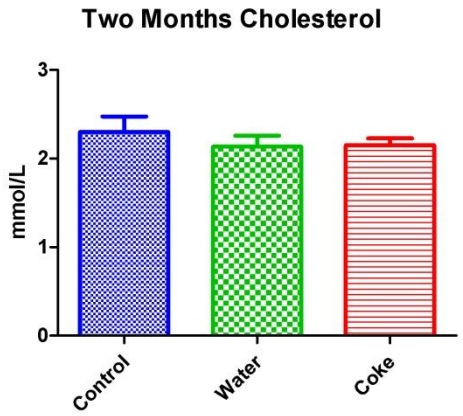

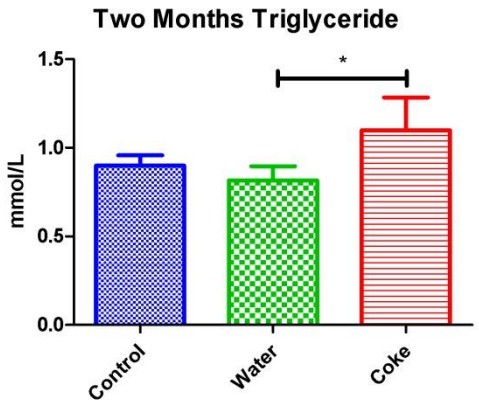

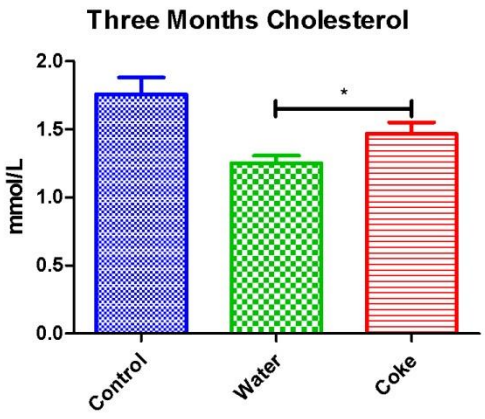

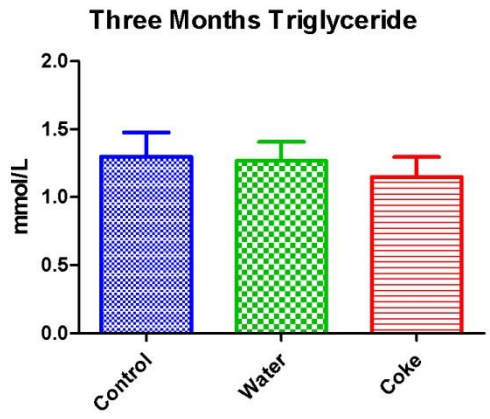

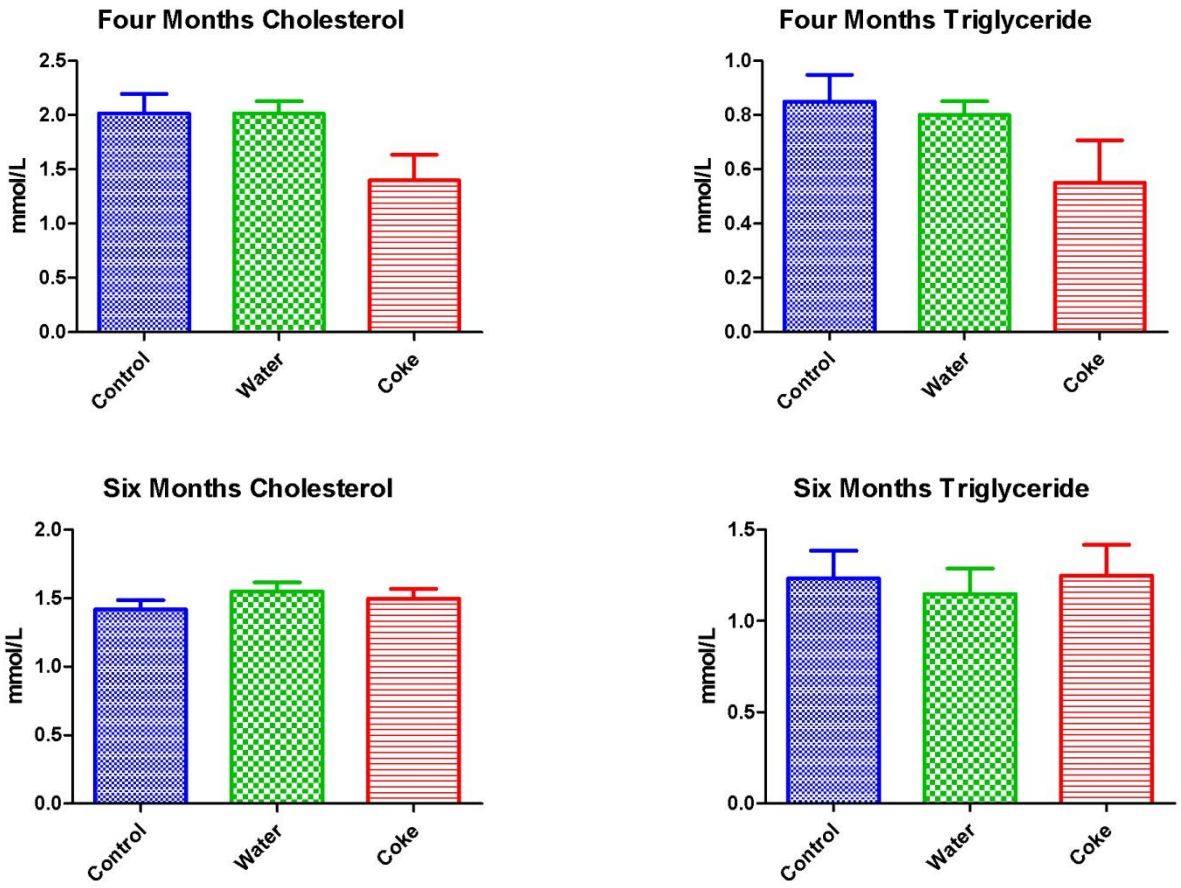

Figure 5.3: Coca Cola®- cholesterol and triglyceride blood metabolites. Blood was collected at 0, 2, 3, 4 and 6 months, respectively (n=12 for baseline to three months; n=6 for four to six months). Values are expressed as mean ± SEM. Significance is shown as * $P<0.05$.

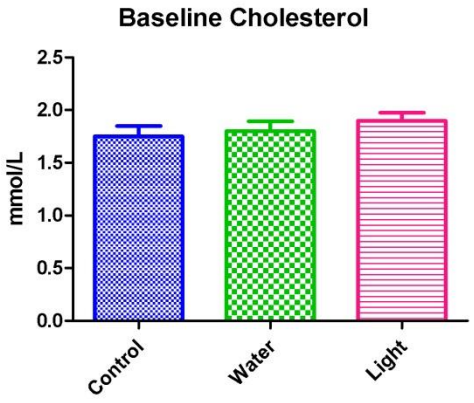

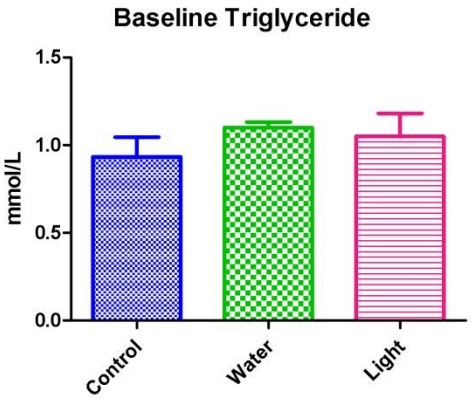

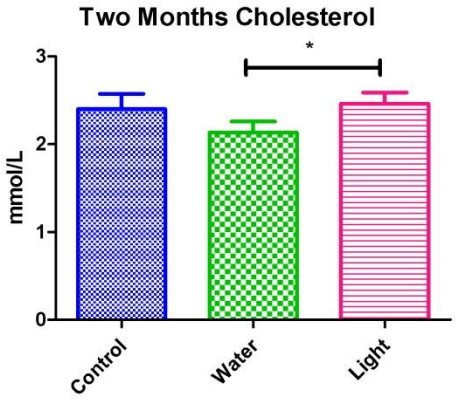

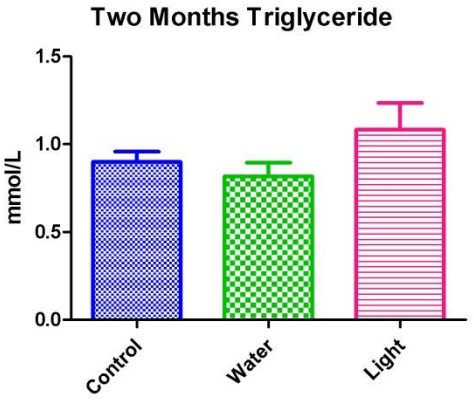

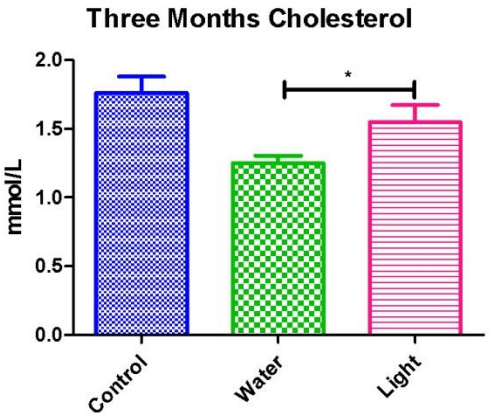

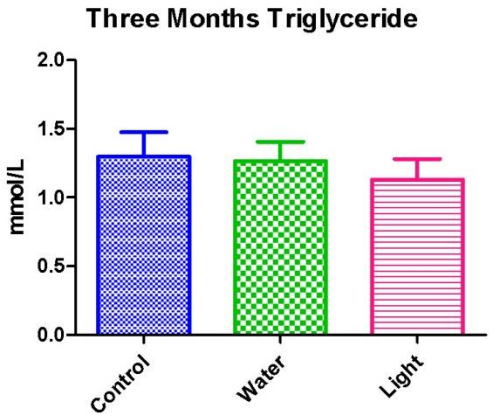

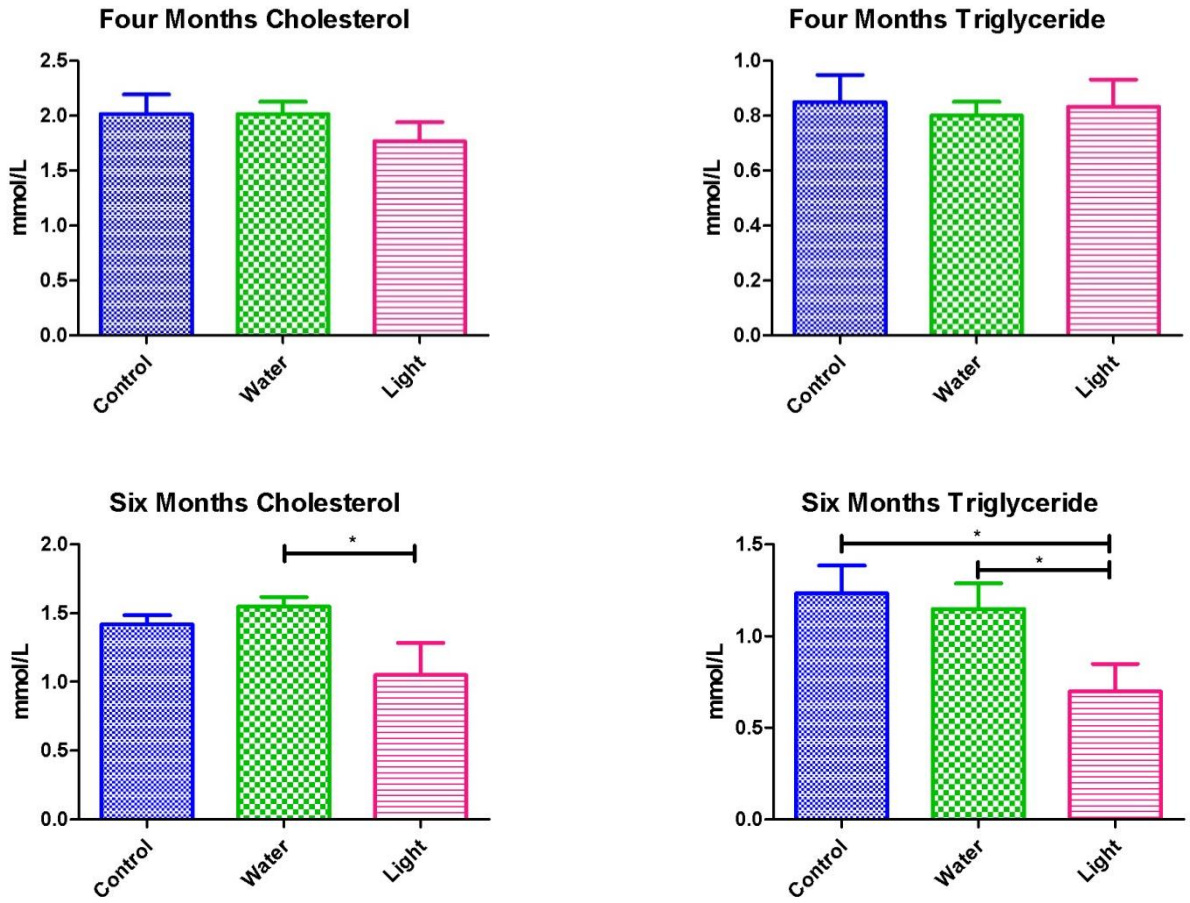

Figure 5.4: Coke Light®- cholesterol and triglyceride blood metabolites. Blood was collected at 0, 2, 3, 4 and 6 months. Values are expressed as mean ± SEM. Baseline to three months n=12 and four to six months n=6. Significance is shown as * $P<0.05$.

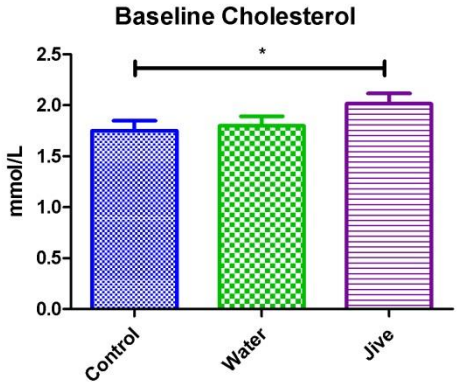

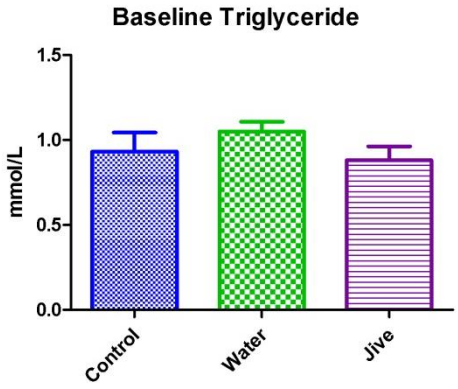

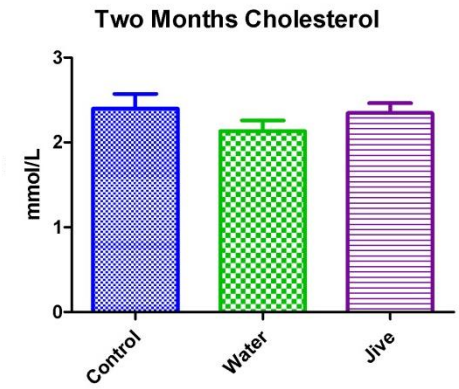

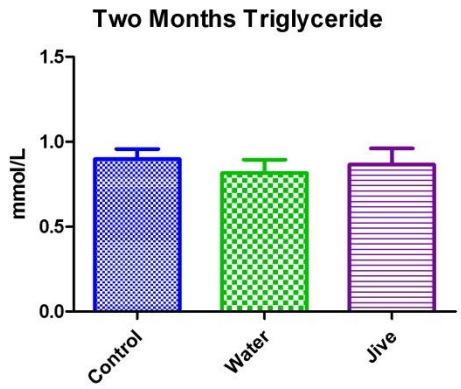

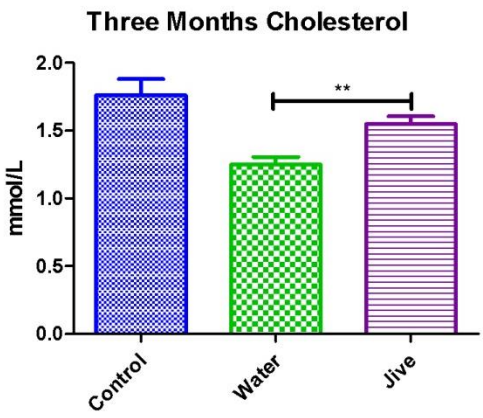

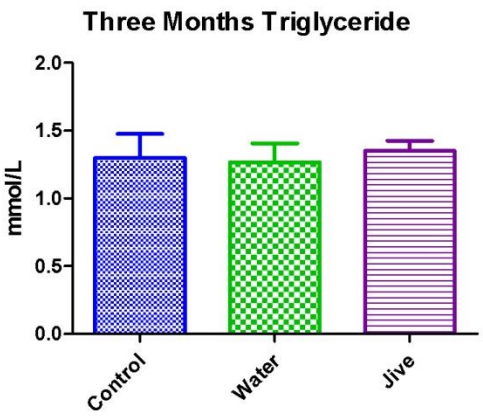

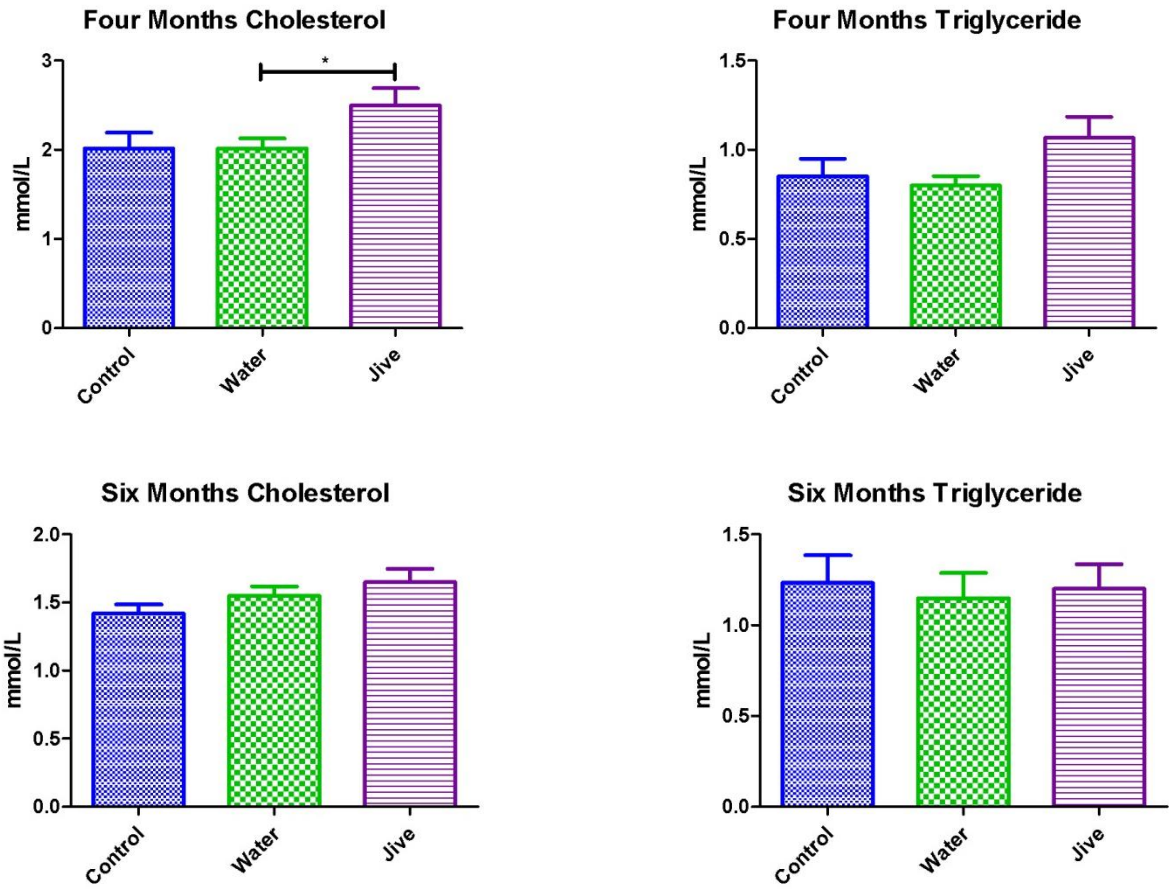

Figure 5.5: Jive®- cholesterol and triglyceride blood metabolites. Blood was collected at 0, 2, 3, 4 and 6 months. Values are expressed as mean ± SEM. Baseline to three months n=12 and four to six months n=6. Significance is shown as * $P<0.05$ and ** $P<0.005$.

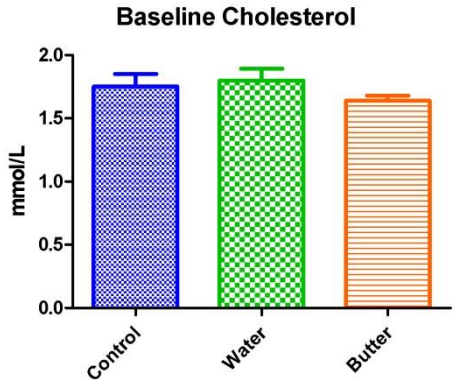

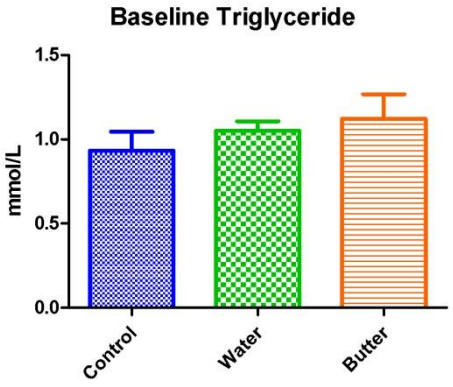

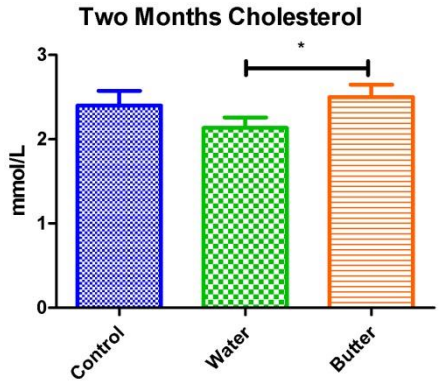

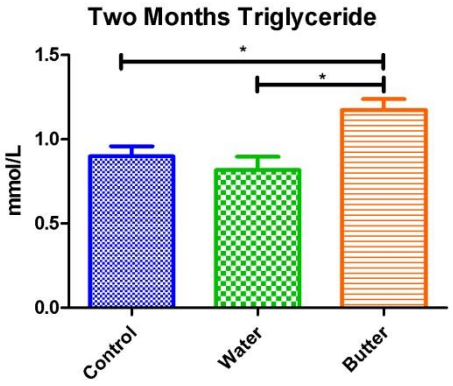

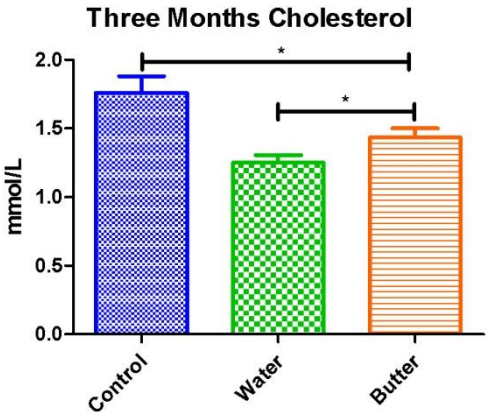

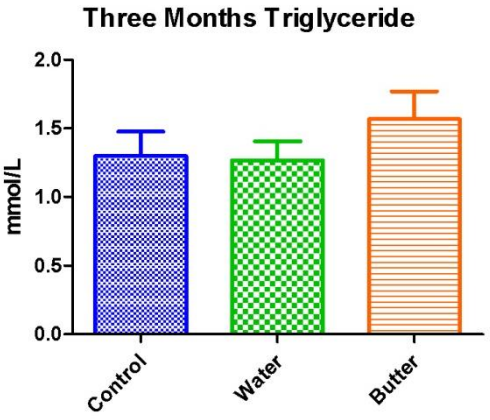

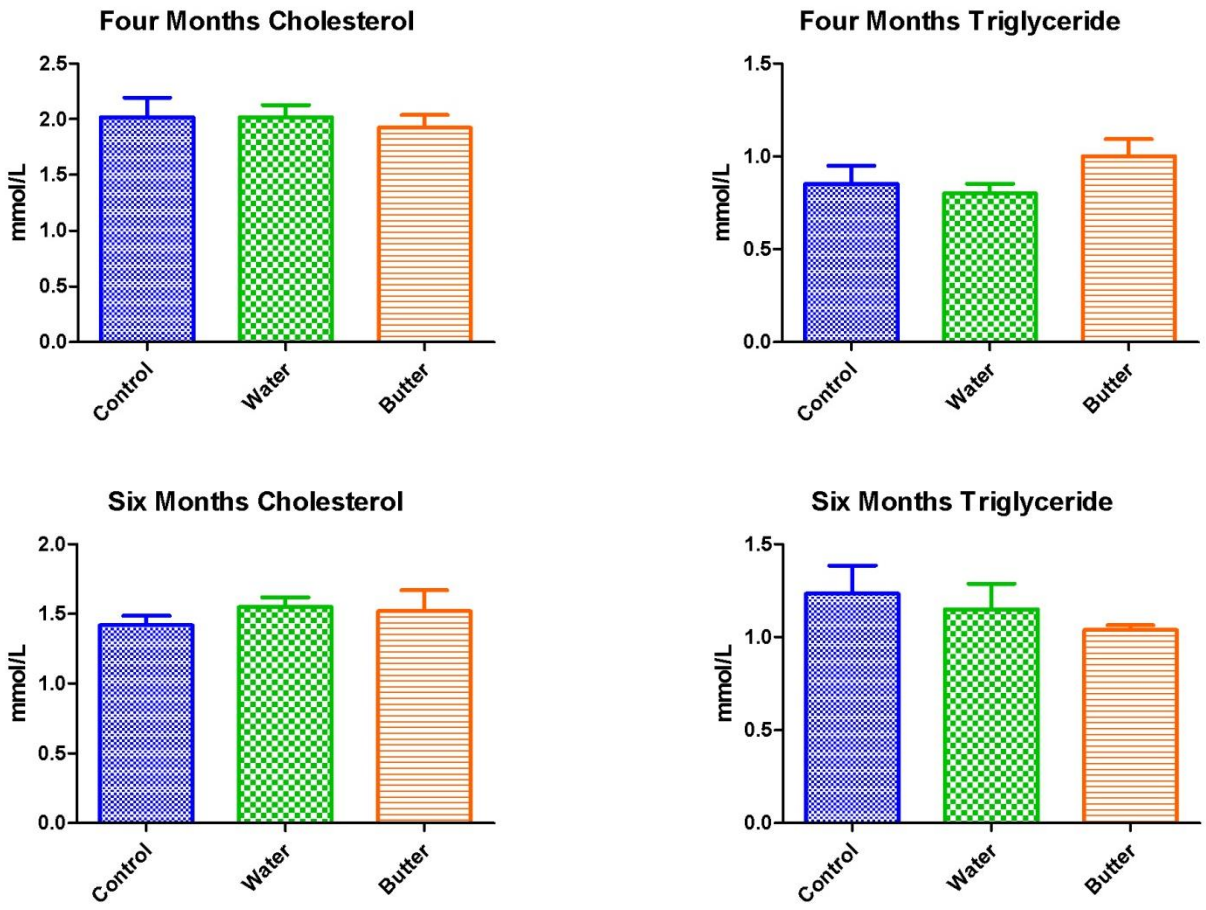

Figure 5.6: Butter- cholesterol and triglyceride blood metabolites. Blood was collected at 0, 2, 3, 4 and 6 months. Values are expressed as mean ± SEM. Baseline to three months n=12 and four to six months n=6. Butter baseline to three months n=11 and four to six months n=5. Significance is shown as * $P<0.05$.

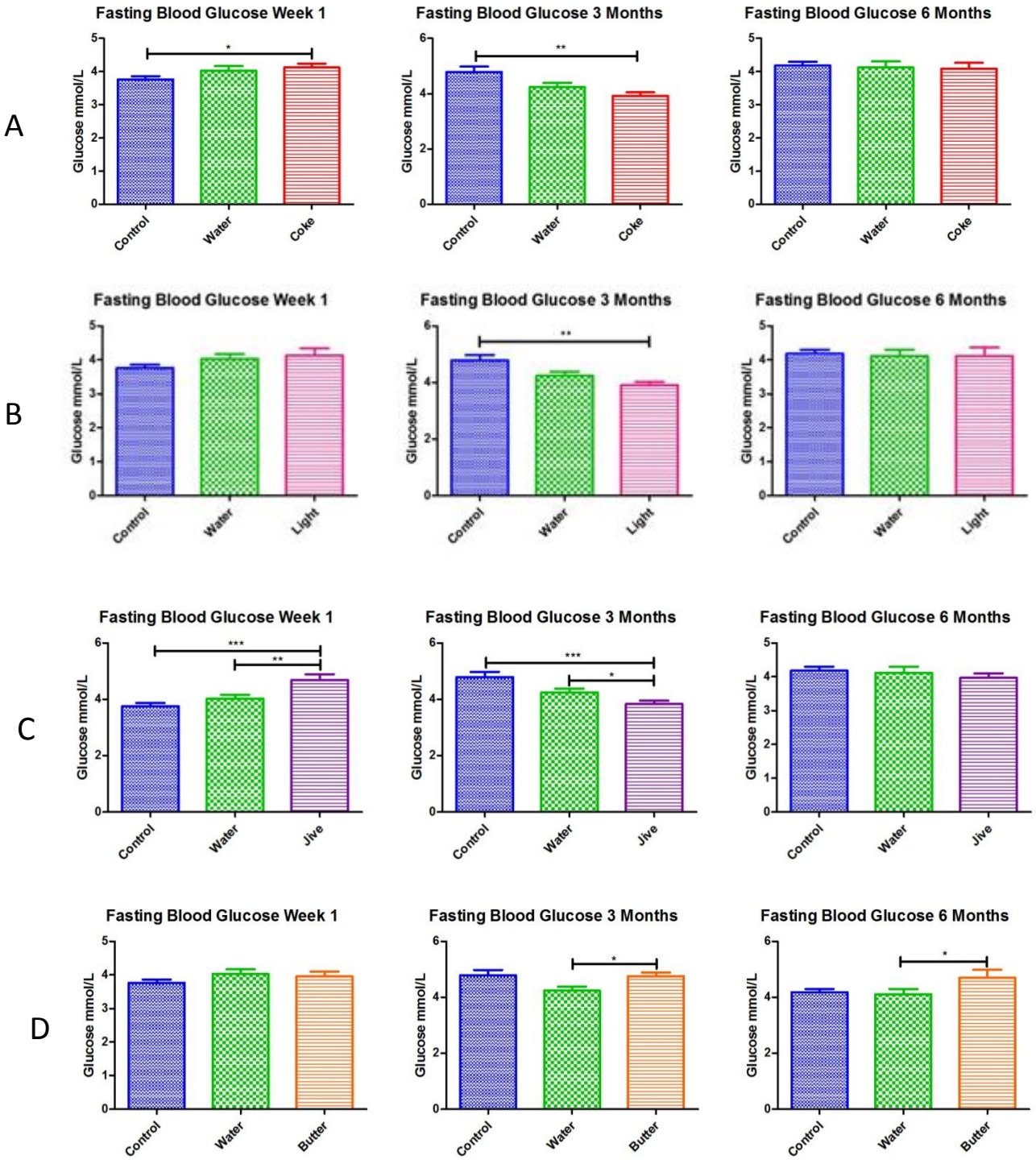

Figure 5.7: Fasted plasma glucose concentrations. A: Coca Cola®, B: Coke Light®, C: Jive®, D: butter. Weeks 1 - 12, n=12; weeks 13 - 24, n=6 – for all experimental groups except the butter group. Butter group: week 1 - 12, n=11; weeks 13 - 24, n=5. Significance is shown as * P<0.05, ** P<0.005 and *** P<0.0005.

5.4 Organ mass analyses

We also determined the weights of various organs and tissues (Figures 5.8 - 5.11).

The Coca Cola® group results after three months revealed no significance between the different groups for heart, muscle, liver or visceral fat weights. A similar pattern was found at the six month time point, except for the liver mass that displayed a decrease compared to both the control and water groups ($P<0.05$ and $P<0.005$, respectively) (Figure 5.8).

For the Coke Light® group we found no differences between the heart, liver and visceral adipose weights after three months. However, the Coke Light® group exhibited heavier muscle weights than the control group ($P<0.005$). After six months there were no significant differences for heart and muscle weights, although we found lowered liver mass versus both the control and water groups ($P<0.005$ and $P<0.001$, respectively). In addition, the Coke Light® group displayed heavier visceral fat mass compared to the control group ($P<0.01$) (Figure 5.9).

For the Jive® group there was no difference between the heart, liver and visceral fat weights after three months despite displaying lighter muscle weight compared to the water group ($P<0.005$). However, the Jive® group exhibited greater heart ($P<0.01$), muscle ($P<0.005$) and liver masses ($P<0.05$ and $P<0.005$, respectively) at six months compared to both the control and water groups. Furthermore, the Jive® group also displayed increased visceral fat mass when compared to the control group ($P<0.01$) (Figure 5.10).

For the butter group the data indicated that there was no significant difference between heart weights after three months. However, the butter group's muscles were lighter than the water group ($P<0.01$) while liver weights were increased versus control and water groups ($P<0.05$ and $P<0.001$, respectively). This group's visceral fat also weighed significantly less than the control group ($P<0.05$). We found no significant differences after six months (Figure 5.11).

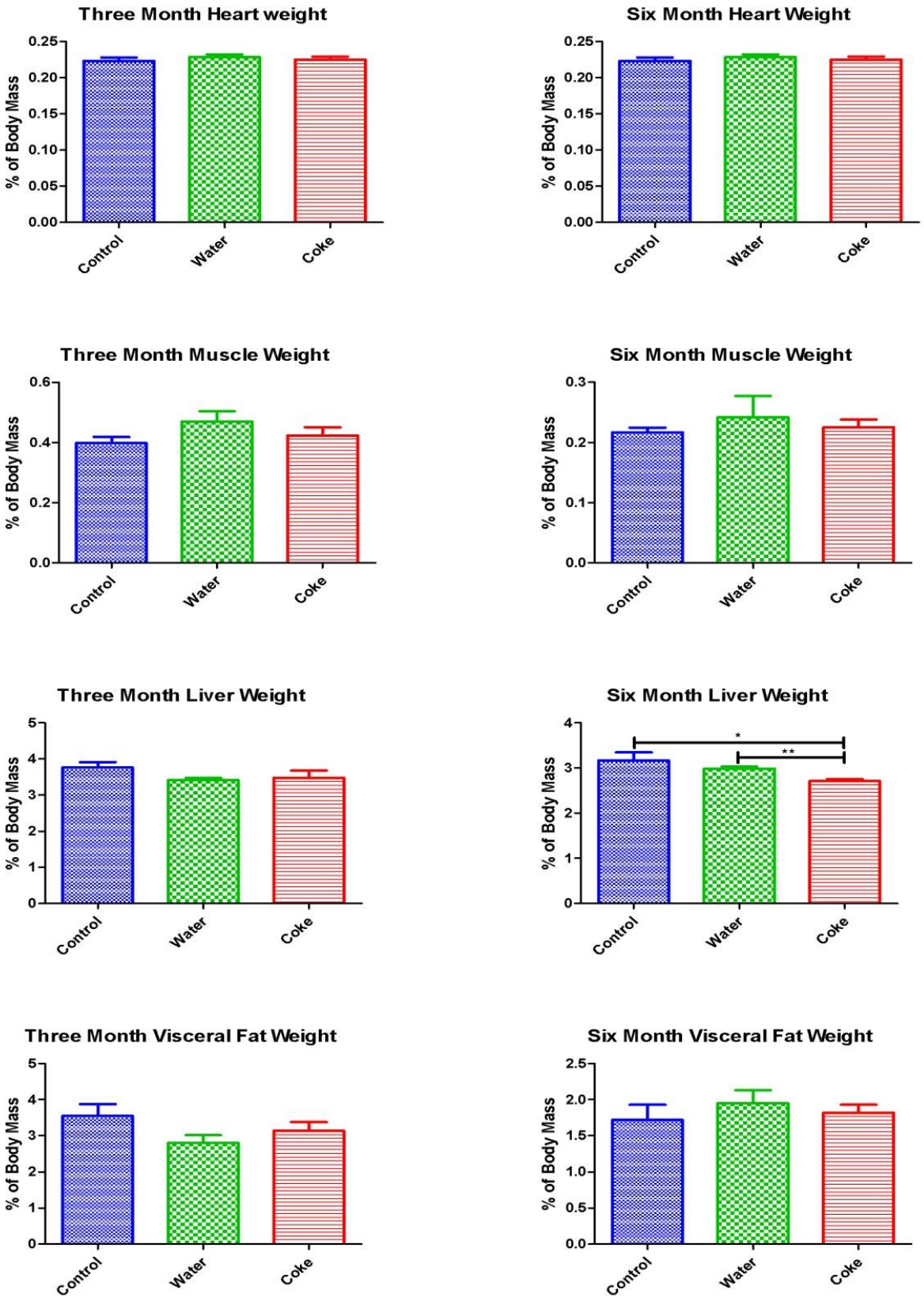

Figure 5.8: *Coca Cola*® *-* organ and tissue weights as a percentage of total body mass (n=6). Values are expressed as mean ± SEM. Significance is shown as * P<0.05 and ** P<0.005.

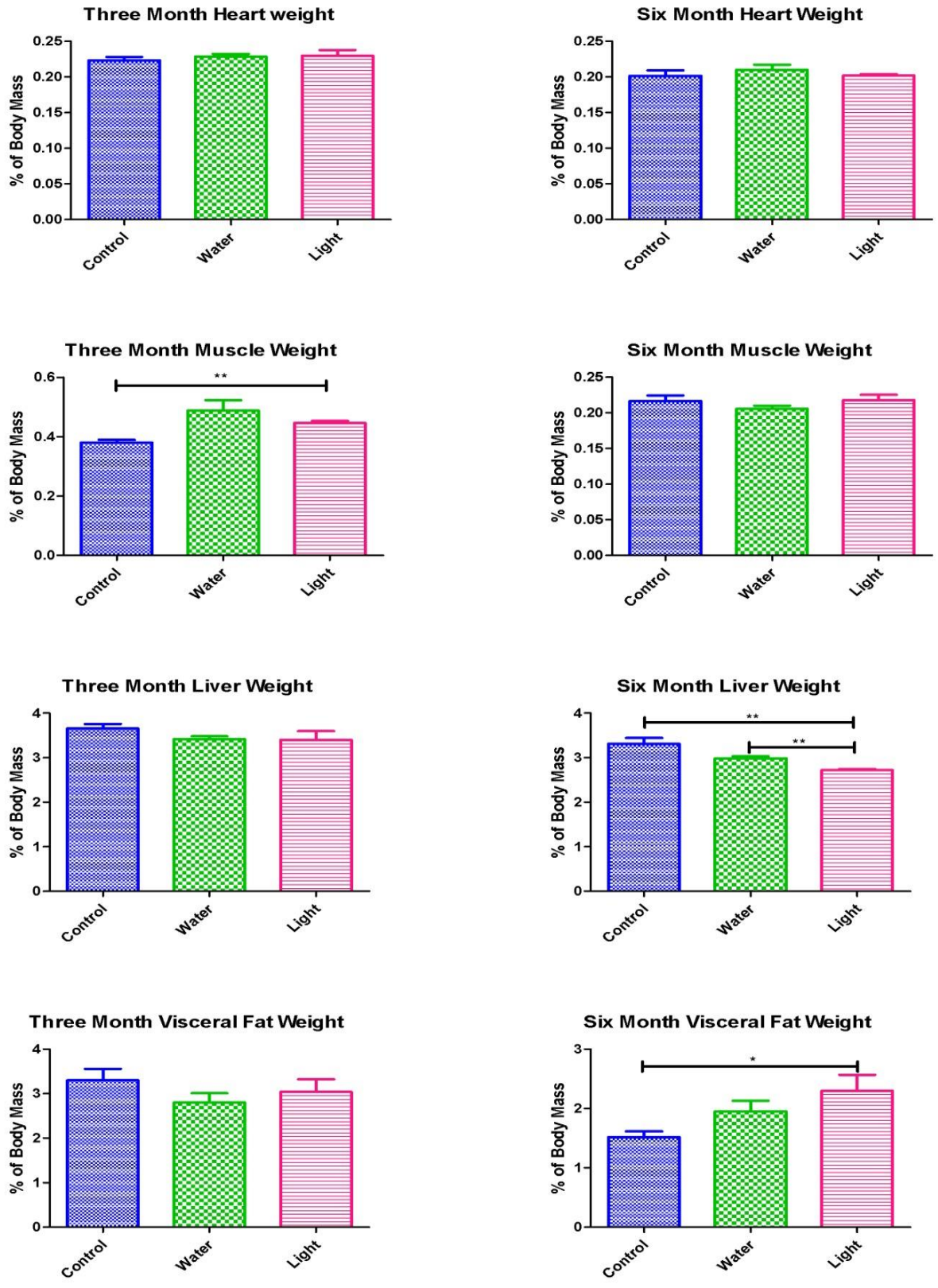

Figure 5.9: Coke Light® - organ and tissue weights as a percentage of total body mass (n=6). Values are expressed as mean ± SEM. Significance is shown as * P<0.05 and ** P<0.005.

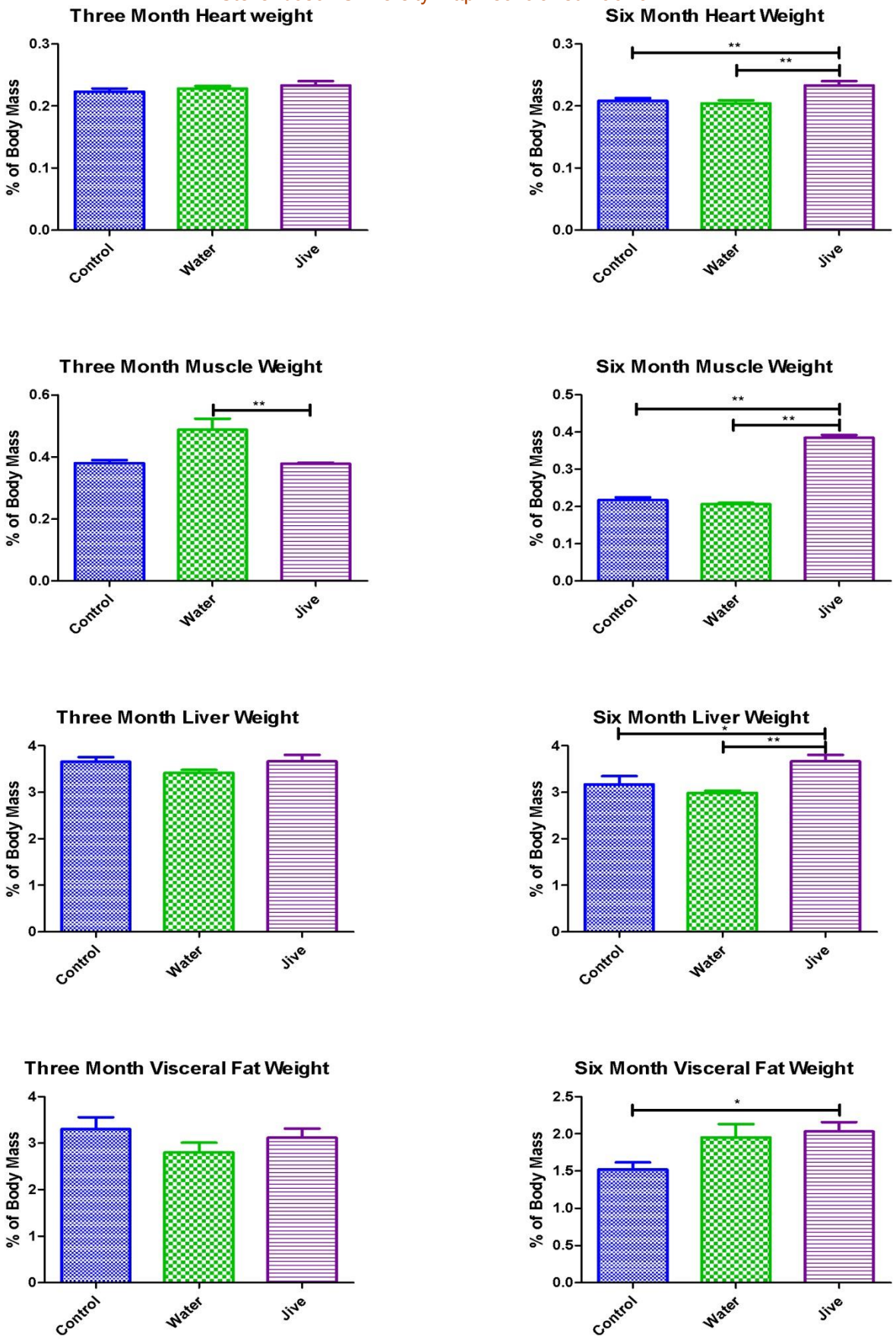

Figure 5.10: Jive® - organ and tissue weights as a percentage of total body mass (n=6). Values are expressed as mean ± SEM. Significance is shown as * P<0.05 and ** P<0.005.

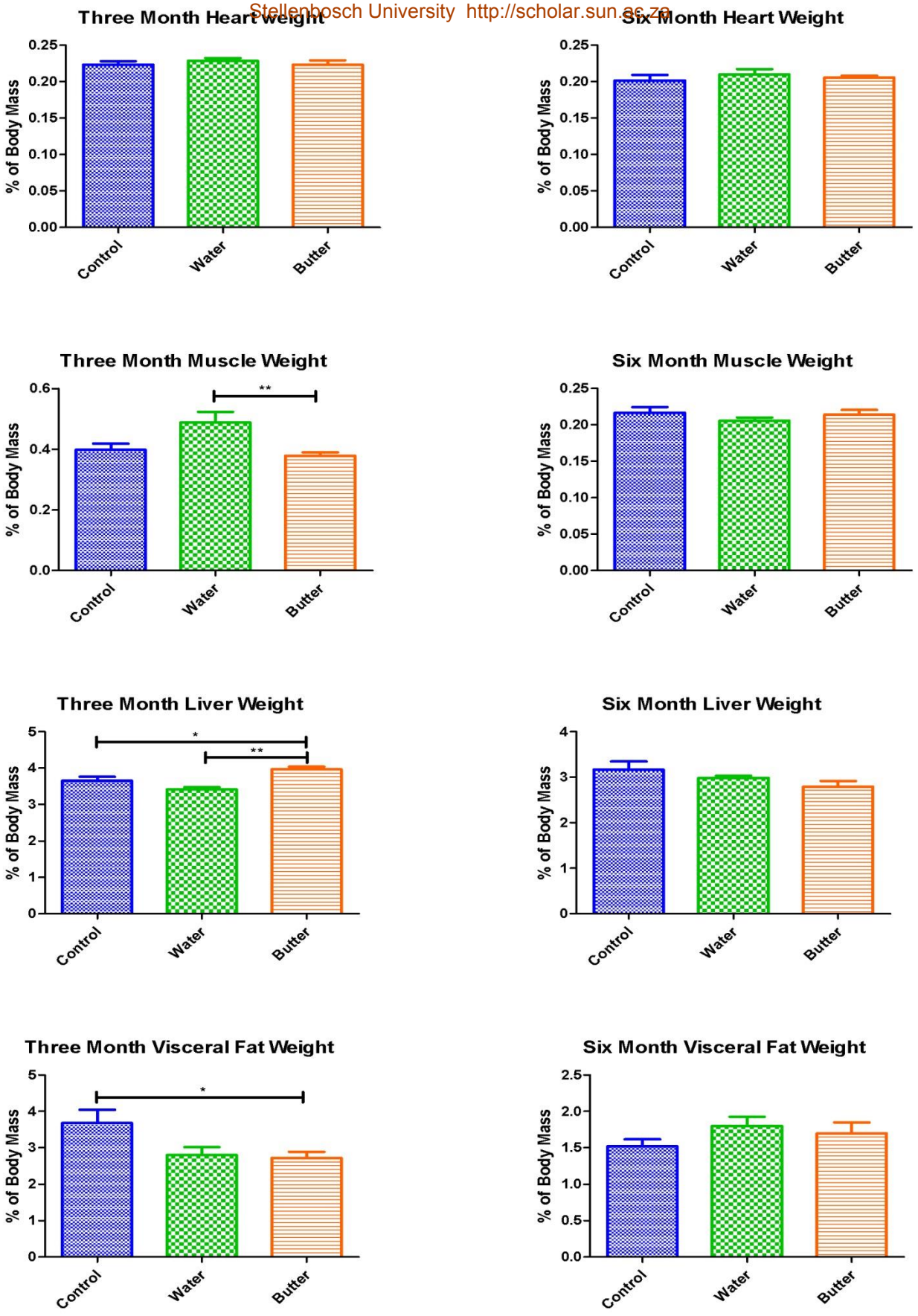

Figure 5.11: Butter- organ and tissue weights as a percentage of total body mass (n=6 for all except n=5 for 6-months butter group). Values are expressed as mean ± SEM. Significance is shown as * P<0.05 and ** P<0.005.

5.5 Adipocyte area analyses

The total area of visceral adipocytes was measured only at six months – due to limited tissue availability (Figure 5.12). The Coca Cola® group displayed increased fat cell surface area compared to both the control and water groups (P< 0.05 and P<0.0001, respectively). A similar result was found for the Coke Light® group, although only significant when compared to the water group (P< 0.005). Conversely, the Jive® group exhibited reduced fat cell surface area compared to both the control and water groups (P<0.0001 and P< 0.005, respectively). No significant differences were found for the butter group. Figure 5.13 display an example of the histological images used to generate the area of the fat cell data.

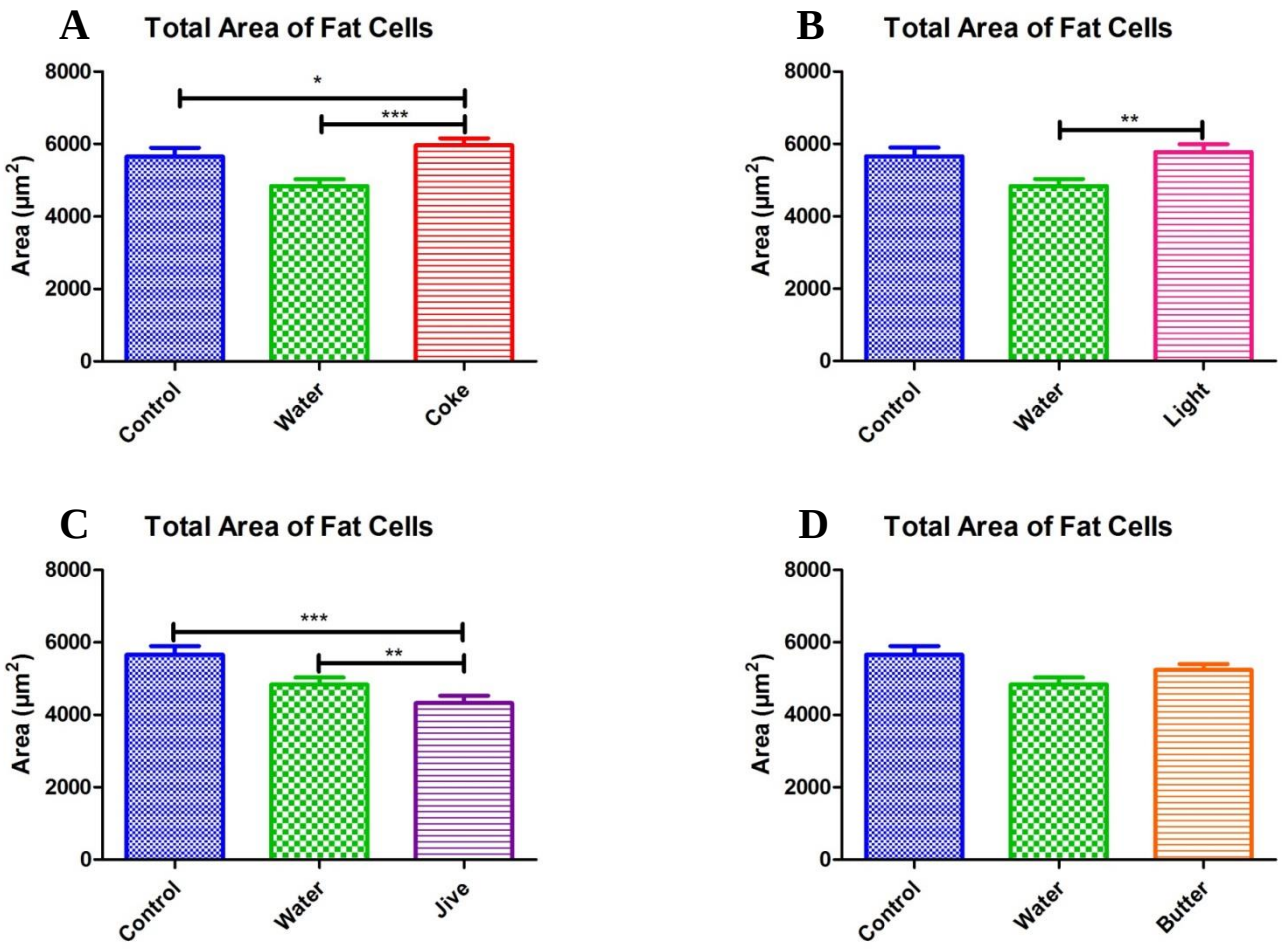

Figure 5.12: The total area of fat cells in the rat's visceral adipose tissue. A: Coca Cola®, B: Coke Light®, C: Jive®, D: butter. The left visceral fat pad was collected from each group (n=6), butter (n=5). Twelve images were taken of each group and 110 adipocytes were measured (μm^2) per group. Values are expressed as mean ± SEM. Significance is shown as * P< 0.05, ** P<0.005 and *** P<0.0005.

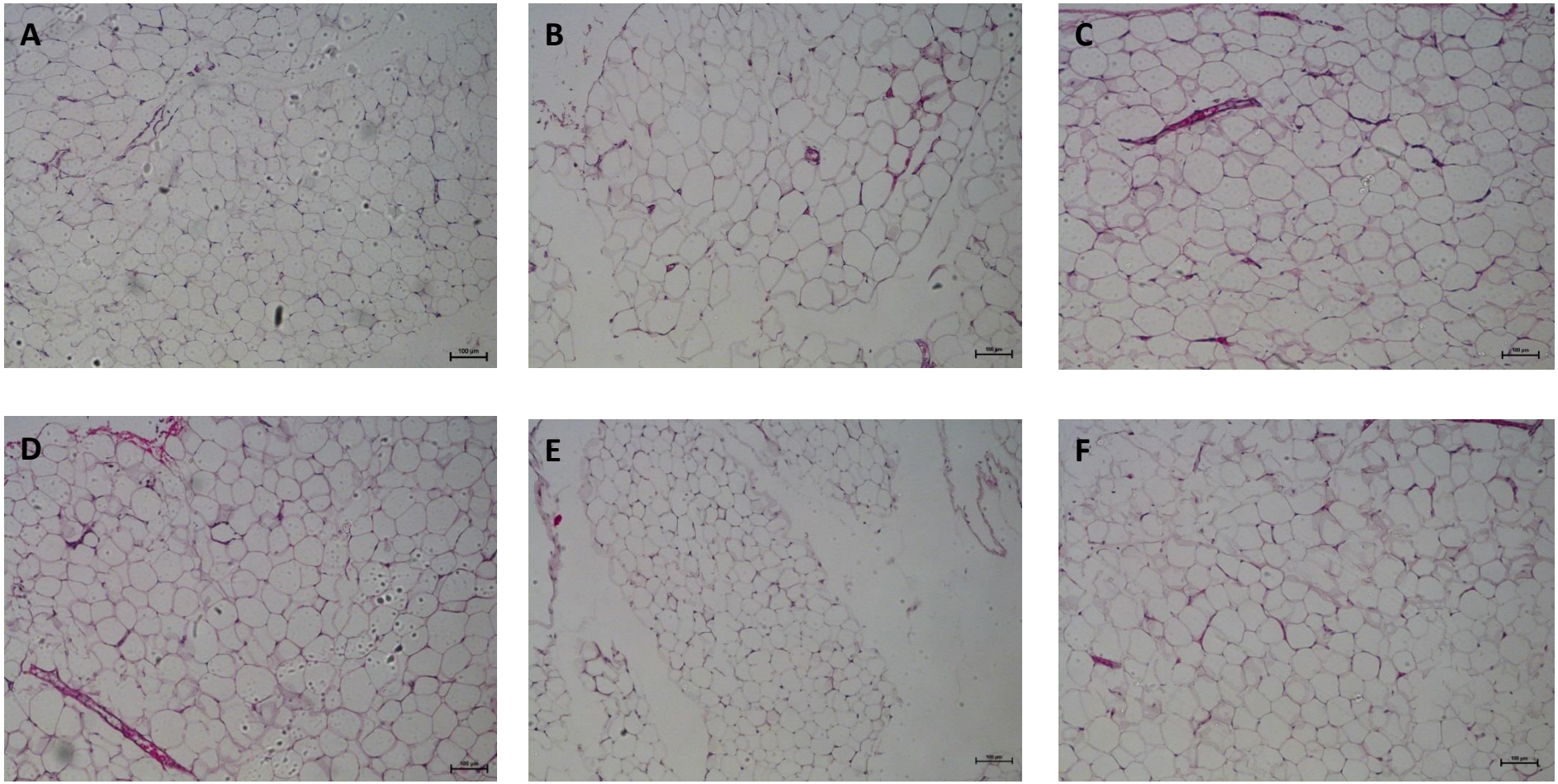

Figure 5.13: Histological images used to calculate the area of the fat cells. Twelve images were taken of each group and 110 adipocytes were measured (μm^2) per group. A: Control, B: Water and C: Coca Cola®, D: Coke Light®, E: Jive®, F: Butter

Chapter 6

Chronic SSB model – baseline characterization (glucose metabolism, NOGP activation)

6.1 Oral glucose tolerance tests

The results of OGTTs, which were performed bi-weekly over a period of six months, are reflected in Figures 6.1 to 6.8. Each treatment group's results are shown separately. Only baseline, three and six months results will be shown, as the animals were sacrificed at three month intervals.

6.1.1 Coca Cola®

Results from week one indicated no significant differences at the 15 minute time point. At 30 minutes the Coca Cola® group displayed significantly reduced blood glucose levels compared to water, while at 120 minutes Coca Cola® generated variable data versus control and water groups, respectively ($P<0.005$ and $P<0.0001$). At three months there was no significance at 30 and 120 minutes, however, at 15 minutes lower glucose levels were observed compared to the control group ($P<0.001$). The six month results indicated no significant differences at 30 minutes. At 15 minutes there was a significant increase in Coca Cola® blood glucose levels compared to both the control and water groups ($P<0.005$ and $P<0.05$, respectively). There was also a significant reduction in the Coca Cola® glucose levels compared to the water group at 120 minutes (refer to Figures 6.1 & 6.2).

6.1.2 Coke Light®

Results from week one indicated significance, at 15 minutes with the Coke Light® group exhibiting significantly elevated glucose levels compared to the water group. After 30 minutes Coke Light® showed diminished glucose levels versus the control and water groups ($P<0.05$ and $P<0.0005$, respectively), while at the 120 minute time point there were various degrees of significance between Coke Light® and the two groups ($P<0.05$ and $P<0.005$, respectively). At three months the Coke Light® had significantly reduced glucose levels at 15, 30 and 120 minutes compared to the control group's respective time points. The six month results revealed no significant differences between the groups at 30 and 120 minutes.

However, at the 15 minute time point the Coke Light® group displayed elevated glucose levels compared to the control and water groups ($P<0.01$ and $P<0.05$, respectively) (refer to Figures 6.3 & 6.4).

6.1.3 Jive®

During week one, Jive® showed significantly elevated glucose levels at 15 minute and variable difference at 120 minute versus both the control and water groups. By contrast, at 30 minutes the Jive® displayed lowered glucose levels compared to the water group ($P<0.0005$). At the three month time point, Jive® presented with lower glucose levels at 15 minutes when compared to respective control and water groups ($P<0.0001$ and $P<0.0005$, respectively). The Jive® group levels were also significantly lower than the water group at the 30 minute time point, but no differences were observed at 120 minutes. At six months there were no significant differences between the groups at 15 and 30 minutes. However, Jive® was significantly lower than both the control and water groups at 120 minutes (refer to Figures 6.5 & 6.6).

6.1.4 Butter

Week one's results revealed no significance at 30 minutes. However, the butter group showed lower blood glucose levels than the control group at 15 minutes ($P<0.05$), while at 120 minutes it showed higher levels versus the control group ($P<0.0001$). At three months the butter group showed reduced blood glucose levels at 15 minutes compared to the control group ($P<0.0005$). No further significance was found at 30 or 120 minutes. At six months, the butter group had significantly greater blood glucose levels than both the control and water groups at 15 minutes. There was no significance at 30 or 120 minutes for the six month time period (refer to Figures 6.7 & 6.8).

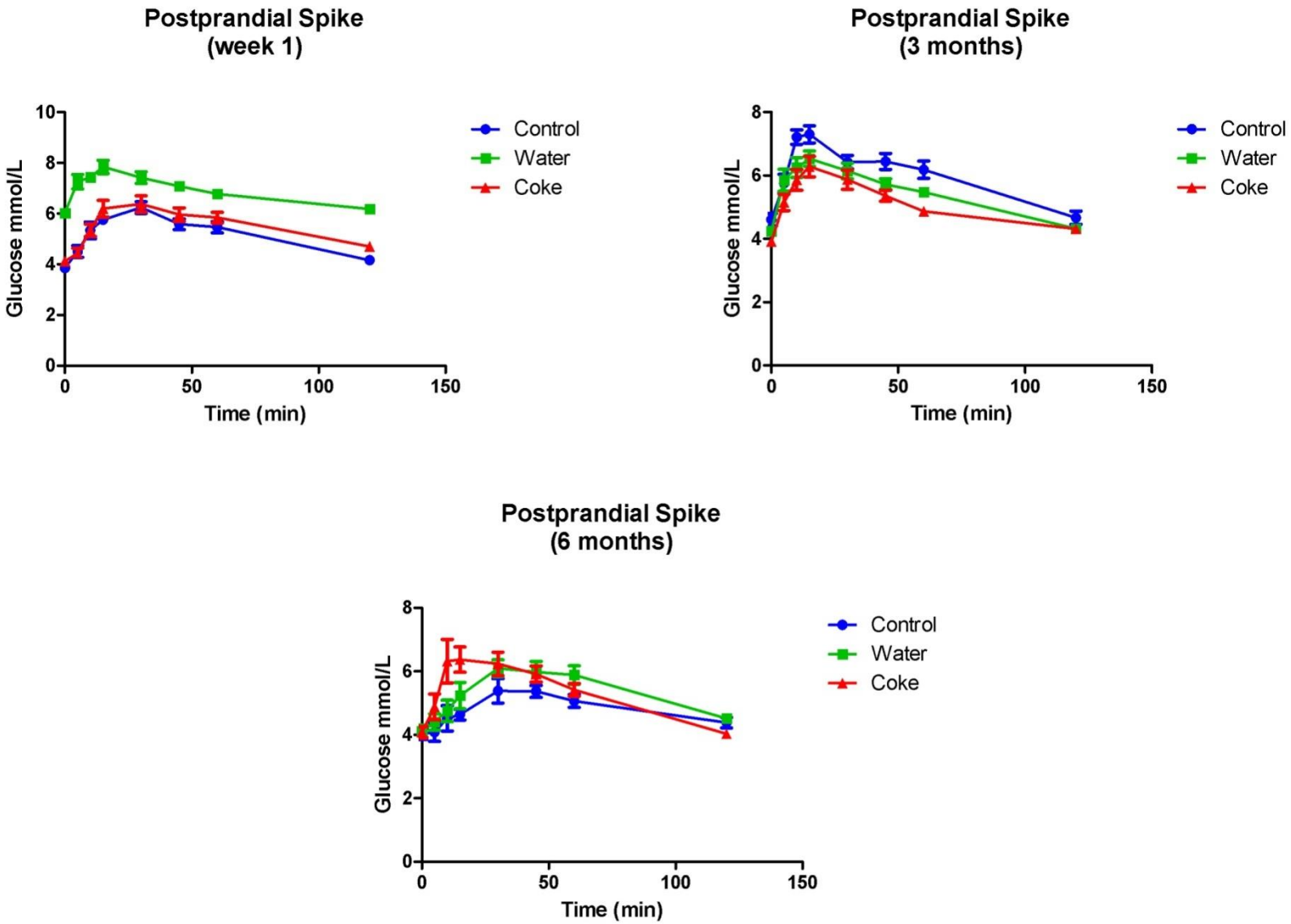

Figure 6.1: Coca Cola®- Oral glucose tolerance tests performed at various stages over the course of the six month experimental period. Glucose levels were tested at 0, 5, 10, 15, 30, 45, 60 and 120 minutes (n=6). Values are expressed as mean ± SEM.

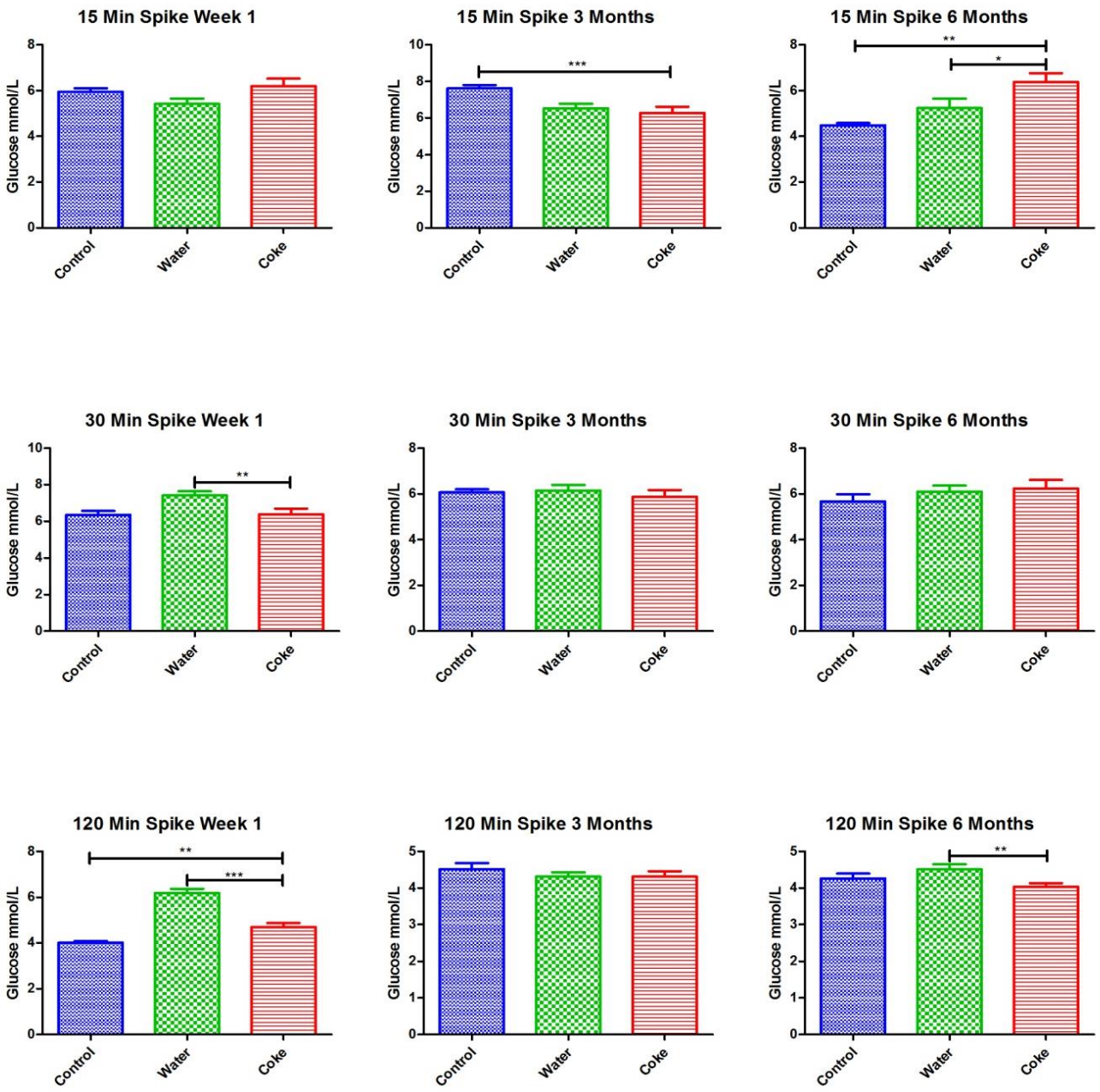

Figure 6.2: Coca Cola®- Oral glucose tolerance tests indicating glycemic state (n=12 for baseline [week 1] to three months; n=6 for six the month time point). Values are expressed as mean ± SEM. Significance is shown as * P<0.05, ** P<0.005 and *** P<0.0005.

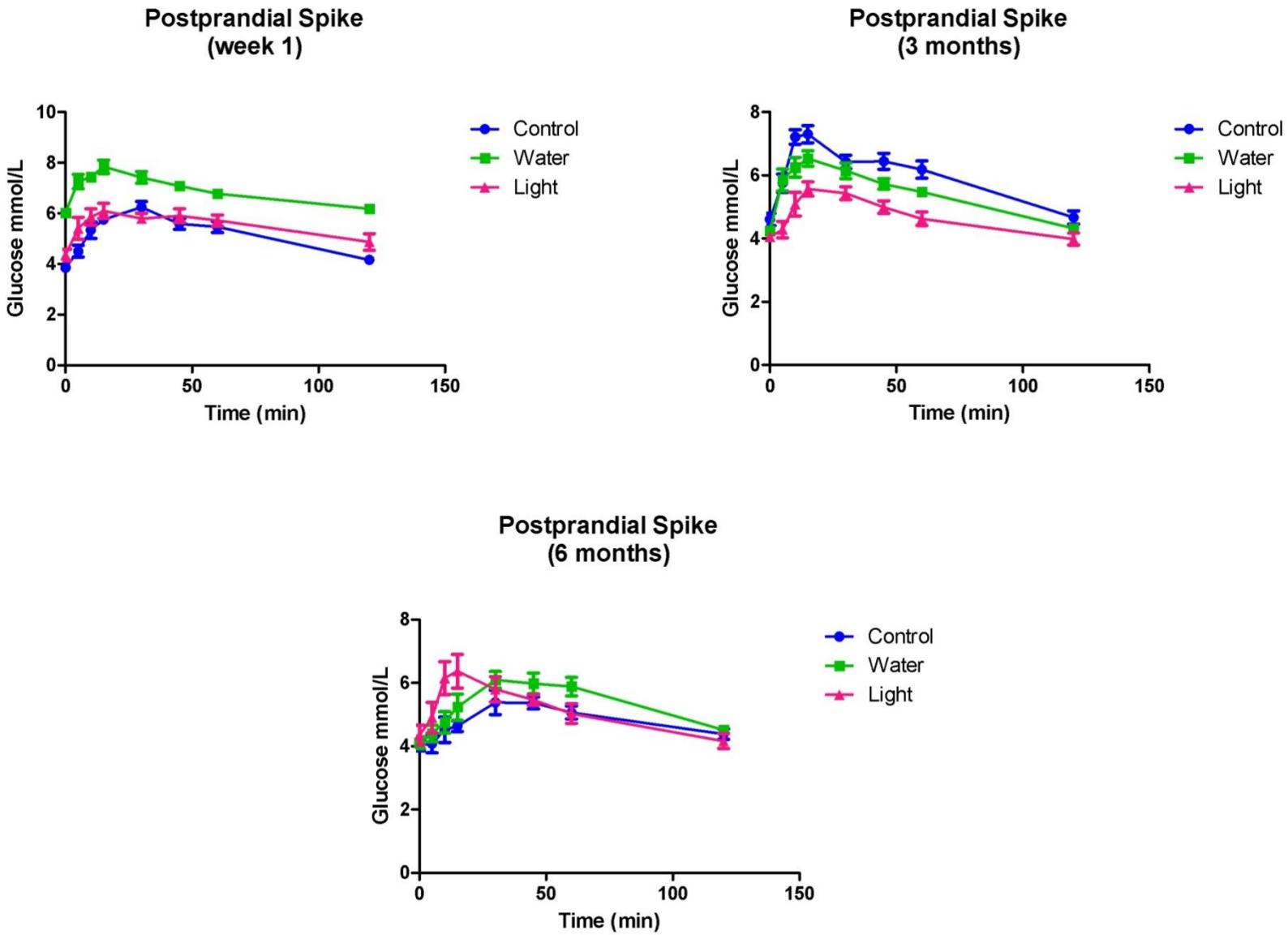

Figure 6.3: Coke Light®- Oral glucose tolerance tests indicating glycemic state. Glucose levels were tested at 0, 5, 10, 15, 30, 45, 60 and 120 minutes (n=12 for baseline [week 1] to three months; n=6 for the six month time point). Values are expressed as mean ± SEM.

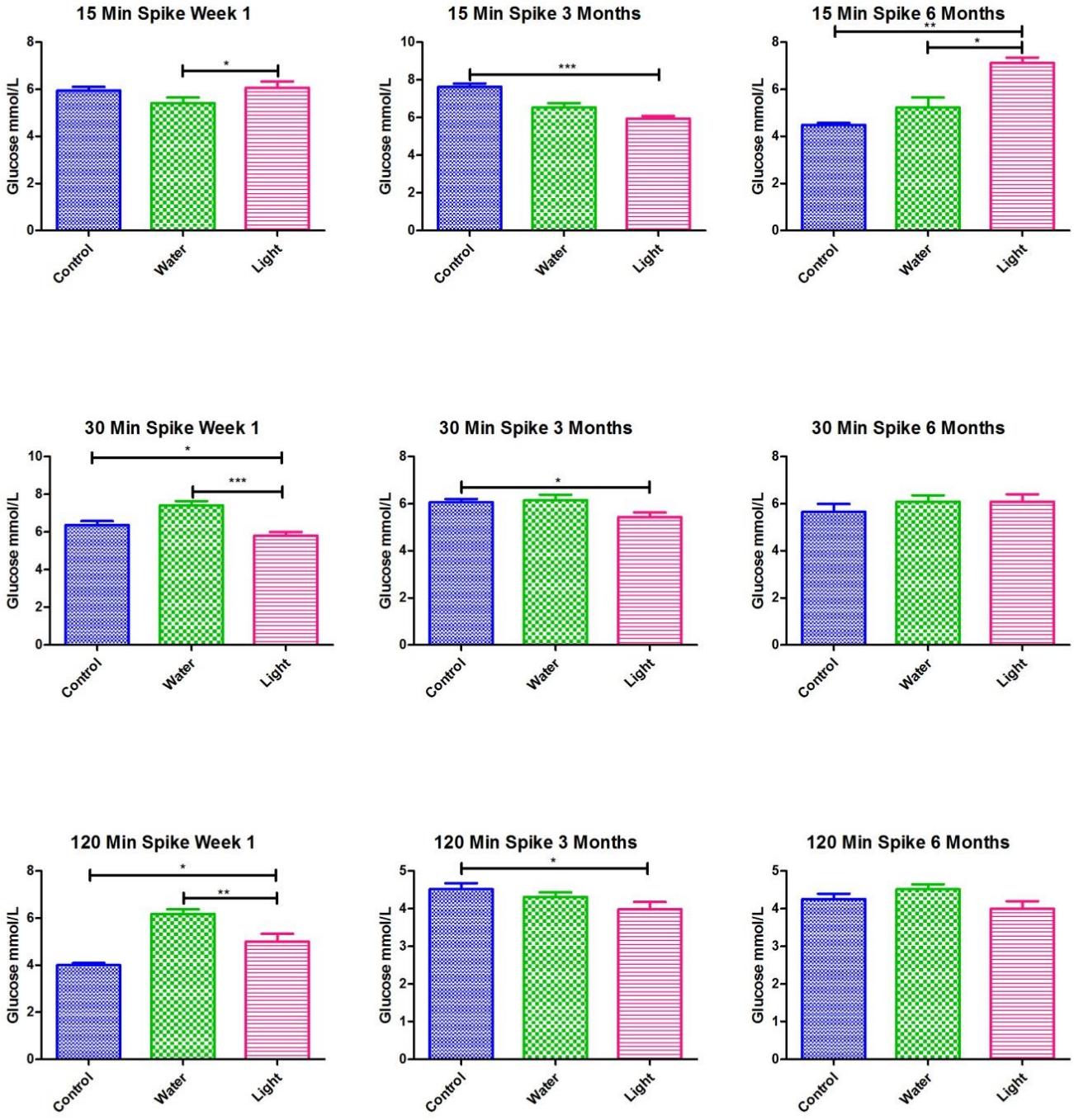

Figure 6.4: Coke Light®- Oral glucose tolerance tests indicating glycemic state. (n=12 for baseline [week 1] to three months; n=6 for the six month time point). Values are expressed as mean ± SEM. Significance is shown as * P<0.05, ** P<0.005 and *** P<0.0005.

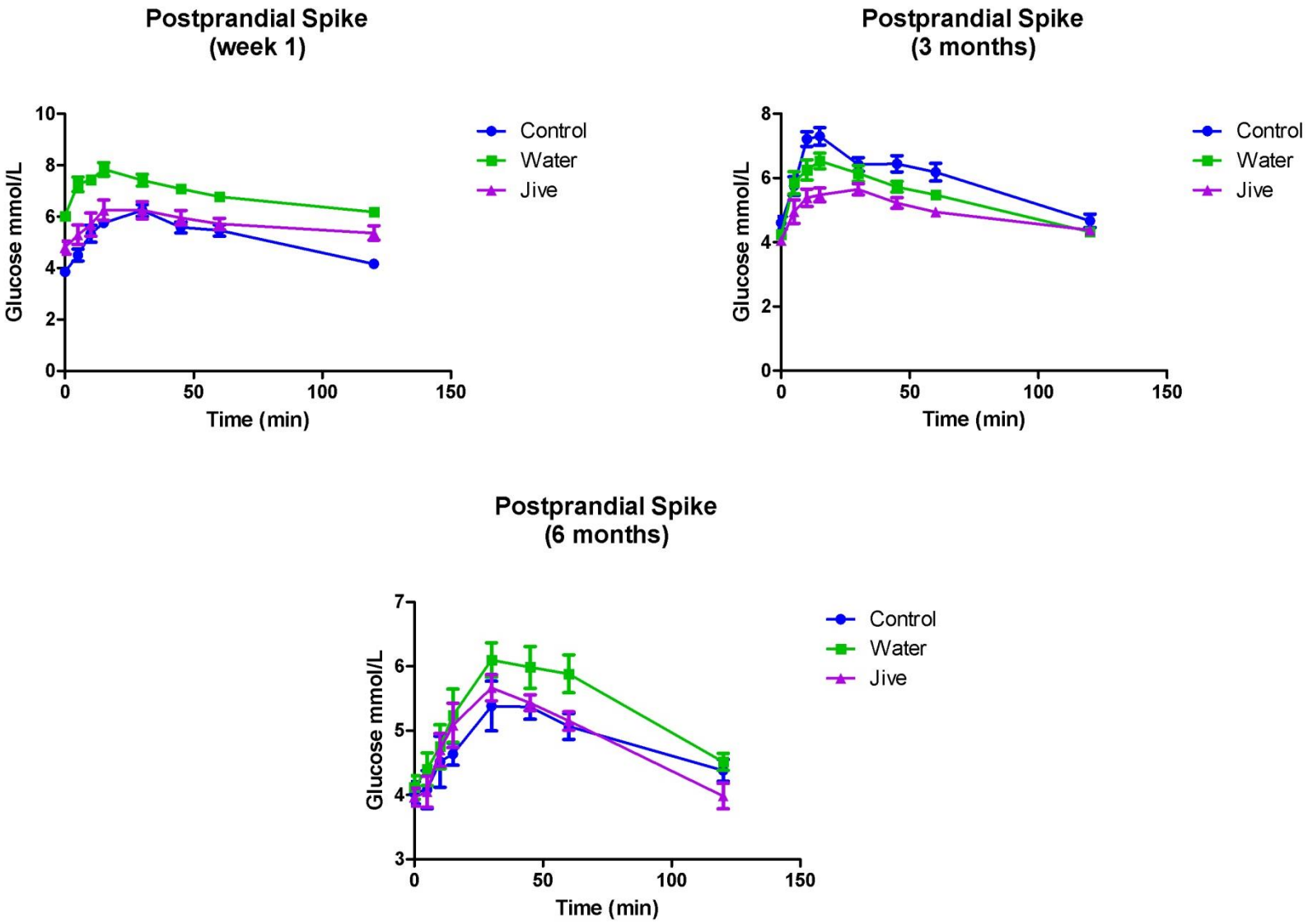

Figure 6.5: Jive®- Oral glucose tolerance tests indicating glycemic state. Glucose levels were tested at 0, 5, 10, 15, 30, 45, 60 and 120 minutes (n=12 for baseline [week 1] to three months; n=6 for the six month time point). Values are expressed as mean ± SEM.

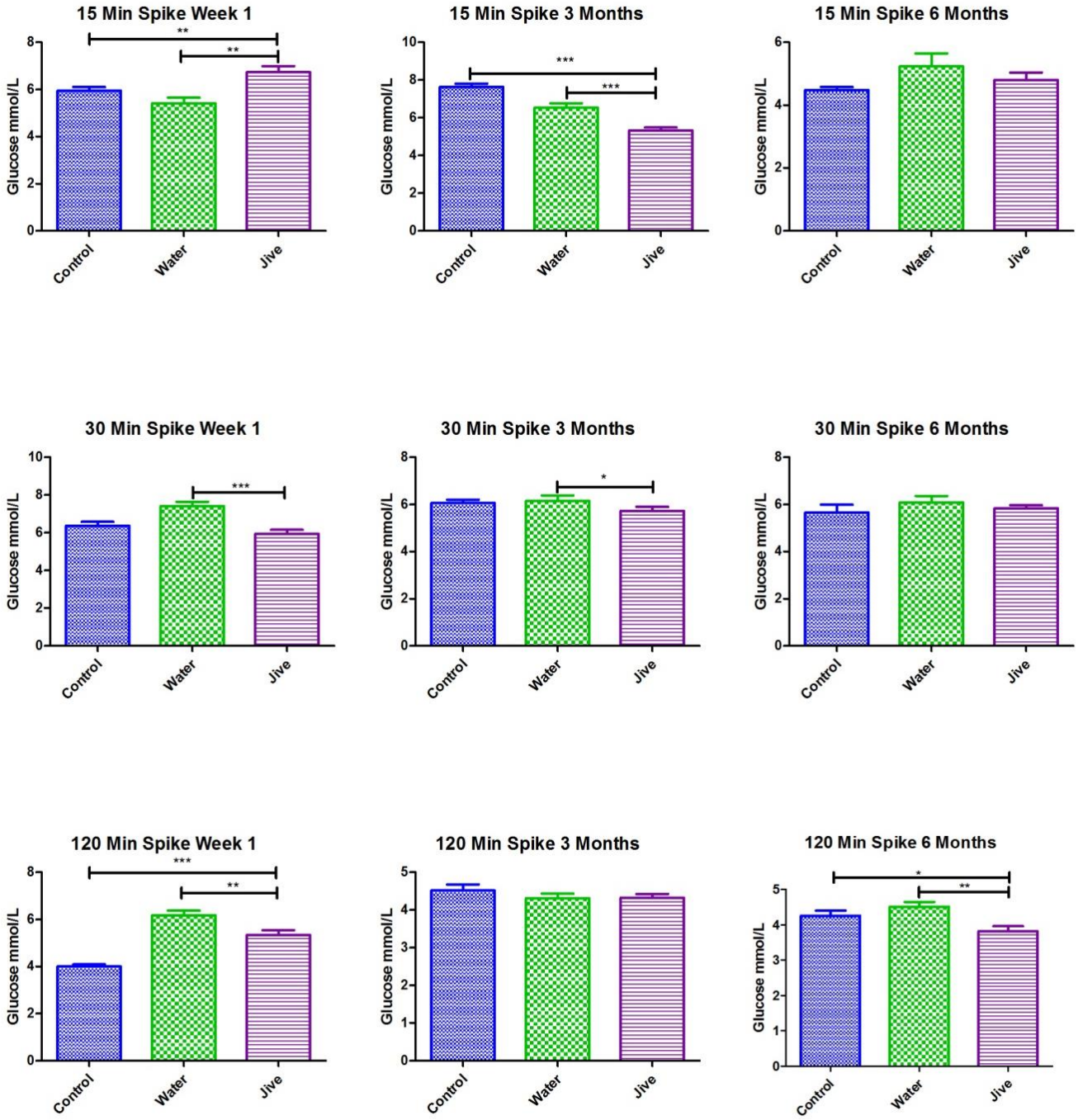

Figure 6.6: Jive®- Oral glucose tolerance tests indicating glycemic state (n=12 for baseline [week 1] to three months; n=6 for the six month time point). Values are expressed as mean ± SEM. Significance is shown as *P<0.05, ** P<0.005 and *** P<0.0005.

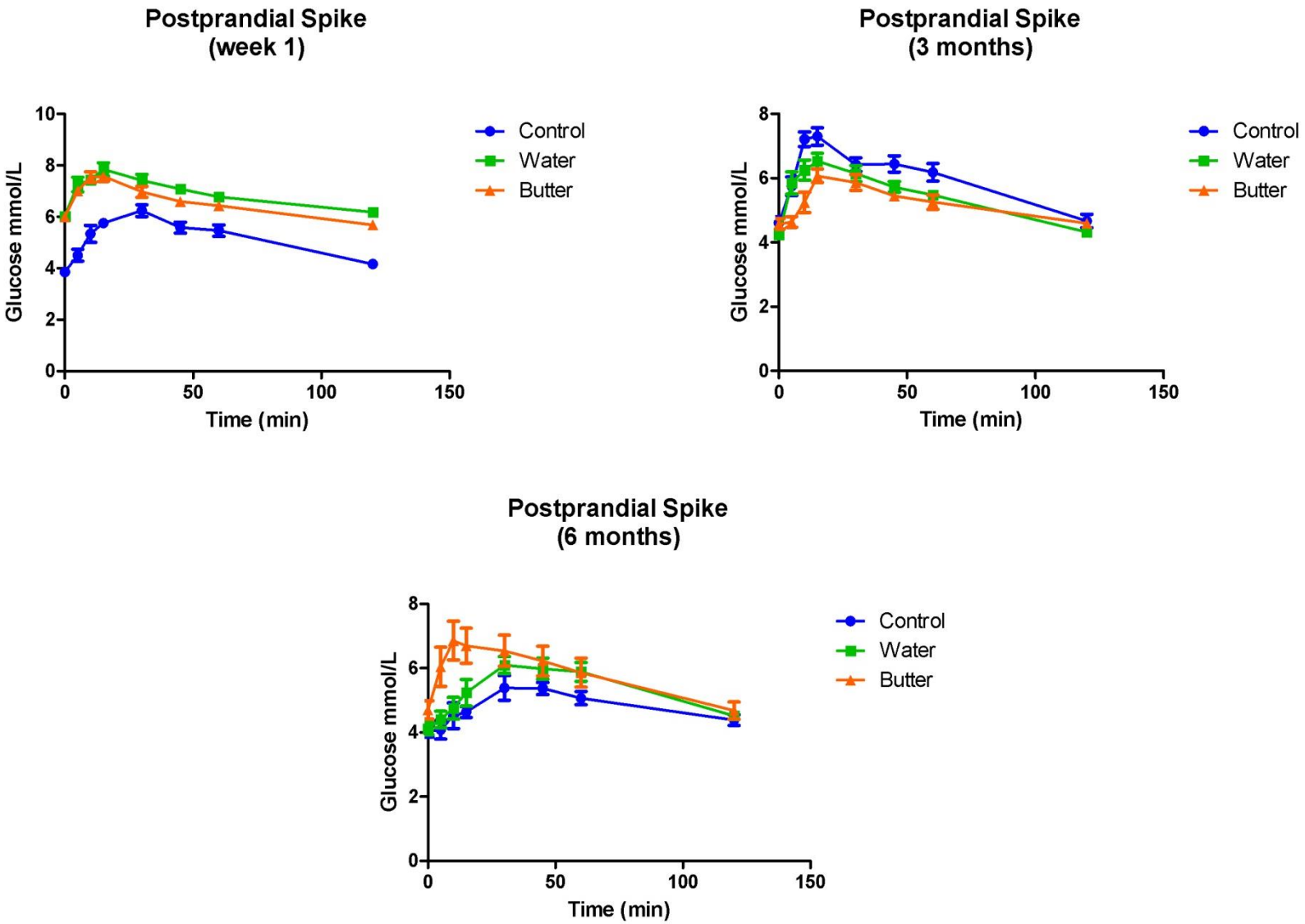

Figure 6.7: Butter- Oral glucose tolerance tests indicating glycemic state. Glucose levels were tested at 0, 5, 10, 15, 30, 45, 60 and 120 minutes (n=12 for baseline [week 1] to three months; n=6 for the six month time point for all experimental groups except the butter group. Butter group: week 1 - 12, n=11; weeks 13 - 24, n=5.). Values are expressed as mean ± SEM.

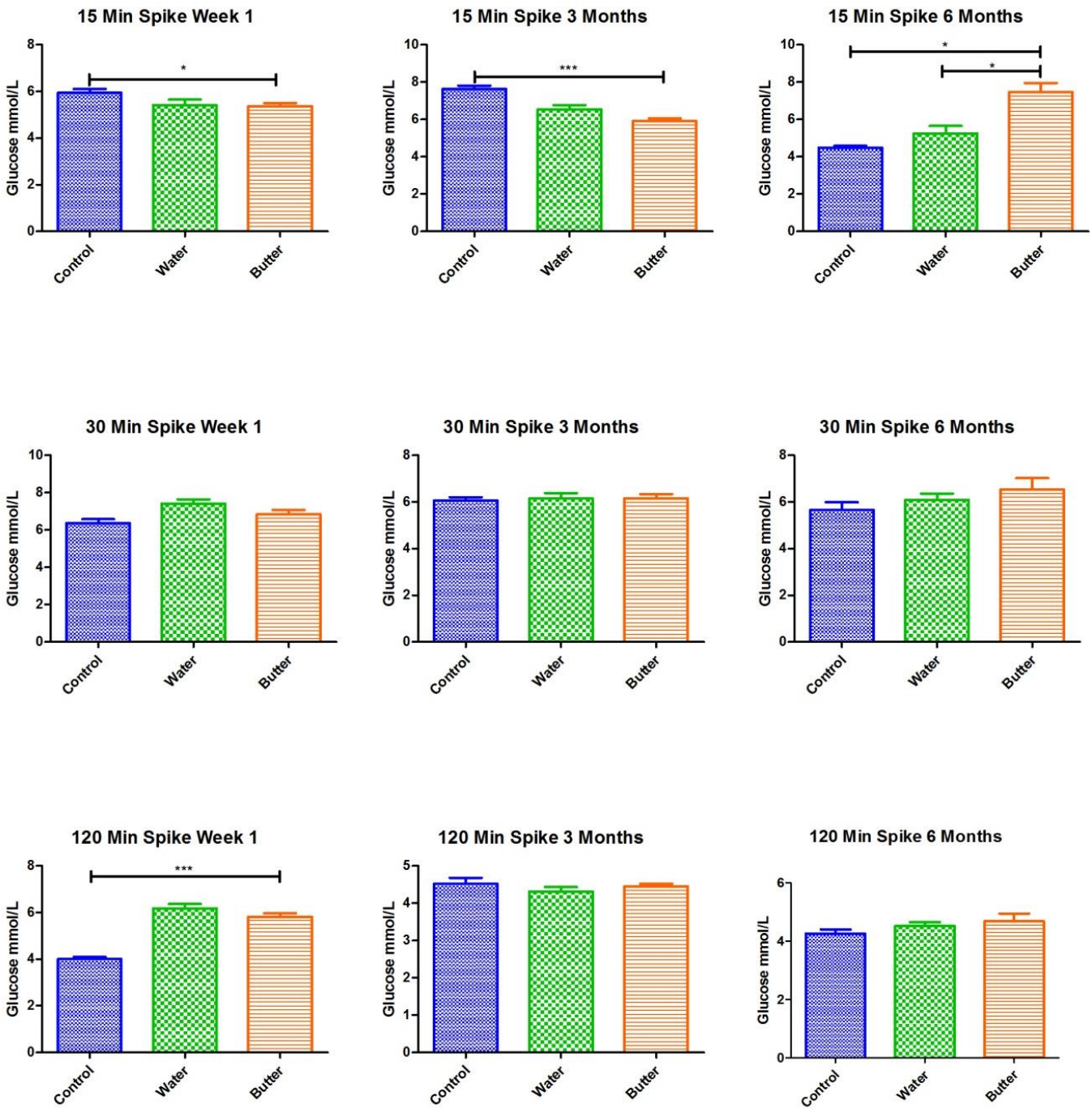

Figure 6.8: Butter- Oral glucose tolerance tests indicating glycemic state. Baseline (week 1) to three months n=12; six months n=6 for the control and water groups; baseline to three months n=11; six months n=5 for the butter group. Values are expressed as mean ± SEM. Significance is shown as * P<0.05 and *** P<0.0005.

6.2 Non-oxidative glucose pathway in the heart

OGTTs were performed biweekly in order to monitor the animal's glycemic states and to evaluate the effects of SSBs, ASBs and butter on postprandial hyperglycemic excursions. This model was created to replicate acute hyperglycemic events by daily gavaging animals with various experimental substances. Although NOGPs are not formal risk factors to test for the development of IR or T2D, they are associated with hyperglycemia, and if activated continually may eventually lead to T2D and cardiac dysfunction. Together hyperglycemia and its downstream activation of NOGPs can lead to metabolic derangements within the myocardium and contribute to the onset of cardiovascular complications.

6.2.1 Advanced glycation end products (AGE)

The levels of MG were measured in order to determine activation of the AGE pathway – refer Figure 6.9. Significant differences were found at three months, i.e. the Coca Cola® group displayed lower MG levels compared to the water group. However, there were no differences at six months.

The Coke Light® group showed a decrease at three months compared to the water group ($P<0.01$). The six month results show elevated MG levels in the Coke Light® group compared to the control group ($P<0.05$).

At three months the Jive® group exhibited significantly higher MG levels compared to the control group but at six months levels were significantly lower than both the control and water groups.

At three months the butter group showed higher MG levels compared to the control groups ($P<0.05$). Conversely, at six months there were no differences found.

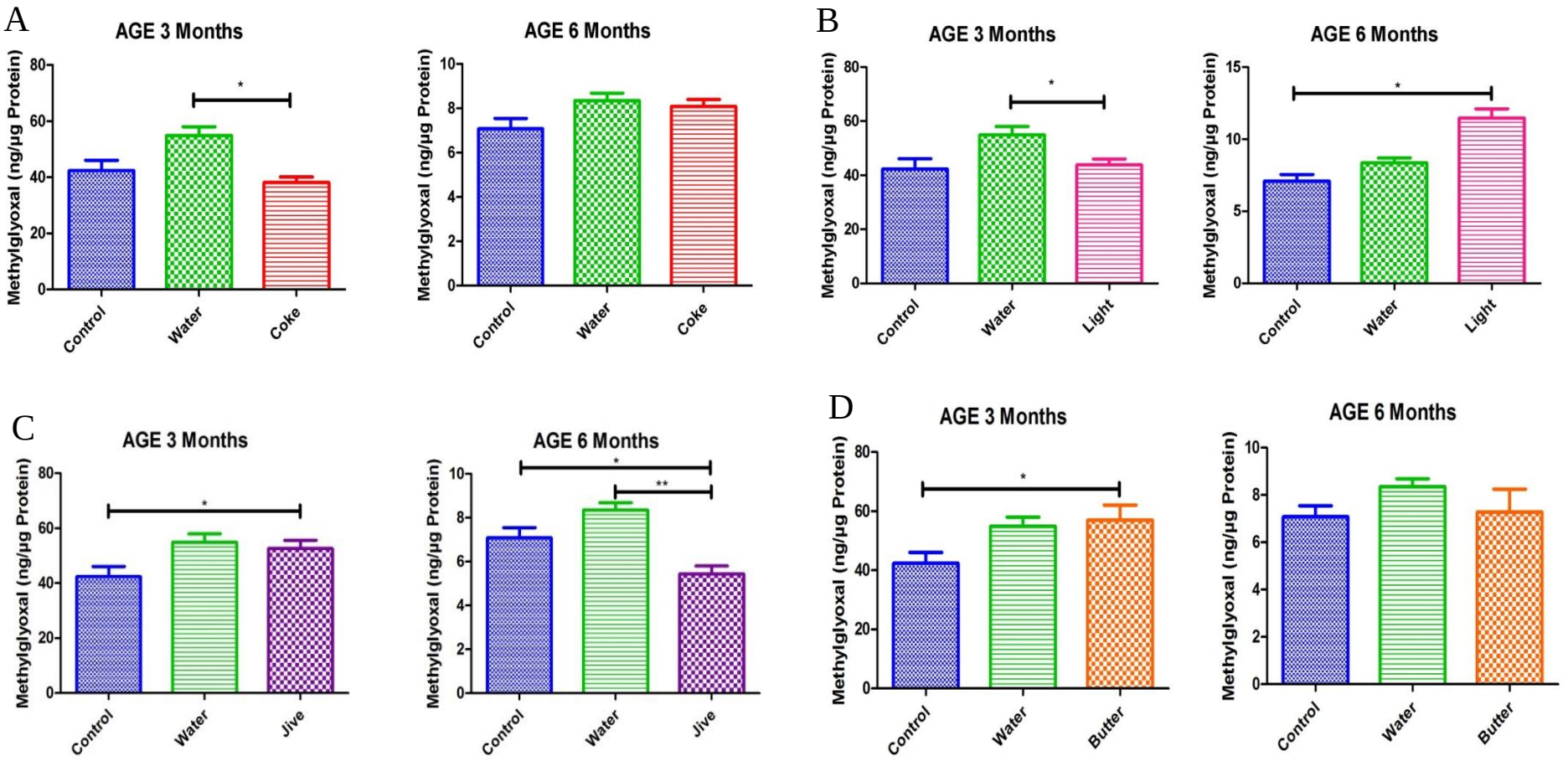

Figure 6.9: Activation of the AGE pathway. A: Coca Cola®, B: Coke Light®, C: Jive®, D: butter (n=6 for all groups except butter group for six months n=5). Values are expressed as mean ± SEM. Significance is shown as * P<0.05 and ** P<0.005.

6.2.2 Protein kinase C (PKC) activity

Heart tissues were analyzed to determine the activation of PKC but no significant differences were observed between the Coca Cola®, control and water groups at three or six months (refer to Figure 6.10).

No significant differences were detected at three months between the control, water and Coke Light® groups. However, at six months there was an increase in PKC activity in the Coke Light® group compared to both the control and water groups ($P<0.01$ and $P<0.05$, respectively).

At three months Jive® displayed significantly greater PKC activity than both the control and water groups, that was largely sustained after six months (compared to control group only) ($P<0.05$).

There was no significant PKC activity found in either the three or six month time points between the control, water and butter groups.

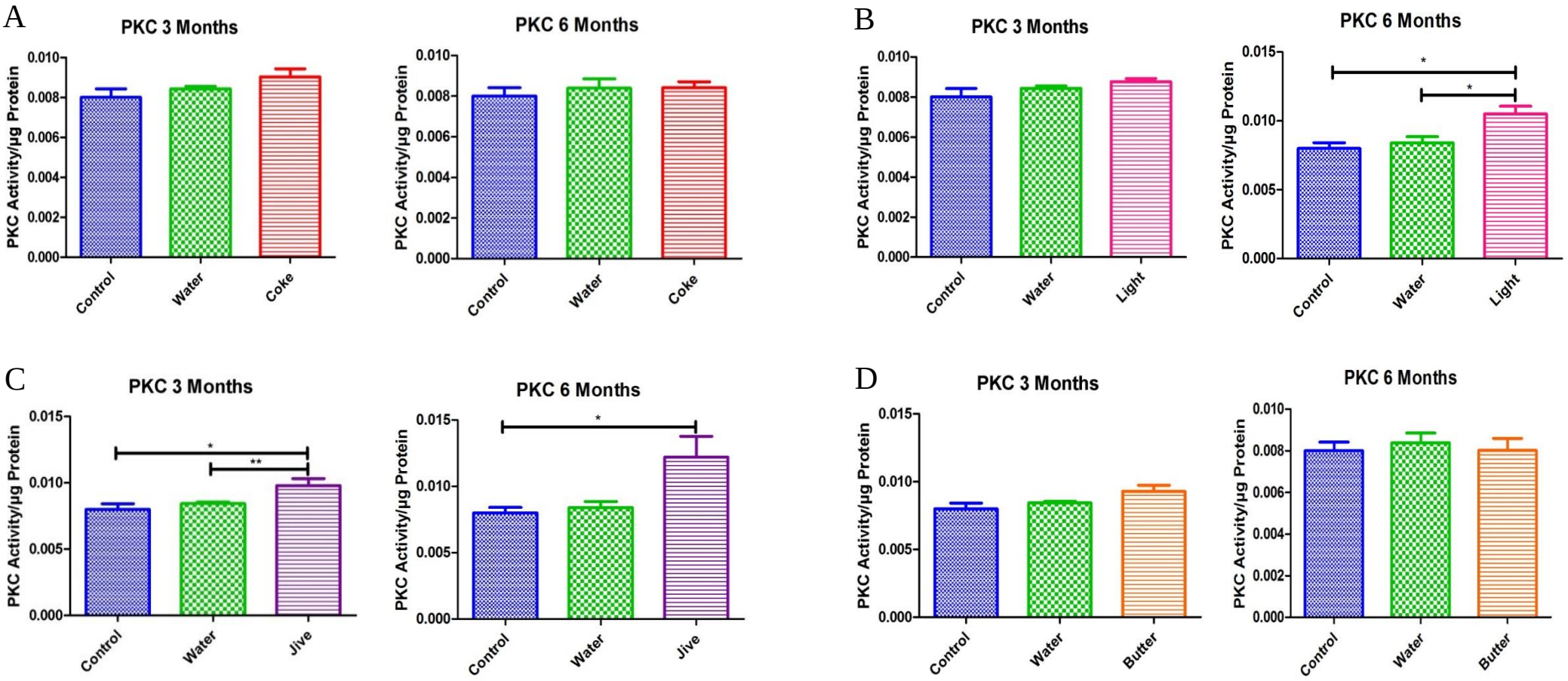

Figure 6.10: PKC activity in cardiac tissues. A: Coca Cola®, B: Coke Light®, C: Jive®, D: butter (n=6 per group except for the butter group at six months [n=5]). Values are expressed as mean ± SEM. Significance is shown as * P<0.05 and ** P<0.005.

6.2.3 Polyol pathway

D-sorbitol levels were measured in order to calculate activation of the polyol pathway – refer Figure 6.11. At three months there were significantly depleted D-sorbitol levels in the Coca Cola® group compared to both the control and water groups ($P<0.01$ and $P<0.005$, respectively). However, at six months no significant differences were identified.

At three months the Coke Light® group showed a significant increase in D-sorbitol levels compared to both the control and water groups, while no differences were found at the six month time point.

At three months the D-sorbitol levels were significantly higher in the Jive® group compared to the control and water groups. The inverse was observed at six months with significantly reduced glucose levels compared to the respective control groups.

At three months the butter group showed higher amounts of D-sorbitol when compared to both the control and water groups ($P<0.01$ and $P<0.005$, respectively). However, at six months there were no significant differences found.

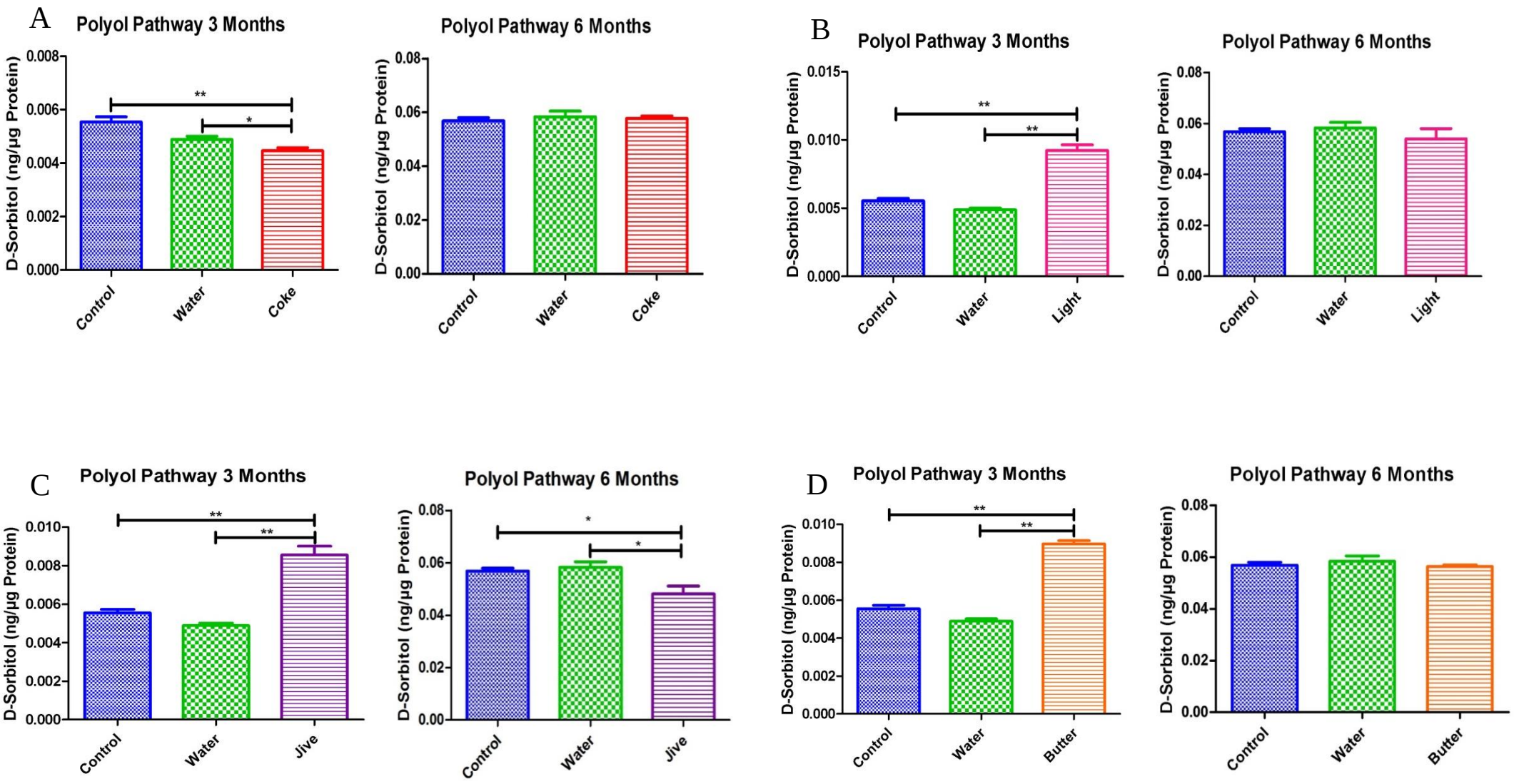

Figure 6.11: Activation of the polyol pathway. A: Coca Cola®, B: Coke Light®, C: Jive®, D: butter (n=6 per group except for the butter group at six months [n=5]). Values are expressed as mean ± SEM. Significance is shown as * P<0.05 and ** P<0.005.

6.2.4 Hexosamine biosynthetic pathway (HBP)

Western blotting techniques were employed to calculate *O*-GlcNAcylated proteins, which were measured in order to determine HBP activation – refer Figures 6.12 and 6.13. Note, Figure 6.13 represents typical Western blot images used to generate the quantified data presented here. The various lanes in the gel, used to separate proteins, were loaded with proteins extracted from the rat hearts.

Three months revealed no significant difference between the control, water and Coca Cola® groups. However, at six months the total *O*-GlcNAcylated proteins were elevated in the Coca Cola® group compared to both the control and water groups ($P<0.01$).

At three and six months there were significantly elevated *O*-GlcNAc protein levels in the Coke Light® group compared to the control and water groups.

At both three and six months the Jive® displayed more *O*-GlcNAcylated proteins when compared to the control ($P<0.005$ and $P<0.01$, respectively) and water ($P<0.01$) groups.

At three months the butter exhibited significantly higher amounts of *O*-GlcNAcylated protein when compared to both the control and water groups. However, no differences were found at six months.

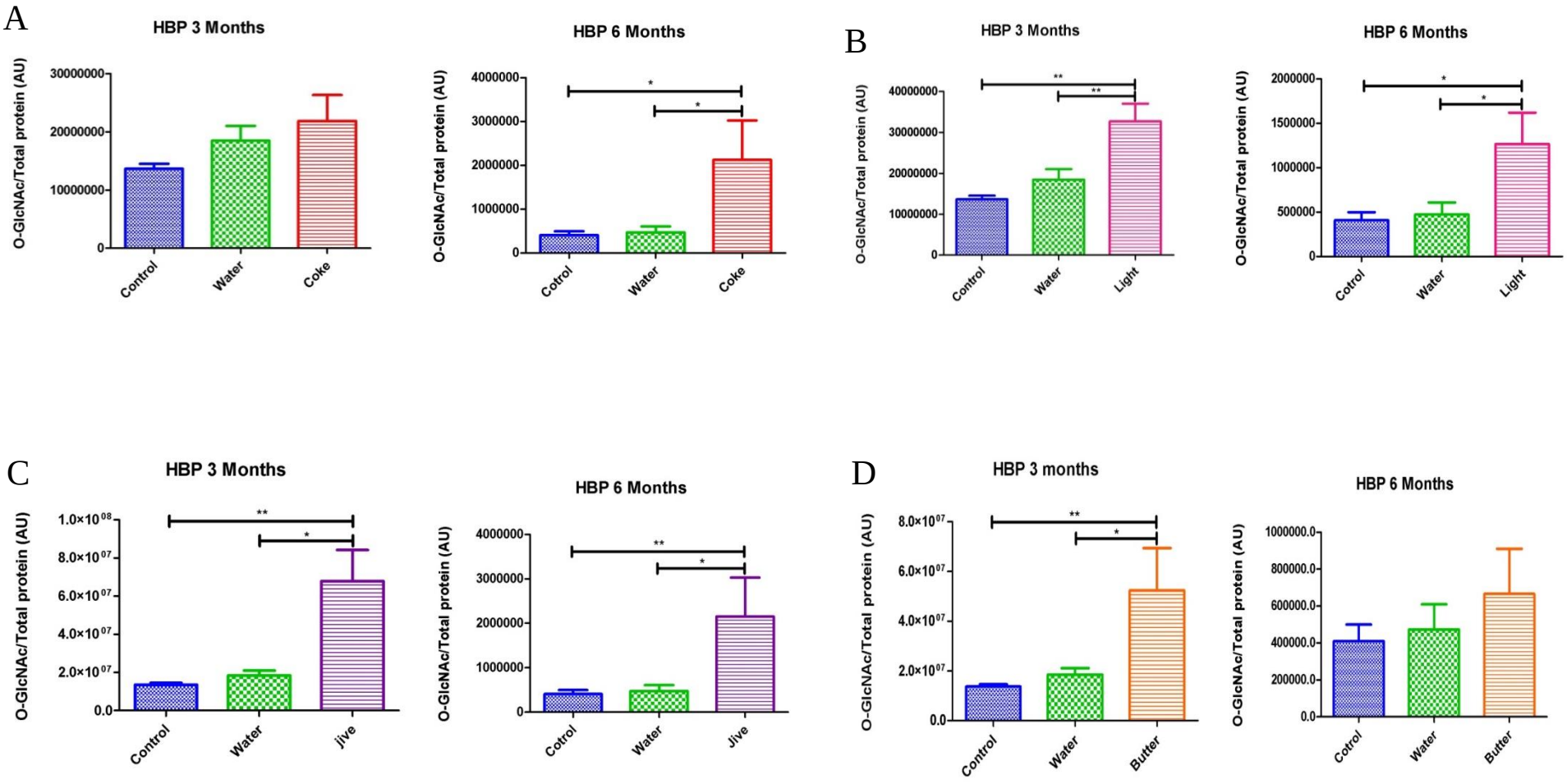

Figure 6.12: Total *O*-GlcNAcylated proteins used to measure activation of the HBP. A: Coca Cola®, B: Coke Light®, C: Jive®, D: butter (n=6 per group except for the butter group at six months [n=5]). Values are expressed as mean ± SEM. Significance is shown as * P<0.05 and ** P< 0.005.

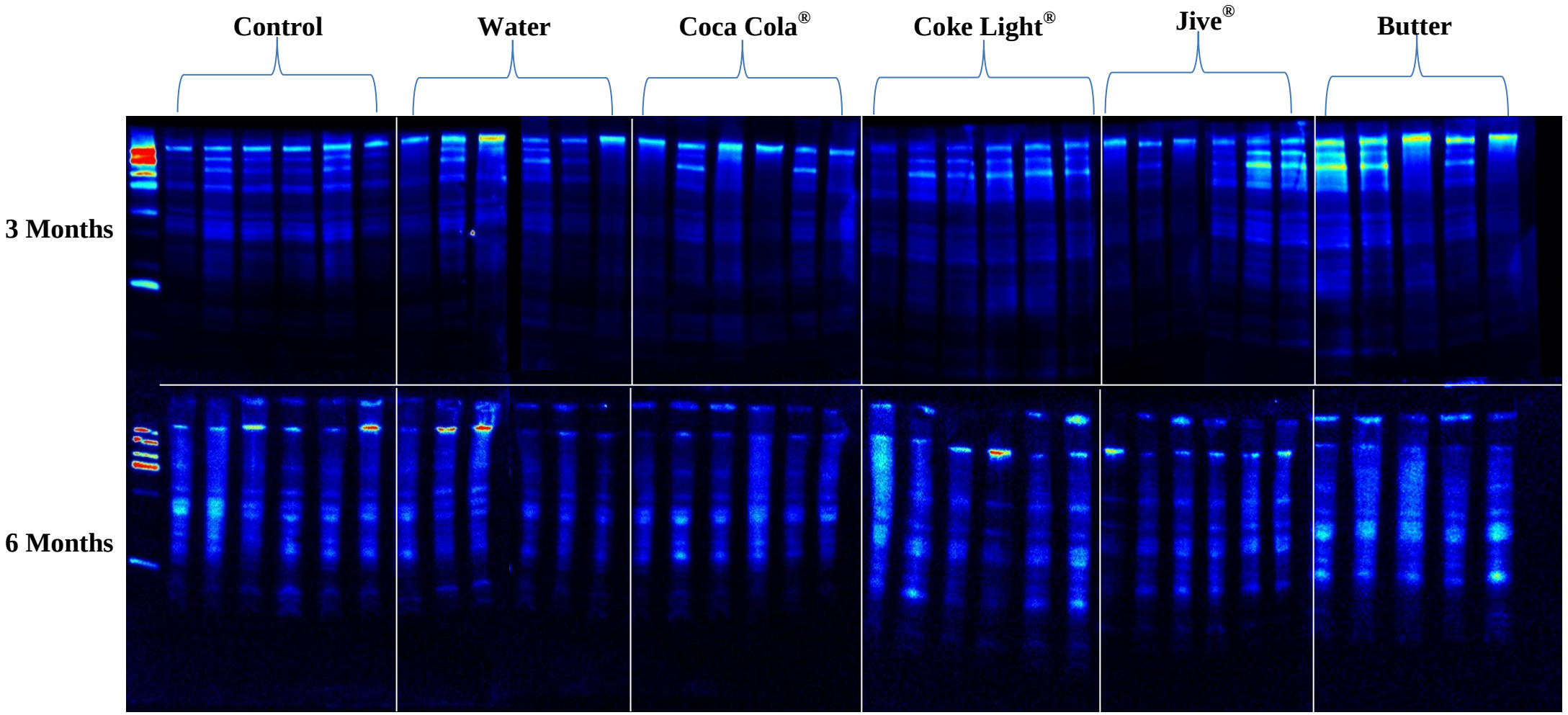

Figure 6.13: Representative Western blot images used to quantify the total *O*-GlcNAcylated proteins in the heart.

Chapter 7
Discussion

7.1 Introduction

Cardiovascular complications contribute dramatically to morbidity and mortality incidence amongst individuals who have developed T2D, with IR in the myocardium playing an important role in such disease progression (Chavali *et al*., 2013). It is well established that effective glucose uptake and metabolism contribute greatly to normal cardiac function and limiting future onset of CVD (Liao, 2002). However, poor lifestyle choices and dietary habits e.g. increased SSB consumption, may give rise to acute hyperglycemic events (Popkin, 2012) and perturb normal cardiac metabolism leading to increased manifestation of risk factors such as increased weight gain, IR and T2D (De Ruyter *et al*., 2012). Despite the proposed risk posed by increased SSB consumption, the underlying mechanisms whereby it can result in cardio-metabolic complications remain poorly understood. In light of this, the experimental design of this study was to establish (and characterize) a unique rat model of chronic SSB consumption with the idea of determining risk factors and mechanisms that contribute to the development of cardio-metabolic diseases.

7.2 Major findings

The current study managed to successfully establish an *in vivo* rat model of chronic SSB consumption. Our data reveal that after six months of consuming the different sodas, the groups display minimal macroscopic changes (similar body weights and circulating metabolite levels), therefore possibly representing a relatively early stage in terms of expected SSB-mediated cardio-metabolic complications. However, we found several changes at the biochemical level with distinct signatures for the Jive® group compared to the Coca Cola® and Coke Light® groups. Here Jive® consumption for six months resulted in early signs of cardiac and skeletal muscle hypertrophy, together with increased liver mass and perturbed adipocyte ultrastructure. Moreover, these animals displayed variable OGTTs suggesting that insulin-mediated glucose metabolism may be altered, although no clear signs of IR were found after six months. In addition, we also established that the majority of the NOGPs were activated in heart tissues isolated from the Jive® group after three months, and sustained after

six months. We propose that such sustained activation may have contributed to some of the changes already found and may also contribute to the onset of future complications. The Coca Cola® and Coke Light® groups exhibited alterations in liver mass and altered adipocyte ultrastructure together with lower glucose clearance after six months (OGTTs). The latter suggests that these groups may be IR or at least in the process of becoming so. Here we established that cardiac NOGPs were activated to a lesser extent compared to the Jive® group, although the HBP was strongly turned on in both Coca Cola® and Coke Light® groups and may thus be implicated in the OGTT response observed, as also likely to contribute to the onset of future cardio-metabolic complications.

7.3 Cardiovascular risk factors

7.3.1 Weight gain and food consumption

For the first part of our study we focused on the weight gain of the animals and their associated food consumption as numerous studies indicate that there is a parallel weight gain with the consumption of SSBs (De Ruyter *et al*., 2012; Ebbeling *et al*., 2012; Qi *et al*., 2012). This relationship is postulated to be due to the increased caloric intake and the inability of SSBs to trigger the satiety response, thus providing an explanation for greater energy intake (Malik *et al*., 2010; Popkin, 2012) which is not utilized perhaps due to sedentary lifestyle choices (Bradshaw *et al*., 2007).

Our data revealed that all the soda groups consumed similar amounts of food regardless of their treatment group, with no significant changes in terms of overall weight gain. These findings therefore show that the consumption of SSBs, ASB or butter did not affect dietary patterns/behavior and weight gain in our experimental model. How does one explain this discrepancy with previously published clinical studies? We propose two reasons. In the first instance, this may relate to the length of time of SSB consumption. For example, clinical studies examined human subjects over a relatively long period, e.g. two years, and under these circumstances found SSB consumption linked to weight gain and/or an increase in BMI (De Ruyter *et al*., 2012; Ebbeling *et al*., 2012). Therefore, we propose that a period of 24 weeks (the entire duration of this study) may not have been long enough to trigger significant changes in terms of weight gain. However, this may provide useful support for any metabolic/signaling changes found, i.e. that this not due to obesity *per se* but rather due to

SSB/ASB effects itself (Malik *et al*., 2010; Van Gaal *et al*., 2006). A second reason may also be due to variations in dosages employed. For the current study, we employed a dosage that is roughly equivalent to half a glass of soda consumed per day (in human terms) while in some clinical studies they typically requested participants to consume ~ 355 ml of soda per day (De Koning *et al*., 2012; Ebbeling *et al*., 2012). The treatment dosages were calculated as described in Chapter 4.

7.3.2 Cholesterol and Triglyceride Blood Markers

We next aimed to test whether the consumption of SSBs would trigger a rise in systemic cardio-metabolic risk factors. Blood metabolites (cholesterol, triglycerides, glucose) associated with the risk of developing CVD were therefore assessed after three and six months, respectively (Swarbrick *et al*., 2008). Our data did not reveal many significant changes and no distinct patterns/trends. We did, however, find sporadic changes, e.g. increased triglyceride levels for the Coca Cola® group at two months, and decreased levels for the Coke Light® group after six months. The same applies for cholesterol and glucose (baseline) measurements and we are of the opinion that such isolated changes may be dependent on the particular context and/or rat grouping at the time of the measurements. Our analyses were further compounded by some minor variations between the control and water groups (also for other measurements) and hence we only took soda-induced changes as real when it differed significantly from both control groups. We are unclear why this may be the case and postulate this may be due to the number of animals examined per group, i.e. higher numbers per group may potentially remove such differences. In addition, animal heterogeneity may also account for such changes. At present, we are also currently conducting further research studies to evaluate additional risk factors e.g. lipid deposition in heart, liver and muscle tissues.

How do such findings match with clinical studies completed? Ludwig (2002) reviewed two separate studies and found that higher glycemic load was accompanied by an agonistic increase in serum lipid concentrations, i.e. cholesterol and triglycerides. Conversely, his additional analyses on six other SSB-related studies showed no significant effects for these metabolites. Several studies support this notion, e.g. by Fung *et al*. (2001) concluded that SSB consumption resulted in no significant differences in terms of cholesterol and triglyceride levels. Moreover, Swarbrick *et al*. (2008) examined the effect of fructose-

sweetened beverages (a component of SSBs) over a period of 10 weeks and also established no significant differences for fasting blood cholesterol and triglyceride levels. Others likewise found no changes in cholesterol levels for individuals consuming SSBs and ASBs, although triglyceride levels were significantly increased with the consumption of SSBs but not with ASBs (De Koning *et al*., 2012). Thus, the overall data are mixed with some studies reporting changes in lipid levels while others do not. It is likely that such variations may be due to the nature and experimental design of different studies and the degree and nature of SSB consumption. In our experimental model, we propose that the time period and the dosages employed represent a moderate stressor and hence we do not observe any significant macroscopic changes after the six-month time period. We are of the opinion that this is actually a strength of our newly established experimental model since it should provide useful insights into biochemical/signaling/gene changes that would occur in the absence of significant weight and circulating metabolite levels. Such molecular changes would therefore represent the earliest changes triggered in response to long-term SSB/ASB consumption.

7.3.3 Organ mass analyzes

Several organs and tissues (heart, muscle, liver and visceral adipose tissue) were weighed at three and six months, respectively. We calculated the mass of each organ as a percentage of body weight in order to gain further insights into the effects of SSBs and ASBs. For the purpose of this discussion each organ/tissue will be discussed separately.

7.3.3.1 Heart mass

Neither our three nor six month results showed any differences with regards to heart mass, except at six months for the Jive® group. This finding is intriguing since the greater heart mass suggests that such hearts may be undergoing a hypertrophic response. We are currently in the process of evaluating additional biomarkers for cardiac hypertrophy such as Atrial natriuretic peptide (ANP) and B-type Natriuretic Peptide BNP. Moreover, we are planning future studies to collect heart tissues for histological analyses in order to assess whether this indeed represents a hypertrophic response. We are unclear at this stage how exactly this phenomenon may occur in response to SSB intake, but Maersk *et al*. (2012) found that SSB exposure resulted in an increase in blood pressure in adult individuals. Thus it is a possibility that Jive® consumption may have increased blood pressure thereby placing hearts under more

strain to pump blood to the entire body and potentially leading to the onset of cardiac hypertrophy. Our future studies will also evaluate blood pressures in especially the Jive® group.

7.3.3.2 Muscle mass

The muscle mass data for the Jive® group correlated well with the heart mass findings earlier discussed. *These data suggest that for the* Jive® group *there may be a general activation of growth signals in muscle (skeletal, heart) tissues and it* correlates with work done by Maersk *et al*. (2012). More research is now required to gain a comprehensive understanding of the effects of SSBs and ASBs on muscle growth and several growth pathways e.g. insulin-like growth factor (IGF)-1 and/or signaling via the Akt/mammalian target of rapamycin pathways that are likely prime candidates in this regard (Tidball, 2005).

7.3.3.3 Liver mass

For the liver mass evaluations we found mixed results with it being increased and decreased, for different groups at varying times. Here the Jive®-treated animals displayed increased liver mass after 6 months, while a similar finding was made for the butter group – but at the 3 month time point. Conversely, both Coca Cola® and Coke Light® exhibited decreased liver mass weights compared to the control groups. We are unclear why such distinct differences manifest and are in the process of completing additional biochemical studies to gain additional insights into these findings. The higher liver mass data are in agreement with Maersk *et al*. (2012) and Popkin (2012) who also found increased liver fat percentages with the consumption of SSBs (clinical studies). Moreover, the same authors also reported that ASB consumption was linked to lower liver weights (Maersk *et al*., 2012). The Coca Cola® data, however, contradict these findings by also showing reduced liver mass, although this may be due to its high fructose content that is rapidly metabolized in the liver (De Koning *et al*., 2012). The Coca Cola® results may also be due to the metabolism of fructose in the liver. The observation that fructose-fed rats develop fatty liver and metabolic syndrome without requiring increased energy intake suggests that the metabolism of fructose may be different from that of other carbohydrate sources.

Another reason why our Coca Cola® data may differ to the literature may be that animal studies using fructose typically use pure fructose as opposed to sucrose or HFCS, which is the primary source of fructose in humans. Rats are moderately resistant to fructose because they generate less uric acid (compared to humans) in response to fructose due to the presence of the uricase gene in their liver. Uricase degrades uric acid to allantoin, and as a consequence, rats degrade uric acid rapidly after it is formed in their liver. The metabolism of fructose in the liver leads to the formation of uric acid, which in turn increases the risk of developing IR and CVD. The mechanism appears to be mediated by uric acid–dependent intracellular and mitochondrial oxidative stress. Although uric acid is a potent antioxidant in the extracellular environment, when uric acid enters cells via specific organic anion transporters, it induces an oxidative stress that has been shown in vascular endothelial cells and adipocytes (Johnson *et al*., 2013). Further studies need to be conducted to calculate the actual fat percentage in the liver in order to draw meaningful conclusions from such findings.

7.3.3.4 Visceral adipose tissue

Although previous studies demonstrated an accumulation of visceral adiposity with SSB consumption (Anton *et al*., 2010; Malik *et al*., 2010; O'Keefe *et al*., 2008; Popkin, 2012), we did not find any meaningful changes. There were some changes but it was not significant versus both the controls here employed and therefore we propose that such changes cannot lead to reliable conclusions. However, the general lack of profound and consistent changes is consistent with our earlier findings that our experimental model represents early changes triggered by SSB consumption. It is thus likely that real changes in visceral adipose tissues may only be found with longer exposure to SSBs, i.e. beyond the six-months here employed.

7.3.4 Adipose tissue analyses

Abdominal obesity is a major risk factor for Diabetes and CVD. Excess visceral fat and subcutaneous adipose tissues are proposed to be key contributors to this process (Swarbrick *et al*., 2008). For example, several studies found that visceral fat and subcutaneous adipose tissues are associated with multiple cardiovascular risk factors as well as markers of inflammation and oxidative stress (Anton *et al*., 2010; Neeland *et al*., 2013). An insufficient subcutaneous adipose tissues reservoir for fat storage promotes ectopic redistribution of FAs to visceral adipose tissue, liver, and skeletal muscle, and predisposing individuals to

increased metabolic risks (Neeland *et al*., 2013). In light of this, we also measured the surface area of adipocytes isolated from the left visceral fat pads to assess whether this may be the case in our experimental model.

Although the Coca Cola® group did not show a significant difference in percentage visceral fat to body weight as discussed earlier, the adipocyte surface area was larger compared to the controls. This could be indicative that more FAs are converted to triglycerides for storage purposes (increasing adipocyte cell surface areas) (Zimmermann *et al*., 2004) and potentially placing the organism at risk for future CVD onset (Swarbrick *et al*., 2008). These results are in accordance with previous studies which show that SSBs is linked to excess visceral fat deposition (Anton *et al*., 2010; Popkin, 2012). For the Jive® group a different scenario was found, i.e. although the overall area of the adipocytes were less than the controls, the total percentage of visceral fat to body weight appears to be increased. This leads us to speculate that there are numerous smaller adipocytes - this may also be as a result of excess FA deposition (Neeland *et al*., 2013) – that may also signal detrimental pathophysiologic outcomes.

Together these findings (first part of this study) demonstrate that our rat model of chronic SSB/ASB consumption represents a relatively early stage during the progression towards the onset of cardio-metabolic complications. We found that there was no significant weight gain or profound changes in key circulating metabolites for any of the sodas employed. Moreover, food consumption remained unaffected for all groups studied while organ weight changes occurred only for some of the experimental groupings. These data therefore indicate that after six months there are limited visible macroscopic changes. However, our findings reveal that Jive® consumption resulted in the most significant changes, with early evidence of cardiac and skeletal muscle hypertrophy together with increased liver weights. In addition, this group also displayed changes in adipocyte ultrastructure that could potentially have detrimental effects in the long-term. Interestingly, these changes were not found in the butter group that was provided with the exact same caloric intake, therefore indicating that SSBs (especially Jive®) *per se* can elicit potentially damaging effects. The next stage of this study involves gaining some additional insights into putative underlying mechanisms that may be responsible for early changes triggered by SSB consumption.

7.4 Insulin resistance/Diabetes risk factors

7.4.1 Oral glucose tolerance tests

OGTTs were performed biweekly in order to evaluate the effects of SSBs, ASBs and butter on postprandial hyperglycemic excursions. Although both chronic and acute hyperglycemia has been linked with the development of CVD, we set out to investigate acute glycemic fluctuations as the literature falls short in this regard. Evidence suggests that acute hyperglycemia plays a vital role in the pathogenesis of developing vascular complications and has been linked with oxidative stress, endothelial dysfunction (Marcovecchio *et al*., 2011) and increased acute myocardial infarction mortalities (Cao *et al*., 2005). Furthermore, repeated changes in postprandial excursions on a daily basis result in an increase in atherosclerotic risk factors and predisposition to coronary artery disease (O'Keefe *et al*., 2008).

The current study found that the different experimental groups exhibited significant variation in their respective OGTTs with the different time points here examined. These data suggest that SSB consumption triggers some effects that impact on insulin-mediated glucose uptake and metabolism. For example, we established that the Coca Cola® and Coke Light® groups displayed a much higher postprandial excursion (especially early on) after the six month time period. The butter group showed a similar result and these data suggest that in this instance there may be an impairment of insulin action on target cells and/or secretion by the pancreatic β–cells. Evidence shows that ASBs trigger the same insulin response as that of SSBs although with a diminished glycemic response (Anton *et al*., 2010). We were unfortunately unable to assess systemic insulin levels in our model (due to loss of sample materials) since this would have allowed us to calculate measures such as the homeostatic model assessment (HOMA) to gain insight regarding insulin sensitivity. For the three month time point, Coke Light® and Jive® groups' postprandial excursions were lower – again suggesting a problem with insulin-regulated glucose metabolism. This indicates that a greater insulin response was likely required as shown in the literature (Anton *et al*., 2010, Swithers, 2013) to reduce the glycemic effects of the Coke Light® and Jive® groups, causing the blood glucose levels to decline significantly as found here. In support, Swarbrick *et al*. (2008) found that the consumption of fructose beverages over a period of ten weeks significantly increased the insulin response in humans and thus could predispose them to diminished insulin sensitivity

and lead to IR. Moreover, Popkin (2012) demonstrated that SSB consumption has adverse effects on insulin sensitivity, thus if this response is continually stimulated it could lead to the onset of IR.

Anton *et al*. (2010) proposed that ASBs also trigger a higher glucose response than normal, although not as high as sucrose containing substances (SSBs). As noted, over the six month period we found lower blood glucose levels at three months and again an increase after six months. This could be indicative of impaired insulin response possibly leading to IR. These data correlate with the literature and add valuable information regarding ASBs and that it could also possibly lead to IR over an extended period of time. However, additional studies are required to gain a fuller understanding, e.g. insulin measurements in order to calculate the HOMA index, and an investigation of molecular markers of insulin-mediated glucose metabolism (heart, muscle, liver tissues).

7.4.2 Non-oxidative glucose pathways

We hypothesized that increased glucose availability (due to SSB consumption) will trigger an enhanced mitochondrial oxidative stress response, leading to upstream glycolytic metabolites being shunted into NOGPs, i.e. polyol, HBP, AGE, and PKC pathways.

We found variable responses for the different NOGPs. Our data reveal that the Jive® group displayed the most significant changes in terms of NOGP activation in the rat heart. Here we found that the HBP, PKC and polyol pathways were coordinately induced after three months, with the AGE pathway remaining essentially unchanged. This pattern continued and remained the same after six months, except the AGE pathway was now downregulated. For the other groups, the HBP also featured strongly, i.e. upregulated at either three and six month time points, or both. This suggests that the HBP is a relatively early and universal metabolic target that is triggered in response to chronic SSB and ASB consumption. For the remainder of the groups, we found that the PKC and polyol pathways were activated in punctuate fashion and sometimes up- or downregulated.

Increased flux through the HBP has been implicated in glucose-induced insulin resistance. Glucosamine (an intermediate in the HBP) is several times more potent than glucose in inducing IR and reducing insulin responsiveness. The latter is a result of the modification of

gene transcription factors, via *O*-GlcNAcytion, relevant to glucose homeostasis/ insulin signaling (Buse *et al*., 2002; McClain and Crook, 1996). Several studies support this notion, e.g. GFAT (HBP rate-limiting enzyme) overexpression in mice develop IR with decreased muscle glucose disposal rates linked to reduced levels of the muscle-enriched glucose transporter, GLUT4 (Hebert *et al*. 1996). Similarly, skeletal muscle GFAT activity is significantly elevated in Type 2 diabetic patients (Rajamani *et al*., 2011; Yki-Jarvinen *et al*. 1996).

The collective activation of the NOGPs are also implicated in the onset of insulin resistance in heart cells and there is a strong interplay between such pathways (Joseph and Essop, 2014). Thus we propose that activation of one or several of such pathways can further fuel activation of the NOGPs therefore creating a vicious metabolic cycle. Excessive NOGP activation can lead to more ROS production and also damaging downstream effects on the heart (Brownlee, 2005; Joseph *et al*., 2014; Mapanga *et al*., 2012). For example, we found that activation of NOGPs with ischemia-reperfusion (under acute hyperglycemic conditions) results in greater damage to hearts (Mapanga *et al*., 2012). Moreover, when these pathways were blunted our data reveal that hearts showed significantly improved functional recovery following ischemia-reperfusion. What are the upstream events that lead to NOGP activation? Oxidative stress is considered the linking mechanism whereby hyperglycemia mediates its activation of the NOGPs and with damaging effects (Brownlee, 2001). Here hyperglycemia-induced ROS is thought to inhibit the glycolytic enzyme GAPDH, thereby increasing flux through upstream glycolytic metabolites into the NOGPs with downstream effects contributing to cardio-metabolic complications (Du *et al*., 2003). Therefore a possible mechanistic pathway may include oxidative stress as an initial downstream target of SSB consumption, followed by NOGP activation and the onset of pathophysiologic complications. We are currently in the process of investigating markers of oxidative stress in our model. It is also highly likely that other signaling pathways are also involved in SSB-mediated effects in our model and we are planning to perform proteomic analyses to gain more insights in this regard.

References

1. Anton, S. D., Martin, C. K., Han, H., Coulon, S., Cefalu, W. T., Geiselman, P., & Williamson, D. A. (2010). Effects of stevia, aspartame, and sucrose on food intake, satiety, and postprandial glucose and insulin levels. *Appetite*, *55*(1), 37–43.

2. Barr, E. L. M., Zimmet, P. Z., Welborn, T. a, Jolley, D., Magliano, D. J., Dunstan, D. W., Shaw, J. E. (2007). Risk of cardiovascular and all-cause mortality in individuals with Diabetes Mellitus, impaired fasting glucose, and impaired glucose tolerance: the Australian Diabetes, Obesity, and Lifestyle Study (AusDiab). *Circulation*, *116*(2), 151–7.

3. Bradshaw, D., Norman, R., Pieterse, D., Levitt, N. (2007). Estimating the burden of disease attributable to Diabetes in South Africa in 2000. *South African MEdical Journal*, *97*(7), 700–706.

4. Brownlee, M. (2001). Biochemistry and molecular cell biology of diabetic complications. *Nature*, *414*(6865), 813–20.

5. Buse, M. G., Robinson, K. A., Marshall, B. A., Hresko, R. C., & Mueckler, M. M. (2002). Enhanced O-GlcNAc protein modification is associated with insulin resistance in GLUT1-overexpressing muscles. *American Journal of Physiology. Endocrinology and Metabolism*, *283*(2), E241–50.

6. Cao, J. J., Hudson, M., Jankowski, M., Whitehouse, F., & Weaver, W. D. (2005). Relation of chronic and acute glycemic control on mortality in acute myocardial infarction with Diabetes Mellitus. *The American Journal of Cardiology*, *96*(2), 183–6.

7. Chavali, V., Tyagi, S. C., & Mishra, P. K. (2013). Predictors and prevention of diabetic cardiomyopathy. *Diabetes, Metabolic Syndrome and Obesity : Targets and Therapy*, *6*, 151–60.

8. De Koning, L., Malik, V. S., Kellogg, M. D., Rimm, E. B., Willett, W. C., & Hu, F. B. (2012). Sweetened beverage consumption, incident coronary heart disease, and biomarkers of risk in men. *Circulation*, *125*(14), 1735–41, S1.

9. De Ruyter, J. C., Olthof, M. R., Seidell, J. C., & Katan, M. B. (2012). A trial of sugar-free or sugar-sweetened beverages and body weight in children. *The New England Journal of Medicine*, *367*(15), 1397–406.

10. Du, X., Matsumura, T., Edelstein, D., Rossetti, L., Zsengellér, Z., Szabó, C., & Brownlee, M. (2003). Inhibition of GAPDH activity by poly(ADP-ribose) polymerase activates three major pathways of hyperglycemic damage in endothelial cells. *The Journal of Clinical Investigation*, *112*(7), 1049–57.

11. Ebbeling, C. B., Feldman, H. A., Chomitz, V. R., Antonelli, T. A., Gortmaker, S. L., Osganian, S. K., & Ludwig, D. S. (2012). A randomized trial of sugar-sweetened beverages and adolescent body weight. *The New England Journal of Medicine*, *367*(15), 1407–16.

12. Fung, T. T., Rimm, E. B., Spiegelman, D., Rifai, N., Tofler, G. H., Willett, W. C., & Hu, F. B. (2001). Association between dietary patterns and plasma biomarkers of obesity and cardiovascular disease risk. *The American Journal of Clinical Nutrition*, *73*(1), 61–7.

13. Hebert, L. F., Daniels, M. C., Zhou, J., Crook, E. D., Turner, R. L., Simmons, S. T., & McClain, D. a. (1996). Overexpression of glutamine:fructose-6-phosphate amidotransferase in transgenic mice leads to insulin resistance. *The Journal of Clinical Investigation*, *98*(4), 930–6.

14. Johnson, R. J., Nakagawa, T., Sanchez-Lozada, L. G., Shafiu, M., Sundaram, S., Le, M., & Lanaspa, M. A. (2013). Sugar, uric acid, and the etiology of diabetes and obesity. *Diabetes*, *62*(10), 3307–15.

15. Joseph, D., & Essop, M. F. (2014). The effects of thiamine treatment on pre-diabetic versus overt diabetic rat hearts: Role of non-oxidative glucose pathways. *International Journal of Cardiology*, *176*(3), 1371–3.

16. Joseph, D., Kimar, C., Symington, B., Milne, R., & Essop, M. F. (2014). The detrimental effects of acute hyperglycemia on myocardial glucose uptake. *Life Sciences*, *105*(1-2), 31–42.

17. Liao, R. (2002). Cardiac-Specific Overexpression of GLUT1 Prevents the Development of Heart Failure Attributable to Pressure Overload in Mice. *Circulation*, *106*(16), 2125–2131.

18. Ludwig, D. S. (2002). The Glycemic Index Physiological Mechanisms Relating to Obesity, Diabetes, and Cardiovascular Disease. *Journal American Medical Association*, *287*(18), 2414–2423.

19. Maersk, M., Belza, A., Stødkilde-Jørgensen, H., Ringgaard, S., Chabanova, E., Thomsen, H., & Richelsen, B. (2012). Sucrose-sweetened beverages increase fat storage in the liver, muscle, and visceral fat depot: a 6-mo randomized intervention study. *The American Journal of Clinical Nutrition*, *95*(2), 283–9.

20. Malik, V. S., Popkin, B. M., Bray, G. a, Després, J.-P., & Hu, F. B. (2010). Sugar-sweetened beverages, obesity, type 2 Diabetes Mellitus, and cardiovascular disease risk. *Circulation*, *121*(11), 1356–64.

21. Mapanga, R. F., Rajamani, U., Dlamini, N., Zungu-Edmondson, M., Kelly-Laubscher, R., Shafiullah, M., Essop, M. F. (2012). Oleanolic acid: a novel cardioprotective agent that blunts hyperglycemia-induced contractile dysfunction. *PloS One*, 7(10), e47322.

22. Marcovecchio, M. L., Lucantoni, M., & Chiarelli, F. (2011). Role of chronic and acute hyperglycemia in the development of Diabetes complications. *Diabetes Technology & Therapeutics*, *13*(3), 389–94.

23. McClain, D. A., & Crook, E. D. (1996). Hexosamines and Insulin Resistance. *Diabetes*, *45*(8), 1003–1009.

24. Neeland, I. J., Ayers, C. R., Rohatgi, A. K., Turer, A. T., Berry, J. D., Das, S. R., de Lemos, J. A. (2013). Associations of visceral and abdominal subcutaneous adipose tissue with markers of cardiac and metabolic risk in obese adults. *Obesity (Silver Spring, Md.)*, *21*(9), E439–47.

25. O'Keefe, J. H., Gheewala, N. M., & O'Keefe, J. O. (2008). Dietary strategies for improving post-prandial glucose, lipids, inflammation, and cardiovascular health. *Journal of the American College of Cardiology*, *51*(3), 249–55.

26. Popkin, B. M. (2012). Sugary beverages represent a threat to global health. *Trends in Endocrinology and Metabolism: TEM*, *23*(12), 591–3.

27. Qi, Q., Chu, A. Y., Kang, J. H., Jensen, M. K., Curhan, G. C., Pasquale, L. R., Qi, L. (2012). Sugar-sweetened beverages and genetic risk of obesity. *The New England Journal of Medicine*, *367*(15), 1387–96.

28. Rajamani, U., Joseph, D., Roux, S., & Essop, M. F. (2011). The hexosamine biosynthetic pathway can mediate myocardial apoptosis in a rat model of diet-induced insulin resistance. *Acta Physiologica*, *202*(2), 151–157.

29. Swarbrick, M. M., Stanhope, K. L., Elliott, S. S., Graham, J. L., Krauss, R. M., Christiansen, M. P., Havel, P. J. (2008). Consumption of fructose-sweetened beverages for 10 weeks increases postprandial triacylglycerol and apolipoprotein-B concentrations in overweight and obese women. *The British Journal of Nutrition*, *100*(5), 947–952.

30. Swithers, S. E. (2013). Artificial sweeteners produce the counterintuitive effect of inducing metabolic derangements. *Trends in Endocrinology and Metabolism*, *24*(9), 431–41.

31. Tidball, J. G. (2005). Mechanical signal transduction in skeletal muscle growth and adaptation. *Journal of Applied Physiology (Bethesda, Md. : 1985)*, *98*(5), 1900–8.

32. Van Gaal, L. F., Mertens, I. L., & De Block, C. E. (2006). Mechanisms linking obesity with cardiovascular disease. *Nature*, *444*(7121), 875–80.

33. Yki-Jarvinen, H., Daniels, M. C., Virkamaki, A., Makimattila, S., DeFronzo, R. A., & McClain, D. (1996). Increased Glutamine:Fructose-6-Phosphate Amidotransferase Activity in Skeletal Muscle of Patients With NIDDM. *Diabetes*, *45*(3), 302–307.

34. Zimmermann, R., Strauss, J. G., Haemmerle, G., Schoiswohl, G., Birner-Gruenberger, R., Riederer, M., & Zechner, R. (2004). Fat mobilization in adipose tissue is promoted by adipose triglyceride lipase. *Science (New York, N.Y.)*, 306(5700), 1383–6.

Chapter 8
Concluding remarks

8.1 Summary of findings

Obesity and CVD are becoming global pandemics, and even more so in developing nations. These diseases are associated with a sedentary lifestyle and unhealthy dietary habits. The molecular mechanisms underlying the etiology of such diseases are still not fully understood. We are of the opinion that a comprehensive understanding of the pathophysiological mechanisms driving the development of T2D and CVD is fundamental to curb the disease progression at an early stage. This thesis therefore evaluated the effects of SSB consumption (as part of the so-called Western diet) by establishing and characterizing a unique in vivo experimental model. Here the idea is to employ this model to gain novel mechanistic insights as to how SSBs can actually elicit cardio-metabolic complications in the long-term. We began by focusing on setting up the model and thereafter specifically focusing on whether NOGPs are activated in the myocardium.

This study managed to successfully establish a novel in vivo rat model of chronic SSB/ASB consumption. Our data reveal that after six months the different soda groups display minimal macroscopic changes, therefore representing a relatively early stage in terms of SSB-mediated cardio-metabolic complications. However, we found several changes at the biochemical level but with distinct signatures for the Jive® group compared to the Coca Cola® and Coke Light® groups. Here Jive® consumption for six months resulted in early signs of cardiac and skeletal muscle hypertrophy, together with increased liver mass and perturbed adipocyte ultrastructure. We also established that the majority of the myocardial NOGPs were activated which may have contributed to some of the changes already found and could also lead to future complications. The Coca Cola® and Coke Light® groups exhibited alterations in liver mass and altered adipocyte ultrastructure together with lower glucose clearance after six months suggesting onset of IR. The HBP also emerged as a universal pathway that was activated in all of the soda groups and may thus represent a useful therapeutic target within this particular context. Therefore, our study alerts to potential side-effects of long-term SSB intake that may place organisms at risk of developing cardio-metabolic complications despite an apparently "healthy" phenotype.

8.2 Limitations

We were unable to assess systemic insulin levels in our model (due to loss of sample materials) since this would have allowed us to calculate measures such as the HOMA to gain insight regarding insulin sensitivity. Blood serum availability was limited and thus only a few systemic metabolites could be evaluated. Due to time constraints we were unable to assess oxidative stress markers and/or anti-oxidant modulators.

8.3 Future direction

For future studies we plan to further evaluate The following: a) *ex vivo* heart perfusions to determine SSB effects on heart function, b) blood pressure assessments, c) endothelial functional analyses, d) oxidative stress markers, e) mitochondrial respiration studies, f) a comprehensive analysis of signaling pathways (cell death, hypertrophy, insulin/glucose metabolism) and g) histological analyses of different tissues (heart, pancreas, muscle, liver)**.**

The damaging downstream effects of the NOGPs also need to be measured, e.g. inflammatory markers such as NFκB as well as NO levels to determine vasodilation capabilities. Future studies are also necessary to pursue reasons behind the continual activation of the HBP. Finally, this experimental system will be replicated in an obese model to simulate the effects of SSB consumption in a person already predisposed to cardio-metabolic complications. Such collective investigations should thus significantly contribute to an improved mechanistic understanding of the damaging effects of SSB consumption and its link to T2D and CVD.

Appendix A

UNIVERSITEIT•STELLENBOSCH•UNIVERSITY
jou kennisvennoot • your knowledge partner

Protocol Approval

Date: 03-Jun-2013

PI Name: DRIESCHER, Natasha

Protocol #: SU-ACUM13-00012

Title: The role of post-prandial hyperglycaemia in the onset of cardio-metabolic diseases

Dear Natasha DRIESCHER, the Response to Modifications, was reviewed on 28-May-2013 by the Research Ethics Committee: Animal Care and Use via committee review procedures and was approved. Please note that this clearance is only valid for a period of twelve months. Ethics clearance of protocols spanning more than one year must be renewed annually through submission of a progress report, up to a maximum of three years.

Applicants are reminded that they are expected to comply with accepted standards for the use of animals in research and teaching as reflected in the South African National Standards 10386: 2008. The SANS 10386: 2008 document is available on the Division for Research Developments website www.sun.ac.za/research.

Please remember to use your protocol number, SU-ACUM13-00012 on any documents or correspondence with the REC: ACU concerning your research protocol.

Please note that the REC: ACU has the prerogative and authority to ask further questions, seek additional information, require further modifications or monitor the conduct of your research.

We wish you the best as you conduct your research.

If you have any questions or need further help, please contact the REC: ACU secretariat at WABEUKES@SUN.AC.ZA or .

Sincerely,

Winston Beukes

REC: ACU Secretariat

Research Ethics Committee: Animal Care and Use

Appendix B

Protein extraction from tissues

Preparation of RIPA buffer

Base ingredients

- **Tris-HCl** (buffering agent prevents protein denaturation)
- **NaCl** (salt prevents non-specific protein aggregation)
- **NP-40** (non-ionic detergent to extract proteins; 10% stock solution in H_2O) or use **Triton X-100**
- **Na-deoxycholate** (ionic detergent to extract proteins; 10% stock solution in H_2O; protect from light). **Adjust the pH** to 9, then boil, cool, and re-adjust the pH to 9. Repeat this process until the solution becomes colorless

Note: Do not add Na-deoxycholate when preparing lysates for kinase assays. Ionic detergents can denature enzymes, causing it to lose its activity.

RIPA protease inhibitors

- **Phenylmethylsulfonyl fluoride** (PMSF) (200 mM stock solution in isopropanol; store at room temperature)
- **EDTA** (calcium chelator; 100 mM stock solution in H_2O, pH 7.4)
- **Leupeptin** (store frozen in aliquots, 1 mg/ml in H_2O)
- **Aprotinin** (store frozen in aliquots, 1 mg/ml in H_2O)
- **Pepstatin** (store frozen in aliquots, 1 mg/ml in methanol)

RIPA phosphatase inhibitors

- **Activated Na_3VO_4** (200 mM stock solution in H_2O; see sodium orthovanadate activation protocol).
- **NaF** (200 mM stock solution: store at room temperature)

Note: Do not add phosphatase inhibitors when preparing lysates for phosphatase assays.

RIPA trypsin inhibitors

- **Soyabean Trypsin Inhibitor (SBTI) (**1 mg/ml in 0.01 M phosphate buffer, pH 6.5 with 0.15 M NaCl- freeze aliquots at -20ºC)
- **Benzamidine** (200 mM stock solution -dissolve in ddH_2O – store at -20ºC)

Sodium orthovanadate activation protocol

1. Sodium orthovanadate should be activated for maximal inhibition of protein phosphotyrosyl-phosphatases.
2. Prepare a 200 mM solution of sodium orthovanadate.
3. Adjust the pH to 10 using either 1 N NaOH or 1 N HCl. The starting pH of the sodium orthovanadate solution may vary depending on different lots of the chemical. The solution will become yellow in color at pH 10.
4. Boil the solution until it turns colorless (~ 10 minutes).
5. Cool to room temperature.
6. Re-adjust the pH to 10 and repeat steps 3 and 4 until the solution remains colorless and the pH stabilizes at 10.
7. Store the activated sodium orthovanadate as aliquots at -20°C.
8. This procedure de-polymerizes the vanadate, converting it into a more potent inhibitor of protein tyrosine phosphatases.

Procedure:

Prepare 100 ml modified RIPA buffer as follows:

- Add 790 mg Tris base to 75 ml distilled water (ddH_2O). Then add 900 mg NaCl and stir the solution until all solids are dissolved. Using HCl, adjust the pH to 7.4.
- Add 10 ml of 10% NP-40 to the solution.
- Add 2.5 ml of 10% Na-deoxycholate and stir until solution is clear.
- Add 1 ml of 100 mM EDTA to the solution. Adjust the volume of the solution to 100 ml using a graduated cylinder.
- Ideally, the remaining protease and phosphatase inhibitors should be added to the solution on the same day for running of the assay. Therefore, it is best to aliquot the buffer in 10 ml aliquots without the protease inhibitors and store at 2-8°C.

- RIPA with inhibitors - on day of use, thaw the required amount of RIPA buffer and add the appropriate volume of protease inhibitors to the buffer.

For 10 ml RIPA add:

10 µL aprotonin; 10 µL of leupeptin; 50 µL of PMSF, Na_3VO_4, and NaF and benzamidine, 100 µL pepstatin and 50 µL Pugnac.

NB: these are the volumes for 10 ml of RIPA, but with the exception of PMSF, the diluted inhibitors are stable in aqueous solution for up to 5 days.

The final concentrations in the modified RIPA buffer should be:

Tris-HCl: 50 mM, pH 7.4
NP-40: 1%
Na-deoxycholate: 0.25%
NaCl: 150 mM
EDTA: 1 mM
PMSF: 1 mM
Leupeptin, benzamidine: 1 µg/ml each
Aprotonin: 1 ug/ml
Pepstatin: 10 ug/ml
Na_3VO_4: 1 mM
NaF: 1 mM
PUGNAc: 1mM

Protein extraction

- Cut tissue samples into small pieces and place into a 2 ml microtube.
- Pour RIPA buffer into the microtubes containing the tiny pieces of tissue samples – (aim to make homogenates that are 1:2 w/v tissue: lysis buffer).

- Using a dounce homogenizer (Ultra-Turrax homogenizer, IKA, China), homogenize the tissue until a fine slurry is obtained; then sonicate (Misonixa ultrasonic liquid processor S-4000, Hielscher, Germany) each sample for 10 seconds at 4 amps.
- Transfer the homogenates to fresh pre-chilled 2 ml microtubes and keep on ice.
- Once the foam has dissipated (~1 hour) collect the content of the microtube and transfer it into a clean tube.
- Centrifuge (Spectrafuge™ 24D, Labnet, Edison NJ) at 17 226 x g. for 15 minutes at 4ºC.
- Transfer the supernatants (protein lysates) to clean pre-chilled microtubes.
- Perform Bradford protein determination and then freeze samples at -80ºC.

Appendix C

Bradford protein determination

Stock solution 5 X concentration:

- Dilute 500mg Coomassie Brilliant blue G250 in 250 ml 95% ethanol.
- Add 500 ml phosphoric acid, mix thoroughly.
- Adjust the volume to 1 L with ddH_2O.
- Filter solution and store at 4ºC.

Working solution

- Dilute stock solution in a 1:5 ratio (100 ml:500 ml) with ddH_2O.
- Filter with two filter papers (Munktell, filter paper, 3HW 240 mm, Sweden).
- The filtered working solution should be a light brown color and is light sensitive.

Method

- Thaw the 1 mg/ml BSA stock solution.
- Dilute the BSA stock solution to a final concentration of 200 µg/ml (100 µL of 1 mg/ml stock + 400 µl ddH_2O).
- Thaw the lysate samples on ice (if frozen) and keep on ice at all times.
- Mark 2 ml microtubes, i.e. n=14 for the standards (each standard in duplicate) and n=2 for each sample (also done in duplicate).
- Prepare a standard curve from the 200 µg/ml BSA solution as shown in Table below:

Standard curve preparation required to determine protein concentrations.

BSA	ddH_2O	Concentration
0	100 µL	Blank
10 µL	90 µL	2 µg
20 µL	80 µL	4 µg
40 µL	60 µL	8 µg
60 µL	40 µL	12 µg
80 µL	20 µL	16 µg
100 µL	0 µL	20 µg

- For the samples, place 95 µL of ddH_2O into each sample tube and add 5 µL of protein sample to appropriately labeled tubes (in duplicate).
- Vortex (Scientific industries, Bohemia NY) all tubes briefly.
- Add 900 µL Bradford working solution to each tube and vortex again.
- Incubate tubes at room temp for at least 5 minutes (reaction is stable for up to 60 minutes).
- Switch on the spectrophotometer (Cecil CE 2021, 2000 series, Cambridge) and allow it to warm up for calibration, then set wavelength to 595 nm.
- Read the absorbance of both the standards and all experimental samples.
- If the absorbance of samples falls outside the range of the highest standard, dilute with RIPA buffer and read again – remember to multiply result by dilution.
- Use the Bradford graph program to obtain a standard curve and unknown protein values (in µg).
- Prepare samples with the loading buffer (1:1 ratio).

Appendix D

Protocols: Western blotting

SAMPLE PREPARATION:

Laemmli's loading buffer

ddH_20	3.8 ml
0.5 M Tris-HCl, pH 6.8	1.0 ml
Glycerol	0.8 ml
10% (w/v) SDS	1.6 ml
0.05% (w/v) Bromophenol blue	0.4 ml

Materials:

1.5 ml microtubes

Sharp tweezers or a syringe needle

β-mercaptoethanol

Ice

Heating block set to 95^{o}C (or beaker of water on hot plate)

Vortex (Scientific industries, Bohemia NY)

Microtube centrifuge (Spectrafuge™ 24D, Labnet, Edison NJ)

Protocol:

Make a working solution of Laemmli's sample buffer – 850 µL Laemmli's stock buffer solution together with 150 µL β-mercaptoethanol (work in fume hood). Vortex (Scientific industries, Bohemia NY) thoroughly.

Calculate the appropriate volume of each sample to give equal loading protein amounts (e.g.: 50 µg protein/sample) and calculate the number of sample sets needed.

Label microtubes for each sample.

Add the appropriate amount of working solution of Laemmli's and RIPA buffer, as calculated, to each appropriate tube (work in fume hood).

Add the appropriate volume of each protein sample to respective microtubes.

Close samples and punch small hole in lid with tweezers or syringe needle.

Heat samples on heating block for 5 minutes.

Centrifuge (Spectrafuge 24D Labnet, Edison NJ) each tube at 17, 226 x g (briefly for ~10 seconds) and place on ice immediately.

Samples can now either be stored at -20^{o}C for future use or directly loaded onto gels.

Gels:

Precast gels (BIO-RAD, Mini-PROTEAN® TGX Stain-Free™ Gels, 4-20%, 10 well combs, 50 µL with stain-free enabled imagers, Hercules CA) were used for all HBP analyses (see details below).

1: Add 7.5 µL of protein marker (BIO-RAD, unstained Precision Plus Protein™ standard, Hercules CA) to the first lane on the far left of each precast gel (BIO-RAD, Hercules CA).

2: Add the appropriate amount (calculated from Bradford protein quantification) of sample slowly into respective lanes using the gel-loading tips.

3: Place the green lid with appropriate leads (black to black: red to red) on top of the tank and connect to the power pack (Power PAC 1000, BIO-RAD, Hercules CA).

4. Add running buffer to just below the line indicated on the tank.

Running buffer: 10x SDS (1L)

- 10 grams SDS
- 30.3 grams Tris-base
- 144.1 grams glycine

Dissolve in 800.ml ddH_2O, adjust volume to 2 L. Make 1x running buffer by adding 100 ml 10x running buffer to 900 ml ddH_2O.

5: Run at 300V (constant), 400 mA for 15-20 minutes to allow samples to migrate through gel.

6: Switch off power and disconnect electrodes. Remove gel plates from the tank and immediately proceed to the electro-transfer step.

7: Image gels to evaluate sample migration as well as visualizing total protein content of each sample (Image Lab™ Software version 4.0, BIO-RAD, Hercules CA).

Transfer using Transfer Turbo and Chemi-Doc:

Open the transfer pack (Trans-Blot® Turbo™, transfer pack, BIO-RAD, mini format, 0.2 µm PVDF, single application, Hercules CA) and place the blotting paper marked "bottom" on bottom of the Transfer Blot (Trans-Blot® Turbo™, transfer system, BIO-RAD, Hercules CA) cassette on top. Gently roll out any air bubbles. Place the gel on top of the membrane with the low molecular weight protein side facing towards the center of the cassette and again gently roll out any trapped air bubbles. Then place the blotting paper marked "top" from the transfer pack over the gel and roll out air bubbles (align the blotting paper tabs in the same manner as when it came out of the transfer pack).

- Place lid on top and lock in place.

- Place the cassette in the Transfer Blot (Trans-Blot® Turbo™, transfer system, BIO-RAD, Hercules CA) and set to transfer for 7 minutes, this will allow the protein to be transferred from the gel onto the membrane.

- Check that protein has transferred and then place in methanol for ~30 seconds then leave to dry completely.

- Rinse membrane 3 x 5 minutes with TBS-T.

10x TBS Buffer:

- 48.4 grams Tris
- 160 grams NaCl

Dissolve in 1.5 L ddH_2O. Set pH to 7.6 with HCl and adjust volume to 2 L.

1x TBS-T buffer:

- 100 ml 10x TBS buffer
- 900 ml ddH_2O
- 1 ml Tween

- Block for 15 minutes in 5% BSA – made up in TBS-T (5 grams BSA 100 ml TBS-T).

- Wash 3 x 5 minutes in TBS-T.

- Place membrane in 50 ml Falcon tube (BD Bioscience, Bedford MA) containing 5 ml of primary antibody – a 1/1000 dilution of the *O*-GlcNAc IGg mouse monoclonal primary antibody (CTD110.6, Santa Cruz Biotechnology, Santa Cruz CA) was used.
- Place on rotator in 4ºC walk-in fridge overnight.

DAY 2:

1:Remove membrane from primary antibody (save antibody – freeze at -20ºC).

2:Wash 3 x 5 minutes in TBS-T.

3: Prepare secondary antibodies by diluting in 5 ml TBS-T in a 50 ml Falcon tube (BD Bioscience, Bedford MA). A 1:1000 dilution was used (5 µl secondary antibody in 5 ml TBS-T). An anti-mouse monoclonal secondary antibody (anti-mouse IgG, HRP-linked, Cell Signaling Technology®, Danvers MA) was employed and placed on roller for 1 hour at room temperature.

4:Pour off secondary antibody into tube and freeze for later use.

5:Wash membrane 3 x 5 minutes in TBS-T.

6: Take ECL reagents (BIO-RAD, Hercules CA) A & B from fridge and equilibrate to room temperature.

7: Prepare ECL substrate in a 1:1 ratio of A:B. Use foil-covered microtubes to prepare solution as ECL is light sensitive.

8: Pour off the TBS-T from membrane and add ECL, spreading evenly over the surface of the membrane by gentle tilting. If MW of protein is known, just add ECL to this area to save on the amount of ECL as it is very costly.

9:Swirl gently for 2 minutes.

10: Place membrane on tray of the ChemiDoc (BIO-RAD, ChemiDoc™, XRS+ system, Hercules CA) taking care to remove any visible bubbles.

Image analysis on Chemi-Doc:

1. Select "Image Lab™ Software version 4.0 (BIO-RAD, Hercules CA), quantification analysis" program from desktop on computer.

2. The ''start'' page will pop up – can choose an existing protocol or create a new one.

3. All protocol settings can be modified by selecting the item on the left under "Protocol Set Up".

4. For self-poured gels: Select "Blot" and then select "Chemi" from drop-down window.

5. Next, set the imaging area to 12 x 9 cm (W x L).

6. Specify the optimum exposure e.g. "intense bands".

7. Default color is auto selected – you can change this if required.

8. Select "Lane and Band Detection".

9. Select either "Low" or "High" for intense or faint bands or use the "custom" slider to set exact sensitivity.

10. Select "Analyze MW" then select MW standard used, the appropriate lane and the regression method (linear, semi-log) - if using Bio-Rad marker you can analyze against this (a stain-free marker was used in order to activate and visualize total protein content before the gel was transferred to the membrane). The stain-free gel does not require a loading control as the total protein content is visualized and

analysed for normalization. Gels are visualized to calculate total protein content (Image Lab™ Software version 4.0, BIO-RAD, Hercules CA)

11. Generate a report: Specific output, then provide a customized name and specify whether to be printed or displayed.

12. Save the protocol summary.

13. Load the gel into the imager and position it on the stage using the "position gel" option – this will produce a live image of the gel's position –adjust by opening the top door of Chemi-doc- adjust the zoom settings and position to obtain image exactly as required.

14. When gel is correctly positioned, click on "Run Protocol".

15. Once protocol has run, the images and report will be displayed with all selected analyses applied.

16. Save the images required to an appropriate folder in ''Documents''.

17. Analyze images using: Image Lab™ Software version 4.0 (BIO-RAD, Hercules CA), quantification analysis.

Appendix E

H &E Staining

Hemalum colors the nuclei of cells blue. The nuclear staining is followed by counterstaining with an aqueous solution of eosin *Y*, which colors other structures in various shades of red and pink (Avwioro, 2011).

Procedure:

1. De-paraffinize sections, 2 changes of xylene, 5 minutes each.

2. Re-hydrate in 2 changes of absolute alcohol, 5 minutes each.

3. 95% alcohol for 2 minutes and 70% alcohol for 2 minutes.

4. Wash briefly in distilled water, (if frozen section – start here).

5. Stain in Mayer hematoxylin solution for 8 minutes.

6. Wash in warm tap water for 10 minutes (place tap water in oven before the start of the stain).

7. Rinse in distilled water.

8. Rinse in 95% alcohol, 10 dips.

9. Counterstain with eosin-phloxine B solution (or eosin Y solution) for 30 seconds (50% ddH_2O to eosin).

10. Dehydrate through 95% alcohol, 2 changes of absolute alcohol, 5 minutes each (mount frozen sections here here).

11. Clear in 2 changes of xylene, 5 minutes each.

12. Mount with xylene-based mounting medium.

Results:

Nuclei ---------- blue
Cytoplasm ---------- pink to red

References

1. Avwioro, G. (2011). Histochemical uses of haematoxylin—a review. *J Pharm Clin Sci (JPCS)*, *1*, 24–34.